

On Monte Carlo Time-Dependent Variational Principles

Von der QUEST-Leibniz-Forschungsschule der Gottfried Wilhelm Leibniz
Universität Hannover zur Erlangung des akademischen Grades

Doktor der Naturwissenschaften
– Doctor rerum naturalium –

genehmigte

Dissertation

von
FABIAN WOLFGANG GÜNTER TRASCHEL
Geboren am 10.01.1987 in Gehrden

2016

0

Erstprüfer : Prof. Dr. Reinhard F. Werner
Zweitprüfer : Prof. Dr. Klemens Hammerer
Beratendes Mitglied des Prüfungsausschusses : Prof. Dr. Tobias J. Osborne
Vorsitzender des Prüfungsausschusses : Prof. Dr. Rolf Haug

Tag der Promotion: 17. Dezember 2015

**On Monte Carlo Time-Dependent Variational
Principles**

Fabian W. G. Transchel

Abstract

The present dissertation is concerned with the development and implementation of a novel scheme for quantitative, numeric approximation of the dynamics of quantum lattice systems based on the Time-Dependent Variational Principle together with Monte Carlo techniques in order to include dissipative interactions. The specific implementation is demonstrated on both common and not yet in-detail explored Heisenberg- and Fermi-Hubbard models in one and two dimensions. Additionally, the technical requirements regarding computational complexity and capacity are discussed, especially with regards toward parallelizable components of the implementation. Concluding remarks include prospects with respect to application and extension of the presented methods.

Keywords: Monte Carlo method, Dissipative Dynamics, Lindblad Equation

Zusammenfassung

Die vorliegende Dissertation befasst sich mit der Entwicklung und Umsetzung eines neuartigen Schemas zur quantitativen numerischen Näherung der Dynamik von Quantengittersystemen auf Grundlage des zeitabhängigen Variationsprinzips unter Zuhilfenahme von Monte-Carlo-Techniken zur Einbeziehung von dissipativen Wechselwirkungen. Die Implementierung wird anhand von Beispielen für Heisenberg- und Fermi-Hubbard-Modellen in einer und zwei Dimensionen gezeigt und erläutert. Ergänzend erfolgt eine Betrachtung der technischen Anforderungen an rechnerische Kapazitäten und komplexitätstheoretische Erwägungen, mit besonderem Augenmerk auf parallelisierbare Komponenten der Implementierung. Abschließend wird ein Ausblick hinsichtlich der weiteren Möglichkeiten von Einsatz und Erweiterung der präsentierten Methoden vorgenommen.

Schlagworte: Monte-Carlo-Simulation, Dissipative Dynamik, Lindblad-Gleichung

Selbständigkeitserklärung

Hiermit bestätige ich, die vorliegende Dissertation selbst verfasst zu haben, keine Textabschnitte von Dritten oder eigenen Prüfungsarbeiten ohne Kennzeichnung übernommen und alle benutzten Hilfsmittel und Quellen in der Arbeit angegeben zu haben.

Hannover, den 09. November 2015

Fabian W. G. Transchel

Dedication

*What is a thesis
But a 148-page love letter?
To nature, to physics
To every qubit in the universe*

*What is a thesis
but a ladder to climb on?
For nature, for physics
For dwarfs on the shoulders of a giant universe*

*What is a thesis
But an awe-struck observation?
Of nature, of physics
Of every qubit in the universe*

*What is a thesis
but a proposition that remains?
When nature, when physics
When everything dissipates*

*To nature
To physics
To you
And to everyone*

Acknowledgments

Although an endeavor as bold as a dissertation in theoretical physics never can be fully understood in terms of a single effort of will that is merely assisted by others, this is exactly what one implies once it comes to the acknowledgments. Accordingly, one enumerates the “relevant” impacts, although in truth every little hint is worth acknowledging. Every conversation, every misplaced index, every syntax error spotted propels us toward the aim of making it a thesis. Much like mathematicians turn coffee into theorems, the whole lot of scientific experience that happens in the meantime is turned into a dissertation through means not fully understood by physicists.

Ignoring the paradox to acknowledge the relevance, I proceed toward a (partially ordered) enumeration and thereby deeply thank Reinhard for the unique opportunity to push the boundary of scientific understanding as well as the possibility to observing indisputable genius, Tobias for the tireless gauging of both possible and impossible research directions, Ash for the wonderful basis of evoMPS upon which the framework for open system could be built, Kais, Fabian F. and Robert for their patient (and particularly uncomplaining) office fellowship that led to much unanticipated insights as well as Bernhard, René, Lars, Tobias G., Jörg and all the other members of the QI group for all the corrections and annotations and entertainment opportunities that finally led to this thesis.

Last but not least, of course it cannot be understated the amount of deprivation my family and especially my girlfriend Wiltrud had to endure. Where the group nourished me scientifically, she helped me keeping the pretense of normal functioning and sanity nonetheless – on a ride that truly cannot be ventured alone.

Contents

| | |
|---|----------|
| Abstract | iii |
| Zusammenfassung | v |
| Selbständigkeitserklärung | vii |
| Dedication | ix |
| Acknowledgments | xi |
| List of abbreviations | 1 |
| Introduction | 3 |
| Part 1. Preliminaries | 7 |
| Chapter 1. Quantum Information | 9 |
| 1. Bases | 9 |
| 2. Products | 9 |
| 2.1. Inner Product | 9 |
| 2.2. Outer Product | 9 |
| 3. Eigenproperties | 10 |
| 4. Dynamics | 11 |
| 5. The Qubit | 12 |
| 5.1. Phase | 12 |
| 6. Composition of quantum systems and entanglement | 13 |
| 7. Density operators | 13 |
| 7.1. Properties | 14 |
| 7.2. Bloch sphere | 15 |
| 7.3. No-cloning Theorem | 17 |
| 7.4. Partial trace | 17 |
| 7.5. Schmidt Decomposition | 18 |
| 7.6. Purification | 19 |
| 8. Entropy | 19 |
| 8.1. Properties of the Von Neumann entropy | 20 |
| 8.2. Entropies of composite systems | 21 |
| 8.3. Monogamy of entanglement | 21 |
| 9. Spin | 22 |
| 10. Spins as logical qubits | 23 |
| 11. Second Quantization | 24 |
| 11.1. Creation and Annihilation operators | 25 |
| Chapter 2. Correlated Spin Systems and its Dynamics | 27 |
| 1. Spin Lattices | 27 |
| 2. Finitely Correlated States | 29 |
| 2.1. Entanglement and Correlations | 29 |

| | |
|--|-----------|
| 2.1.1. Bell Inequality | 30 |
| 2.1.2. Area laws | 31 |
| 3. From FCS to MPS | 32 |
| 3.1. Explicit MPS examples | 33 |
| 3.1.1. GHZ state | 33 |
| 3.1.2. W state | 33 |
| 3.2. Properties and applications of MPS | 34 |
| 3.2.1. Expectation values | 34 |
| 3.2.2. MPS from slightly entangled states | 34 |
| 3.2.3. Connection to DMRG | 35 |
| 3.3. The canonical form | 36 |
| 3.4. Translation invariance | 38 |
| 3.5. Gapless and frustration-free Hamiltonians | 39 |
| 3.6. AKLT model | 41 |
| 3.7. Criticality | 41 |
| 3.8. Heisenberg model | 42 |
| 3.9. Hubbard model | 44 |
| 3.9.1. Jordan-Wigner transformation | 44 |
| Chapter 3. Variational Ansatzes in numerical Many-body Physics | 45 |
| 1. The variational principle | 45 |
| 1.1. Derivation | 46 |
| 2. DMRG | 47 |
| 3. Matrix Product Operators | 48 |
| 4. The Time-Dependent Variational Principle | 50 |
| 4.1. Derivation | 50 |
| 4.2. Properties | 53 |
| 4.3. Examples and algorithms: evoMPS | 53 |
| 4.3.1. Imaginary time evolution | 55 |
| 4.3.2. Real time evolution | 55 |
| 5. Variational Monte Carlo | 56 |
| 5.1. Time-Dependent Variational Monte Carlo | 57 |
| Chapter 4. Stochastic Calculus | 59 |
| 1. Markov Processes | 59 |
| 1.1. The Fokker-Planck Equation | 62 |
| 1.2. Itô's Lemma | 63 |
| 2. The Stochastic Integral | 64 |
| 3. The Glivenko-Cantelli theorem | 64 |
| 4. The Quantum Master Equation | 65 |
| Part 2. Monte Carlo Dissipation Models | 69 |
| Chapter 5. A Monte Carlo Time-Dependent Variational Principle | 71 |
| 1. Motivation | 71 |
| 2. Derivation of the method | 72 |
| 3. Algorithm and implementation | 76 |
| 3.1. Preparations | 76 |
| 3.2. Iteration step | 77 |
| 3.3. Distributed computation and sampling | 79 |
| 3.4. Post-processing and analysis | 81 |
| 4. Possible extensions | 83 |
| Chapter 6. Applications to the Heisenberg model | 85 |

| | |
|---|-----|
| 1. Introduction | 85 |
| 2. Results for edge-driven models | 86 |
| 3. Probing the steady state | 87 |
| 4. Quasi-homogenous models | 88 |
| 4.1. Introduction | 88 |
| 4.2. Homogenous dissipation | 88 |
| 4.2.1. Results | 88 |
| 4.3. Bihomogenous case | 90 |
| 4.4. Results for bihomogenous case | 90 |
| 5. Outlook | 92 |
| Chapter 7. Applications to the Fermi-Hubbard model | 93 |
| 1. Introduction | 93 |
| 2. Model-specific adaptations to the Monte Carlo TDVP | 94 |
| 2.1. Jordan-Wigner transform | 94 |
| 2.2. Algorithm | 97 |
| 2.3. Results for the one-dimensional case | 97 |
| 3. Treatment of higher spatial dimensions | 99 |
| 3.1. The memory scaling problem | 100 |
| 3.2. Results for the two-dimensional case | 103 |
| 4. Outlook | 105 |
| 4.1. One-dimensional super sites | 105 |
| 4.2. Nested MPS | 106 |
| Conclusion | 109 |
| Appendix. List of tables | 111 |
| Appendix. List of figures | 113 |
| Appendix. Resources / Hilfsmittel | 117 |
| Appendix. Curriculum Vitae | 119 |
| Appendix. Bibliography | 121 |

List of abbreviations

| | |
|----------|---|
| ALS | Alternating Least Squares method |
| DMRG | Density Matrix Renormalization Group |
| BOINC | Berkeley Open Infrastructure for Network Computing |
| evoMPS | Python many-body simulation package implementing the TDVP |
| ITE | Imaginary Time Evolution |
| LAPACK | Linear Algebra Package |
| LCF | Left Canonical Form |
| LHS | left-hand side |
| MCTDVP | Monte Carlo Time-Dependent Variational Principle |
| MPS | Matrix Product State |
| MPO | Matrix Product Operator |
| NRG | Numerical Renormalization Group |
| NumPy | Python extension for large array/matrix representations |
| openBLAS | Basic Linear Algebra Subprograms |
| RCF | Right Canonical Form |
| RHS | right-hand side |
| RNG | Random Number Generator |
| RTE | Real-Time Evolution |
| SciPy | Python extension for scientific calculations |
| TDVP | Time-Dependent Variational Principle |
| TEBD | Time-Evolving Block Decimation |
| VMC | Variational Monte Carlo |

Introduction

The quest of the physical sciences is to enhance our understanding of reality. While the scientific method has many different manifestations, its principles within will always stay the same: Based upon experience, the scientist formulates a hypothesis about empirically accessible experiments that can deepen a conviction about certain causal relations, be it about fundamentals like the law of gravity or its generalization in relativity as well as the advent of quantum theory. The role of theoretical work cannot be overstated as it provides a foundation for the inference step by precisely defining the necessary variables and interactions.

Depending on the discipline and question, the relation between theory and experiment becomes more and more dialectic – without going into detail, we can already understand from the above definition that without theory, there is no basis for a sound experiment, regardless of its sophistication – while, on the other hand, without experimental validation, any theory becomes hollow and scientifically meaningless.

The present dissertation treads precisely the thin line in between theory and practice because it provides both validation for existing models as well as predictive potential about experiments that have yet to be performed. More concretely, the discipline pursued in this dissertation is that of Quantum Information, the subbranch of Quantum Mechanics that concerns itself with the treatment of information and its transformations where classical information theory fails as badly as classical mechanics to address the various and wondrous phenomena the quantum world provides. Topics like Quantum Teleportation, Quantum Key Distribution and the like have elicited public interest from which Quantum Information has profoundly benefited. From the scientific point of view, however, the systematic research of many-body systems seems much more valuable in terms of understanding reality, because these systems are much more common than the highly-engineered and undisturbed models of Quantum Information theorems and, as we will see, show a rich variety of quantum effects that shape the macroscopic behavior of the larger building blocks – like phase transitions on spin lattice systems – that quantum many body systems aspire to treat.

These many body systems we are concerned with consist of chains of single particles in one or more spatial dimensions, coupled to one another by individually targeted interaction terms that model e.g. magnetic or spin interactions. Spin chains are governed in their behavior by two different kinds of dynamics: First of all, the coherent propagation with time given by the system's Hamilton operator, extended by so-called dissipation, which represents the irreversibility of thermodynamic processes during the flow of time that inevitably appear in real systems of interest. Although it has to be said that dissipation does not necessarily mean that the system is purged of its quantum correlations, one can never truly insulate an experiment from the outside world, which poses a practical, not necessarily theoretical challenge. Dissipation ultimately models the exchange of heat, information, i.e. the creation and annihilation of quantum correlations. While the research of many-body systems is often limited by the sheer number of degrees of freedom and

by the question of which of them to ignore, with dissipation the situation is worse: More often than not an experimentalist observes energy dissipation but cannot tell which path the lost energy took, i.e. the coupling itself is not merely part of the equation, but to some extent up for debate. It is one of the primary objectives of this work to prepare a framework that can systematically determine the form of dissipation at hand.

The tools at our disposal include concepts such as the variational principle, i.e. the method that sets out how to minimize a functional on a manifold. By applying it, we seek answers to the question of how to optimize an algebraic expression given some constraints. While this seems very broad indeed, its application to Quantum Information has given rise to both specific and computationally efficient sets of variational classes. E.g. we introduce why it is useful to stay within a certain class of states that can be realized as matrix products. The variational class of Matrix Product States has been applied to many-body systems with great success – first in the form of density matrix renormalization group ansatzes, and in recent years through the application of the Time-Dependent Variational Principle, the latter being shown to be a generalization of the former.

The great benefit of parametrizing the dynamics on Hilbert spaces exponentially big in the system size by means of MPS is that we have a bounded number of variational parameters to treat – again, bounded in the system size, i.e. number of particles – that scale much more favorably with regards to the increase of degrees of freedom when adding particles to the system, when compared to direct diagonalization. In some cases this means that we can get better answers than other approximate methods, in others we get answers at all, where other methods are not practical – which in itself indicates increased insight into the structure and dynamics of the many-body systems.

Going forth, we show how to introduce stochastic methods that enable the treatment of dissipative dynamics within the Time-Dependent Variational Principle through adding Monte Carlo sampling on the level of the variational manifold, i.e. changing the tangent vector of the variational class on its variational manifold, i.e. the subspace of infinitesimal action with respect to the effect of the dissipative dynamics.

By applying the solution of the respective stochastic differential equation, derived from the Quantum Master Equation to the TDVP, we can successfully simulate the time evolution of mixed states, which cannot in general be treated by numerical studies and are approximated by sampling from the correct superposition of product state basis vectors instead of trying to represent them by truncation schemes. By choosing this approach we gain knowledge about ensemble averages of interesting system properties, be it an approximation of the (mixed) steady state or other constants of motion. We then go on to show that the interaction between the coherent treatment of the Time-Dependent Variational Principle and its dissipative extension can be performed in a way that permits computational treatment in a parallel manner such that hundreds of dissipating samples can be calculated in the time a single coherent treatment would take. It is important to note, though, that neither is finding a steady state always the primary goal of an investigation, nor does every setup feature steady states.

Although sampling thousands of instances of stochastically equivalent (and identically distributed) time evolutions of the same system seems inefficient at first, the correct reference of computational complexity is the exact solution of quantum dynamics, achieved by direct diagonalization. This way of solving dynamics is exponentially more expensive than the numerical schemes developed from the variational principle and alike, and for the treatment of extensive system we aim to

investigate outright impossible. As such, the presented method is among the few numerical schemes that can tackle complex tasks of investigating not only a few (i.e. $\mathcal{O}(10)$), but dozens (i.e. $\mathcal{O}(100)$) of interacting quantum particles, which is a vast improvement over exact analytic treatment, albeit penalized by giving up infinite accuracy.

While the thorough investigation of experimentally accessible systems was not the primary aim of this work, we discuss exemplary results of dissipative dynamics on Heisenberg-type systems as well as Fermi-Hubbard models, which are among the most-studied many-body schemes in physics. The particular benefits of this approach include both being able to check the method against established treatments of dissipation and the opportunity to make specific predictions about configurations that could previously not be treated theoretically within the realm of existing methods, like the case of experimentally accessible chains of ^{40}K atoms subject to the specific interaction induced by laser driving.

The content of this dissertation is arranged as follows. The first part starts with a short introduction to the basic terminology of Quantum Information Theory in Chapter 1. Afterward, we review the state of the art of the treatment of quantum spin chains in Chapter 2, followed by a discussion of necessary notions from Stochastic Calculus in Chapter 4. The remaining technical requirements are introduced in a thorough review of the Time-Dependent Variational Principle as a means of solving ground state problems and unitary time evolution in Chapter 3.

In the second part, the research results of this dissertation are presented, starting with Chapter 5, including the derivation of the Monte Carlo Time-Dependent Variational Principle. We review basic exemplary results on Heisenberg chains of the XZ, XXZ and ZZ form in Chapter 6, while Chapter 7 treats research performed on Fermi-Hubbard models providing insights into, e.g. representing the actual form of Quantum Optical dissipation operators on strongly interacting Rydberg atoms in optical cavities, such as ^{40}K .

The final chapter is comprised of concluding remarks together with an outlook regarding future research possibilities enabled by dissipative methods presented here.

Part 1

Preliminaries

Quantum Information

1. Bases

Before we start fleshing out the tools of Quantum Mechanics, we need to introduce a minimal set of Linear Algebra to make sense of the more advanced definitions. A spanning set of a vector space is a set of vectors $|s_1\rangle, \dots, |s_N\rangle$ such that $|a\rangle = \sum_i a_i |s_i\rangle$ is a linear combination that can describe any vector in the space. In mathematics, we call this a basis. Note, however, that even for a one-dimensional vector space the definition allows for overcompleteness. Thus, we will usually identify an orthonormal basis of minimal rank, i.e. the number of basis vectors is $\dim A$ and they are mutually orthogonal:

$$\langle s_i, s_j \rangle = \delta_{ij} \quad \forall i, j \in 1, \dots, \dim A, \quad (1)$$

where δ_{ij} is the Kronecker symbol, evaluating as 1 if and only if i equals j and giving 0 otherwise.

2. Products

2.1. Inner Product

In Quantum Information, just like in the rest of Physics, it all starts with the Hilbert Space, i.e. a vector space \mathcal{H} with an Inner Product that maps two vectors $|a\rangle$ and $|b\rangle$ to a scalar. In finite dimension N , this can be explicitly stated as

$$|a\rangle = \begin{pmatrix} a_1 \\ a_2 \\ \vdots \\ a_N \end{pmatrix}, |b\rangle = \begin{pmatrix} b_1 \\ b_2 \\ \vdots \\ b_N \end{pmatrix}, \langle a |, |b\rangle = \sum_{i=1}^N a_i \cdot b_i = \langle a|b\rangle, \quad (2)$$

where $\langle a, b \rangle$ is the so-called Dirac notation, $\langle a|$ being the dual vector of $|a\rangle$. In the following we will introduce all necessary tools to explain the research we performed, but will not deal with the subtleties of vector spaces and functional calculus, where reference to a textbook like [127] can explain the technical details much better.

2.2. Outer Product

Apart from the inner product, useful for calculating overlaps, we need to explore the Outer Product as well. Without a proper definition how to compose Hilbert Spaces, thus facilitating the sheer necessity of dealing with multi-particle systems, Quantum Information would be a hell of models that cannot be plugged together but have to be reinvented every time you want to add or remove a degree of freedom. But since there is an Outer Product, also known as the Tensor Product or Kronecker Product, we don't have to worry about the question what a system composed of two formally independent subsystems looks like. Instead of taking $\langle a|b\rangle$ as a product of a row vector and a column vector, we transpose the operation. Thus, we have to explain how $|a\rangle\langle b|$ is defined:

$$|a\rangle\langle b| = a \otimes b = \begin{pmatrix} a_1 \\ a_2 \\ \vdots \\ a_N \end{pmatrix} \otimes (b_1 \ b_2 \ \dots \ b_N) = \begin{pmatrix} a_1 b_1 & a_1 b_2 & \dots & a_1 b_N \\ a_2 b_1 & a_2 b_2 & \dots & a_2 b_N \\ \vdots & \vdots & \ddots & \vdots \\ a_N b_1 & a_N b_2 & \dots & a_N b_N \end{pmatrix}, \quad (3)$$

where we define $a \otimes b = \sum_{(i,j) \in I \times J} v_i w_j (e_i \otimes f_j)$, based on the vectors $a = \sum_{i \in I} v_i e_i \in A$ on a vector space A and $b = \sum_{j \in J} w_j f_j \in B$ on a vector space B with respective index sets I and J giving rise to the basis vectors $e_i \in A$ and $f_j \in B$. Since tensor products of basis vectors are basis vectors of the tensor space, all we have to explain is the respective tensor basis obtained from $\{e\}$ and $\{f\}$ following the ordered Cartesian product $E \times F = \{(e_i, f_j) \mid i \in I, j \in J\}$. Note that the field of the vector spaces is \mathbb{C} unless otherwise specified.

Now this construction gives rise to some interesting structure. Basic properties include

- (1) Linearity in both tensor factors:

$$\alpha(|a\rangle \otimes |b\rangle) = (\alpha|a\rangle) \otimes |b\rangle = |a\rangle \otimes (\alpha|b\rangle) \quad (4)$$

- (2) Distributivity:

$$(|a_1\rangle + |a_2\rangle) \otimes |b\rangle = |a_1\rangle \otimes |b\rangle + |a_2\rangle \otimes |b\rangle \quad (5)$$

This holds for the other subspace *mutatis mutandis*.

Equipped with these basic properties, we can easily check that scalar products of tensor products are mapped to the tensor product of scalar products. For vectors $|a\rangle, |a'\rangle \in \mathcal{H}_A$ and $|b\rangle, |b'\rangle \in \mathcal{H}_B$, we find that for orthonormal bases $\{e_i\} \in \mathcal{H}_A$ and $\{f_j\} \in \mathcal{H}_B$ the scalar product indeed factorizes:

$$\begin{aligned} \langle a \otimes b | a' \otimes b' \rangle &= \langle ab | a'b' \rangle \\ &= \sum_i \langle a | e_i \rangle \langle e_i | a' \rangle \sum_j \langle b | f_j \rangle \langle f_j | b' \rangle \\ &= \langle a | a' \rangle \langle b | b' \rangle. \end{aligned} \quad (6)$$

Note that we used the notation agreement that

$$|0\rangle \otimes |0\rangle \equiv |0\rangle |0\rangle \equiv |00\rangle. \quad (7)$$

Since $\langle \cdot | \cdot \rangle$ maps elements of the Hilbert spaces to (real) scalars, the tensor product of the scalar product is mapped to a regular product.

3. Eigenproperties

Before we can explore more exotic properties of operators on Hilbert spaces, we need to learn about Eigenproperties – i.e. Eigenvectors and Eigenvalues of operators. The first term refers to a vector $|a\rangle$ with the property that for an operator O , $|a\rangle$ is an Eigenvector if and only if

$$O|a\rangle = a|a\rangle, \quad (8)$$

where in turn a is a complex number called the eigenvalue of A . In cases with more than two dimensions – that is, you cannot guess the Eigenproperties by *looking* at the problem, we resort to the characteristic function. Then, the solutions of $c(\lambda) = 0 \equiv \det|O - \lambda\mathbb{1}|$ are the eigenvalues of O , while the eigenvectors can be found by reinserting the particular eigenvalues λ_i into the eigenvalue Eq. (8)).

This furthermore gives rise to the first of many useful representations of an operator, the diagonal representation, or orthonormal decomposition. Note that by using the eigenvectors as a unique basis, that albeit is not necessarily complete with regard to the whole vector space (because the Eigenvalues can be degenerate, resulting in non-maximal rank of $O - \lambda\mathbb{1}$), we can describe the operator O as

$$O = \sum_i \lambda_i |a_i\rangle \langle a_i|, \quad (9)$$

where $\{|a_i\rangle\}$ is the set of eigenvectors. For example, for the Pauli matrix σ_y (we learn about them in Section 9), the decomposition would read

$$\sigma_y = \begin{pmatrix} 0 & -\mathbf{i} \\ \mathbf{i} & 0 \end{pmatrix} = \mathbf{i}(|0\rangle\langle 1| - |1\rangle\langle 0|). \quad (10)$$

Although possible, numerical determination of large eigenvalue problems is costly. Advanced and established algorithms like the Lanczos algorithm [110] generally scale like $\mathcal{O}(N^3)$ in the number of parameters. While not an issue for static problems like the identification of atomic orbitals, as we will see, the state space of a modestly large many-body system can easily comprise a dimension of $N = 10^{10}$ if no truncations are applied. Although, under special conditions, this can be improved to $\mathcal{O}(N^2)$, it is still computationally intractable. Thus, diagonalization of density matrices of the whole state space is under no circumstances a feasible method to solve the kind of system we have in mind.

4. Dynamics

While we will later see more detailed considerations about the evolution of quantum states, let us briefly discuss, what the basic **Postulate of Unitarity** means. In short, after defining Hilbert space, we would like to know how a state $|\Psi\rangle \in \mathcal{H}$ changes with time. Note that we are considering closed systems, i.e. \mathcal{H} is all we concern ourselves with. Only after discussing Stochastic Calculus will we talk about thermodynamically 'open' systems.

DEFINITION 1. *The **time evolution** of a closed quantum system on \mathcal{H} is given by the transformation created by a unitary operator U such that $|\Psi(t_0)\rangle = U|\Psi(t_1)\rangle$, with $t_0 \leq t_1$. U may depend only on t_0 and t_1 .*

It is important to note that Quantum Theory does not hand this operator to us, it only assures us of its existence. Finding and evaluating the *correct* operator is one of the prime problems in dissipative systems.

A direct consequence, however, is the existence of a differential equation of motion, if one explores the classical considerations of Hamilton-Jacobi formalism. We will not explore the underlying correspondence principle or the classical limit, but instead look at the Schrödinger equation in its most common form:

$$\mathbf{i}\hbar \frac{d|\Psi\rangle}{dt} = H|\Psi\rangle. \quad (11)$$

The Planck constant \hbar is only of practical importance and will be identified with identity in this work: $\hbar \equiv 1$. The entity H is a Hermitian operator known (for historical reasons emerging from said Hamilton-Jacobi formalism) as the Hamiltonian.

Equipped with these tools we may now conclude that H can be decomposed as

$$H = \sum_i e_i |E_i\rangle\langle E_i| \quad (12)$$

with Eigenvalues $\{e_i\}$ and Eigenfunctions $\{E_i\}$, the latter known as the **energy Eigenstates** of H . If the Hilbert Space is finite, as we will assume unless noted otherwise, the spectral decomposition also has finitely many contributing terms. Educated about this property, we can conclude that the time evolution of any closed system whose Hamiltonian is not time-dependent is particularly easy to obtain if one has knowledge about the *diagonalization*, i.e. the Hamiltonian's eigenvalues. In this case we write

$$U(t) = e^{-iHt/\hbar} \quad (13)$$

and find for an arbitrary state vector

$$|\psi(t)\rangle = U(t)|\psi(0)\rangle. \quad (14)$$

In this situation the ground state, i.e. the eigenstate with the lowest energy, is of prime interest, as we will later see in Section 8, because oftentimes we can learn much about the system’s characteristic behavior. For example, a non-degenerate ground state has zero entropy. Furthermore, although their preparation is often inconvenient in practice, in quantum information theory ground states are often used as basis states for either computational or cryptographic protocols as well as tools for proving various statements because of the fact that we have a certified lower bound for the system energy: Any operation on the ground state will either increase the system energy or leave it invariant.

5. The Qubit

Knowing about state spaces, we need to know about “things” in them. Just like the system does not tell us how its ground state looks like, for some models we don’t even know how the state space itself looks like. The most basic object of Quantum Information Theory is the **Qubit**. While the term usually describes the two-dimensional state space $\mathcal{H} = \mathbb{C}^2$, it will very well also denote the abstract concept of a quantum system with two orthogonal basis states, $|0\rangle$ and $|1\rangle$. Somewhat analogous to a classical bit of information, the information density of the qubit is 1 bit per qubit, albeit allowing for superpositions of its basis states: $|\Psi\rangle = a|0\rangle + b|1\rangle$. Note that we used the normalization condition $\langle\Psi|\Psi\rangle = 1$, ensuring that $|\Psi\rangle$ is a proper probability density. While the system is in such a superposition state, we cannot with certainty tell what information the qubit will bear: We have to make a measurement.

Quantum measurements are represented by positive operators $\{O_i^\dagger O_i \geq 0\}$ on the Hilbert space \mathcal{H} , where its index i refers to the set of outcomes. Since producing a measurement will have an outcome, we demand that the probabilities p_i for each outcome must sum to unity:

$$\sum_i p_i = \sum_i \langle\Psi|O_i^\dagger O_i|\Psi\rangle = 1 \quad (15)$$

Sneakily we introduced here the correct notation for the operators O_i acting on the state $|\Psi\rangle$. The most common way of *representing* operators on Hilbert spaces is the use of a matrix algebra with elements from the $n \times n$ matrices denoted $\mathcal{M}_{n \times n}$, that is, if we have a basis of dimension n , the corresponding vectors are $1 \times n$ -matrices.

If the sum in Eq. (15) evaluates to one because all outcomes together must be of stochastic nature, we can infer how probabilities are calculated:

$$p_i = \langle\Psi|O_i^\dagger O_i|\Psi\rangle. \quad (16)$$

We will now use this notation to exemplify the computational basis $\{|0\rangle, |1\rangle\}$ of the qubit. Note that we can define a measurement O as e.g. $O_0 = |0\rangle\langle 0|$, $O_1 = |1\rangle\langle 1|$.

Using $\langle i|j\rangle = \delta_{ij}$ for an orthonormal basis, it is easy to see that

$$p_1 = \langle\Psi|O_1^\dagger O_1|\Psi\rangle = (a\langle 0| + b\langle 1|)|1\rangle\langle 1||1\rangle\langle 1|(a|0\rangle + b|1\rangle) = b^2, \quad (17)$$

since $\langle 0|1\rangle = 0$. It should also be noted that in this particular case O_0 and O_1 are projections: $O_i^2 = O_i$. While observables need not have this property, it is useful, when available, since it allows for effortless spectral decomposition that we already know.

5.1. Phase

Together with “*topological*”, an abomination of a term, the notion of **Phase** is one of the most diversely and variously used throughout all of physics. As we will see later, even throughout this monograph we will have more than one concept called

a phase. Still, considering the qubit only, the phase is one of the more accessible concepts.

If we, for example, look at the state vector $e^{i\theta} |\Psi\rangle$, where $|\Psi\rangle$ itself is a state vector on the state space and θ is a real number, we say that the two states $|\Psi\rangle$ and $e^{i\theta} |\Psi\rangle$ are unitary equivalent, since they give the same measurement statistics. We may furthermore call both $e^{i\theta}$ and the number θ itself the **global phase** of $|\Psi\rangle$.

Regarding unitary equivalence, it should be easy to see that

$$\langle \Psi | e^{-i\theta} O_i^\dagger O_i e^{i\theta} | \Psi \rangle = \langle \Psi | O_i^\dagger O_i | \Psi \rangle, \quad (18)$$

since $e^{i\theta}$ is a complex number thus commuting with operators $O_i^\dagger O_i$ and clearing out with $e^{-i\theta}$ to one.

6. Composition of quantum systems and entanglement

If we remember the tensor product of Eq. (3), we now should expose one of the more peculiar aspects of quantum mechanics: **entanglement**.

Looking at states on a system of *two qubits*, more precisely given as

$$\mathcal{H}_{comp} = \mathcal{H}_1 \otimes \mathcal{H}_2, \quad \mathcal{H}_{1+2} = \mathbb{C}^2 \Rightarrow \mathcal{H}_{comp} = \mathbb{C}^4, \quad (19)$$

we can define a state $|\Psi\rangle$ on \mathcal{H}_{comp} as

$$|\Psi\rangle = \frac{|00\rangle + |11\rangle}{\sqrt{2}} \quad (20)$$

and subsequently notice that it has a most puzzling property: We cannot decompose it into a product of single qubit states, i.e.

$$\forall |a\rangle \in \mathcal{H}_1 \wedge \forall |b\rangle \in \mathcal{H}_2 : |\Psi\rangle \neq |a\rangle |b\rangle. \quad (21)$$

7. Density operators

While it is common and useful to introduce the language of quantum mechanics in terms of state vectors, the **density operator** is a much more powerful concept. We will review basic properties in this section, but only understand its benefits when discussing the peculiar nature of mixed state sampling in Chapter 5. The usual definition is given by

$$\rho \equiv \sum_i p_i |\Psi_i\rangle \langle \Psi_i|, \quad (22)$$

where the vectors $|\Psi_i\rangle$ represent the pure states of the respective system and p_i is a probability distribution, such that for every possible contribution i there is a non-vanishing probability to prepare the term $|\Psi_i\rangle \langle \Psi_i|$.

The resulting density operator for a system $\mathcal{H} = d$ is a matrix of dimension $d \times d$, hence coining the synonymous term **density matrix**. It provides a way of talking about systems where the state of the quantum system is not completely known. Also, this is a more thorough way to highlight the inherent stochastic nature of quantum mechanics, since the density matrix can be interpreted as an ensemble of systems all prepared in the same state and subject to the same dynamics:

$$\rho \xrightarrow{U} U \rho U^\dagger = \sum_i p_i U |\Psi_i\rangle \langle \Psi_i| U^\dagger. \quad (23)$$

Note how ρ transforms like a second-order tensor, while $|\Psi\rangle$ transforms like a first-order tensor, just like matrices and vectors respectively and we can thus calculate probabilities as

$$p(i) = \text{tr}(O_i^\dagger O_i \rho), \quad (24)$$

where tr denotes the trace of a matrix, i.e. for $A \in \mathcal{M}_n$

$$\text{tr}(A) = \sum_i^n A_{ii}. \quad (25)$$

7.1. Properties

If a system can be described by $\rho = |\Psi\rangle\langle\Psi|$, i.e. if and only if it can be represented by a single unique wave vector (up to unitary equivalence), the system is in a *pure state*.

If, on the other hand, the state is comprised of a decomposition of pure states, like $\rho = \sum_i p_i |\Psi_i\rangle\langle\Psi_i|$, it is called a mixture or, more precisely, *mixed state*. This concept of a mixture is more pronounced in settings where the preparation of a pure state is not feasible and one ends up with an ensemble of states, weighed by their respective probability, i.e. if one were to measure specifically pure state amplitudes.

Of all statements about density operators, particularly the positivity condition and trace condition seem useful:

THEOREM 1. *Any density operator $\rho = \sum_i p_i |\Psi_i\rangle\langle\Psi_i|$ is a positive operator, i.e. suppose that $|\varphi\rangle$ is an arbitrary wave function in state space. Then we can check that*

$$\langle\varphi|\rho|\varphi\rangle \geq 0, \quad (26)$$

since

$$\sum_i p_i \langle\varphi|\Psi_i\rangle\langle\Psi_i|\varphi\rangle = \sum_i p_i |\langle\varphi|\Psi_i\rangle|^2 \geq 0. \quad (27)$$

Please note: Proofs for the following elementary statements can be found in [127] unless explicitly proved or otherwise noted.

THEOREM 2. *Any density operator $\rho = \sum_i p_i |\Psi_i\rangle\langle\Psi_i|$ obeys the trace condition:*

$$\text{tr} \rho = \sum_i p_i \text{tr}(|\Psi_i\rangle\langle\Psi_i|) = \sum_i p_i = 1. \quad (28)$$

Furthermore, only knowing about pure and mixed states is enlightening as far as state space structure is concerned, but not beneficial on its physical regard. We need to be able to distinguish the two possibilities.

THEOREM 3. *ρ is pure if and only if $\text{tr}(\rho^2) = 1$. Whenever $\text{tr}(\rho^2) < 1$, ρ is a mixed state.*

Before discussing statistic properties of the density operator, it seems appropriate to address a common misconception. Although we can usually determine Eigenproperties with relative ease (if the system complexity allows for practical ways of doing it), their significance is diminished by the fact that the density operator, unless pure, portrays really an ensemble average of mixed states. Let us look at an example.

EXAMPLE 1. *Suppose we are given a density matrix*

$$\rho = \frac{2}{5} |0\rangle\langle 0| + \frac{3}{5} |1\rangle\langle 1|, \quad (29)$$

then the system is in the state $|0\rangle$ with probability $\frac{2}{5}$ and in the state $|1\rangle$ with probability $\frac{3}{5}$. If we furthermore define wave functions as superpositions of the basis vectors with different amplitudes, say

$$|\varphi\rangle = \sqrt{\frac{2}{5}} |0\rangle + \sqrt{\frac{3}{5}} |1\rangle, |\mu\rangle = \sqrt{\frac{2}{5}} |0\rangle - \sqrt{\frac{3}{5}} |1\rangle, \quad (30)$$

we can check that indeed, if we chose a preparation $\rho' = \frac{1}{2} |\varphi\rangle \langle\varphi| + \frac{1}{2} |\mu\rangle \langle\mu|$ that assigns equal probabilities to $|\varphi\rangle$ and $|\mu\rangle$,

$$\rho' = \frac{1}{2} |\varphi\rangle \langle\varphi| + \frac{1}{2} |\mu\rangle \langle\mu| = \frac{2}{5} |0\rangle \langle 0| + \frac{3}{5} |1\rangle \langle 1| = \rho, \quad (31)$$

albeit realizing a different preparation. Since the identical density matrices cannot exhibit different behaviors for different preparations, i.e. being statistically equivalent, one should, as far as arguments about stochastic characteristics are concerned, not attribute special relevance to the basis choice of Eigenproperties.

As a consequence, we can pose the question, what conditions can be given for two ensembles to share the same density operator. But actually that is given by the orbit the global phase of the density matrix generates:

Using Eq. (18), we can state a similar statement for density operators. Supposing two (not necessarily normalized) sets of basis vectors $|\psi\rangle$ and $|\varphi\rangle$, we furthermore suppose that

$$\rho = \sum_i |\psi_i\rangle \langle\psi_i| = \sum_j |\varphi_j\rangle \langle\varphi_j|. \quad (32)$$

To find the conditions for when this is true, we decompose $\rho = \sum_k \lambda_k |k\rangle \langle k|$ with orthogonal states $|k\rangle$ and positive coefficients λ_k . But then we can deduce that

$$|\psi_i\rangle = \sum_k v_{ik} \sqrt{\lambda_k} |k\rangle \quad (33)$$

as well as

$$|\varphi_j\rangle = \sum_l w_{jl} \sqrt{\lambda_l} |l\rangle. \quad (34)$$

Combining Eq. (33) with Eq. (34), we immediately see that for a unitary matrix $u = vw^\dagger$ we have that

$$|\psi_i\rangle = \sum_j u_{ij} \sqrt{\lambda_j} |\varphi_j\rangle, \quad (35)$$

such that

$$\sum_i \lambda_i |\psi_i\rangle \langle\psi_i| = \sum_{i,j,k} u_{ij} u_{ik}^\dagger \sqrt{\lambda_j \lambda_k} |\varphi_j\rangle \langle\varphi_k| \quad (36)$$

$$= \sum_{jk} \left(\sum_i u_{ij} u_{ik}^\dagger \right) \sqrt{\lambda_j \lambda_k} |\varphi_j\rangle \langle\varphi_k| \quad (37)$$

$$= \sum_j \lambda_j |\varphi_j\rangle \langle\varphi_j|. \quad (38)$$

We conclude that two ensembles generate the same density matrix if and only if they are connected by a unitary transformation like that of Eq. (35).

7.2. Bloch sphere

One important representation of this phenomenon can be realized in two dimensions with the notion of the **Bloch sphere**. Although only illustrative in nature, it will help in understanding the very structure of the state space. Given a state in a superposition of basis states $|\Psi\rangle = \Lambda |0\rangle + \gamma |1\rangle$, we first remember that normalization demands that $|\Lambda|^2 + |\gamma|^2 = 1$. But then this condition is identical to Euler's identity $\sin^2 x + \cos^2 x = 1$, hence

$$|\Psi\rangle = e^{i\mu} \left(\cos \frac{\Theta}{2} |0\rangle + e^{i\varphi} \sin \frac{\Theta}{2} |1\rangle \right), \quad (39)$$

where μ , Θ and φ are real numbers. First we notice that since $e^{i\mu}$ is a global factor, it does not at all change the statistics of the state. Secondly, however, we realize

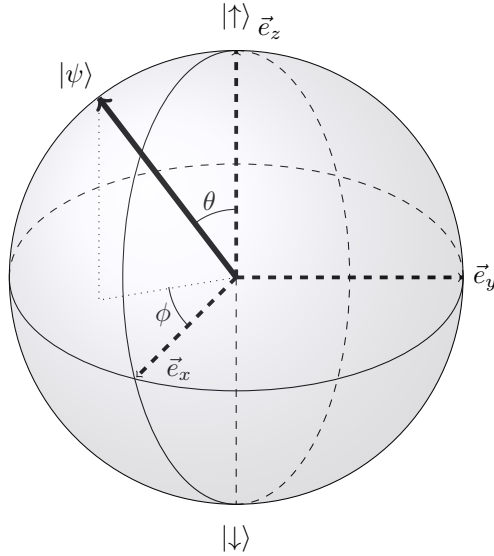


FIGURE 1. **The Bloch sphere.** The 2-dimensional state space of a qubit with basis states $|\uparrow\rangle = r$ and $|\downarrow\rangle = -r$ along the central axis. The convex hull is spanned by the polar decomposition (r, θ, ϕ) of the convex combinations $|\psi\rangle = \cos(\frac{\theta}{2})|\downarrow\rangle + e^{i\phi}\sin(\frac{\theta}{2})|\uparrow\rangle = \cos(\frac{\theta}{2})|\downarrow\rangle + (\cos\phi + i\sin\phi)\sin(\frac{\theta}{2})|\uparrow\rangle$.

that this parametrization of the state is like a unit vector on a 2-Sphere. We can see that the particular sphere is dual to the state space of a qubit, which as we have already seen, is $\mathcal{H} \cong \mathbb{C}^2$. With these tools we are able to draw the state, a vector in two dimensions, into the diagram of the state space in Fig. 1.

Notice that for pure states and the condition $\text{tr } \rho = 1$, the Bloch vector has unit length and is thus lying *on the surface* of the unit sphere while mixed states will lie within the volume. This has far-reaching implications using measure theory, i.e. mixed states are dense in the state space, while the pure states (again, up to unitary equivalence), are finite. However, in this examination we want to concentrate on representations for a moment. While it is already clear how to put a vector into the Bloch sphere, we can also find representations for density matrices. By means of writing

$$\rho = \frac{\mathbf{1} + \vec{r} \cdot \vec{\sigma}}{2}, \quad (40)$$

where \vec{r} is a three-dimensional vector with length $|\vec{r}| \leq 1$ and $\vec{\sigma}$ is the vector whose three components are the Pauli matrices

$$\sigma_0 = \begin{pmatrix} 1 & 0 \\ 0 & 1 \end{pmatrix}, \sigma_1 = \begin{pmatrix} 0 & 1 \\ -1 & 0 \end{pmatrix}, \sigma_2 = \begin{pmatrix} 0 & -i \\ i & 0 \end{pmatrix}, \sigma_3 = \begin{pmatrix} 1 & 0 \\ 0 & -1 \end{pmatrix}, \quad (41)$$

we can directly identify \vec{r} with the state ρ . Note that the indices $\{1, 2, 3\}$ are typically identified with the spatial directions $\{x, y, z\}$.

Unfortunately, the human brain is not good at imagining n -spheres for $n \geq 3$ (and most people, like the author of this dissertation, will have problems with $n = 3$ already), such that visualizations of higher-dimensional state spaces are hard to produce. Also, higher-dimensional convex hulls are in general not spherical. We will thus either come back to this picture and try to find ways to project them to a low-dimensional submanifold or refrain from giving a certain imaginable representation altogether.

7.3. No-cloning Theorem

Although algebraically simple, the impact of the no-cloning theorem by Wootters and Zurek [187] is even more important in quantum information than the uncertainty principle, because it touches the level of elementary computability: if a quantum state cannot be cloned, no measurement-based tomography can answer the question to a mixed state what its “real” coefficients were – we can only observe what (pure) state it became. Moreover, prohibited cloning means that we cannot use classical error correction in quantum communication.

THEOREM 4. *Suppose there are two identical Hilbert spaces \mathcal{H}_A and \mathcal{H}_B , with $|\Phi\rangle_A \in \mathcal{H}_A$. We also suppose that $|e\rangle_B \in \mathcal{H}_B$ is independent of $|\Phi\rangle_A$, i.e. the total state can be described as*

$$|\Psi\rangle_{AB} = |\Phi\rangle_A \otimes |e\rangle_B \quad \forall |\Phi\rangle_A \in \mathcal{H}_A. \quad (42)$$

There is no operation such that $\hat{O}(|\Phi\rangle_A \otimes |e\rangle_B) = |\Phi\rangle_A \otimes |\Phi\rangle_B$, unless $|e\rangle_B = |\Phi\rangle_B$, obviously.

Proof. *The only way we can ever hope to clone the system would be to apply a unitary $U = e^{-iHt} \in (\mathcal{H}_A \otimes \mathcal{H}_B)$, since we must not perform a (projective) measurement on $|\Phi\rangle_A$, because it would project the state into an Eigenstate. But this means that U cannot act in such a way for an arbitrary state in \mathcal{H}_A and hence*

$$\langle e|_B \langle \phi|_A |\psi\rangle_A |e\rangle_B = \langle e|_B \langle \phi|_A U^\dagger U |\psi\rangle_A |e\rangle_B = \langle \phi|_B \langle \phi|_A |\psi\rangle_A |\psi\rangle_B, \quad (43)$$

*which implies that either $\langle \phi|\psi\rangle = 1$ or $\langle \psi|\phi\rangle = 0$. By contradiction Wootters and Zurek concluded that pure quantum states cannot be cloned. Note that the result has been generalized to mixed states by the **Non-Broadcast Theorem** in [9]. ■*

Note that although rarely stated this way, product states, being separable, can be cloned just like classical states. But since the interesting parts of quantum mechanics cannot be performed with just product states, it is usually omitted in the conception of the no-cloning theorem as a no-go theorem.

7.4. Partial trace

By now we got a basic understanding of composite systems and why entangled states are the precise reason that composite systems cannot be described by the individual evolutions of its subsystems. We will now review properties of composite systems, further developing the understanding of the operational structure they feature.

First of all, we will introduce the *reduced density operator*. For a composite system $\rho_{AB} \in \mathcal{H}_A \otimes \mathcal{H}_B$ comprised of distinct, yet interacting physical systems A and B , we can define the reduced density matrix by

$$\rho^A = \text{tr}_B(\rho^{AB}). \quad (44)$$

This operation is known as taking the *partial trace*. In [127] it is defined as

$$\text{tr}_B(|a_1\rangle\langle a_2| \otimes |b_1\rangle\langle b_2|) \equiv |a_1\rangle\langle a_2| \text{tr}(|b_1\rangle\langle b_2|), \quad (45)$$

where $|a_1\rangle \neq |a_2\rangle \in \mathcal{H}_A$ and $|b_1\rangle \neq |b_2\rangle \in \mathcal{H}_B$. Note that there is the additional requirement that the partial trace is linear in its input, but since it is straightforward to see that this has to be the case unless one does not want to keep normalization of states on the respective Hilbert space, we will not comment on this. With this new tool, however, it is not *a priori* clear whether the result of a partial trace tr_B does imply any useful information about system A , but we will show that it produces the correct statistical measurements of the subsystem A . Looking at a product state $\rho_{AB} = \rho \otimes \mu$ first, we check that

$$\rho_A = \text{tr}_B(\rho \otimes \mu) = \rho \text{tr}(\mu) = \rho. \quad (46)$$

This is the expected result, because product states will just decompose into products when taking the partial trace. Now what about a state whose decomposition is not separable? A famous example is the so-called *Bell state*

$$\rho = \left(\frac{|00\rangle + |11\rangle}{\sqrt{2}} \right) \left(\frac{\langle 00| + \langle 11|}{\sqrt{2}} \right), \quad (47)$$

because it shows entanglement – a property we already talked about briefly. It does particularly mean that it cannot be decomposed into products of density matrices, hence

$$\rho_1 = \text{tr}_2(\rho) \quad (48)$$

$$\begin{aligned} &= \frac{1}{2} (\text{tr}_2(|00\rangle\langle 00|) + \text{tr}_2(|00\rangle\langle 11|) + \text{tr}_2(|11\rangle\langle 00|) + \text{tr}_2(|11\rangle\langle 11|)) \\ &= \frac{1}{2} (|0\rangle\langle 0| + |1\rangle\langle 1|) = \frac{\mathbb{1}}{2}. \end{aligned} \quad (49)$$

One of the most puzzling properties of this example is that, while ρ_{12} being a pure state, its components are mixed states, because

$$\text{tr} \left(\left(\frac{\mathbb{1}}{2} \right)^2 \right) = \frac{1}{2} < 1. \quad (50)$$

In other words, the composite state ρ is completely determined while both subsystems ρ_1 and ρ_2 are completely unknown.

7.5. Schmidt Decomposition

While the importance of Erhard Schmidt's work on linear algebra cannot be overstated in any way, especially the **decomposition** named after him will serve us dearly, because it enables a new view on composite systems that is vital in the later formulation of Finitely Correlated States and consequently Matrix Product States in Chapter 2. The statement goes as follows:

THEOREM 5. *Suppose Ψ is a pure state on a composite system $A \otimes B$. Then there exists a set of orthonormal basis vectors $|e_A\rangle \in A$ and another set of orthonormal basis vectors $|e_B\rangle \in B$ with equal properties, such that*

$$|\Psi\rangle = \sum_i \lambda_i |e_A\rangle |e_B\rangle, \quad (51)$$

with $0 \leq \lambda_i \in \mathbb{R}$ and $\sum_i \lambda_i^2 = 1$. The numbers λ_i are called *Schmidt coefficients*.

An important consequence of this observation is that for pure states of composite systems many properties of its constituents are identical until measurement as well. To see this, we can look at the decompositions

$$\begin{aligned} \rho_A &= \sum_i \lambda_i^2 |e_A\rangle\langle e_A|, \\ \rho_B &= \sum_i \lambda_i^2 |e_B\rangle\langle e_B| \end{aligned}$$

and readily check that the eigenvalues and Schmidt coefficients are identical for both systems. Note that for this property to hold there is no need to consider identical systems only. The Eigenvectors might have different interpretations, but we can be sure of the Eigenvalues by all means.

7.6. Purification

Entanglement can be somewhat puzzling, but we want to present an even more surprising property of non-separable states now: If a system \mathcal{H}_A is finite and embodies a mixed state ρ , we can always certify that there is a system \mathcal{H}_B and a pure state $|\Psi\rangle \in \mathcal{H}_A \otimes \mathcal{H}_B$, such that $\text{tr}_B(|\Psi\rangle\langle\Psi|) = \rho$. The basic idea in this case is, beneath positivity of the density operator, the Schmidt decomposition from above. While we already learned that for identical systems we will have identical Schmidt decompositions for a bipartition, a similar argument can be made for arbitrary systems. First observe that, of course, we can write

$$\rho = \sum_{i=1}^n \mu_i |i\rangle\langle i| \quad (52)$$

for some basis $\{|i\rangle\} \in \mathcal{H}_A$. If we now add some system \mathcal{H}_B (with some basis $\{|j\rangle\}$) and compose them as by a tensor product $\mathcal{H}_A \otimes \mathcal{H}_B$, we can write the total state as $|\Psi\rangle = \sum_i \sqrt{\mu_i} |i\rangle \otimes |i\rangle$ and prove by expanding the partial trace:

$$\begin{aligned} \text{tr}_B(\rho) &= \text{tr}_B(|\Psi\rangle\langle\Psi|) \\ &= \text{tr}_B \left[\left(\sum_i \sqrt{\mu_i} |i\rangle \otimes |i\rangle \right) \left(\sum_k \sqrt{\mu_k} \langle k| \otimes \langle k| \right) \right] \\ &= \text{tr}_B \left(\sum_{i,k} \sqrt{\mu_i \mu_k} |i\rangle \langle k| \otimes |i\rangle \langle k| \right) \\ &= \sum_{i,k} \delta_{ik} \sqrt{\mu_i \mu_k} |i\rangle \langle k| = \rho. \end{aligned} \quad (53)$$

Note that the purification need not be unique, since the decomposition of Eigenvalues into square roots is not either. This is usually not of practical interest, since the whole construction is virtual in the sense that the purified system $\mathcal{H}_A \otimes \mathcal{H}_B$ in general will not be of practical interest – for this reason many publications call it a reference system only – if we were to purify every mixed state we encounter, if a comment on this matter is allowed, we might as well wait for the universe to terminate to determine its (purified) wave function.

8. Entropy

To understand the supposed paradox of entanglement better, we will introduce the information theoretic measure of uncertainty, the quantity **entropy** introduced by C. Shannon in [157]. We will shortly review the classical side of things because it will be crucial in understanding both similarities and disparities of the Quantum approach to Information Theory. In classical terms, the uncertainty about any classical random variable X can be quantified in the following way.

DEFINITION 2. *Suppose that X be a classical random variable with associated probabilities $\{p_1, \dots, p_n\}$, then the expression*

$$H(X) = H(p_1, \dots, p_n) = \sum_x p_x \log p_x \quad (54)$$

*is called the **Shannon entropy** of X .*

By log we denote the logarithm to base 2, which can be considered “natural” as far as bits and qubits are concerned. An operational motivation for this quantity is that the entropy precisely gives the amount of bits needed for an optimal coding scheme, given we wanted to transfer information about a “source” X over some physical channel. This result, known as *Shannons noiseless coding theorem* is true

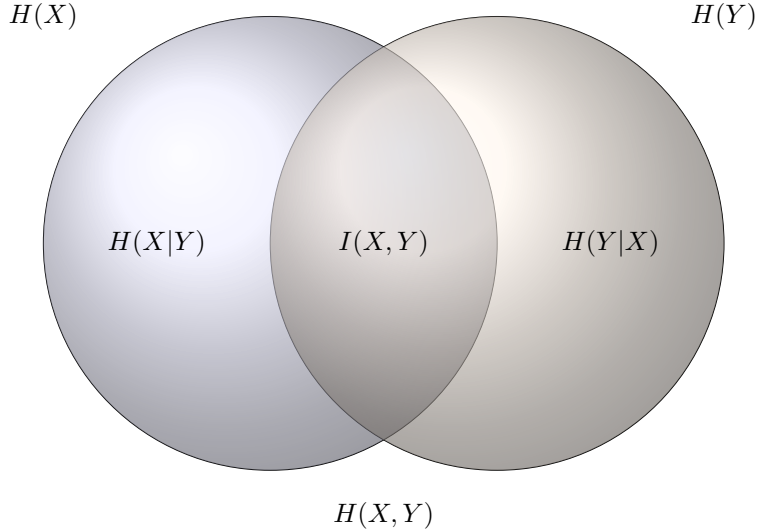


FIGURE 2. **Conditional entropy.** Entropy overview for two non-separable random variables: The blue and green circles stand for the entropies $H(X)$ and $H(Y)$ respectively, while the parts without the intersection give the conditional entropies $H(X|Y)$ and $H(Y|X)$. The central, overlapping part is the mutual information $I(X, Y)$ and both sets together form the joint entropy $H(X, Y)$.

for both classical and quantum channels and can be reviewed for example in [94], such that we may simply conclude that the Shannon entropy is a good measure of information, or, more precisely, uncertainty. If we are to use the somewhat foggy expression of “information” throughout this thesis, it will denote bits of certainty relative to some entropy measure. The close analogue of the smallest classical and quantum information units – bits and qubits – also gives rise to the analogue formulation of a quantum version of entropy [177].

DEFINITION 3. For a quantum ensemble ρ , we call

$$S(\rho) \equiv -\text{tr}(\rho \log \rho) \equiv -\sum_i \lambda_i \log \lambda_i \quad (55)$$

the **Von Neumann entropy** of ρ , whereas the λ_i denote the Eigenvalues of ρ .

We will not go into great detail why this analog is a good definition because one can explain a great deal about different approaches. In our case the quantum analog proved to be useful over time, and thus we might as well occupy ourselves with the *how*, while we refer to [5, 88, 103] for a more thorough discussion of the *why* and discuss some important elementary properties instead. Also, note that from now on we will only deal with Von Neumann entropies, and will thus use the term entropy exclusively for its quantum version.

8.1. Properties of the Von Neumann entropy

- (1) The entropy is non-negative. While this seems clear from the definition, note that it is zero if and only if the state is pure.
- (2) Conversely, the entropy is maximal for the completely mixed state: $S(\frac{1}{d}) = \log d$ with $\dim(\mathcal{H}) = d$.
- (3) Following from the Schmidt decomposition, we can see that for a composite system $\rho_{AB} \in \mathcal{H}_A \otimes \mathcal{H}_B$ we have that $S(\rho_A) = S(\rho_B)$.

8.2. Entropies of composite systems

Now we will explore the last statement a bit further. The implications of entropy behavior for composite systems will prove to be quite illuminating. First of all, note that one can show that $S(\rho \otimes \sigma) = S(\rho) + S(\sigma)$. This is of particular interest since we will often explore systems comprised of products. While this statement is not true for mixed states, it provides a solid starting point when using Matrix Product States that factorize, because it will give rise to so-called area-laws (see Section 2.1.2). There are a number of additional derivative properties worth discussing.

(1) **Joint entropy:**

$$S(A, B) \equiv -\text{tr}(\rho^{AB} \log(\rho^{AB})). \quad (56)$$

(2) **Conditional entropy:**

$$S(A|B) \equiv S(A, B) - S(B). \quad (57)$$

(3) **Mutual Information:**

$$S(A : B) \equiv S(A) + S(B) - S(A, B) = S(A) - S(A|B) = S(B) - S(B|A). \quad (58)$$

Please refer to Fig. 2 for a more pictorial representation of these statements. Also note that while the Shannon entropy expression $H(X) \leq H(X, Y)$ holds, this is not true for Von Neumann entropy. We can invoke the entangled Bell state $|\Psi\rangle = \frac{|00\rangle - |11\rangle}{\sqrt{2}}$ again to see that indeed $S(A, B)|_{\rho^{AB}} = 0$, since $|\Psi\rangle$ is pure, albeit its subsystems being maximally mixed, thus resolving $S(A|B)$ to being actually *negative*. One of the more prominent properties of the Von Neumann entropy is subadditivity [160]. Besides more exotic statements, the basic quantum analogue is the **Araki-Lieb inequality**:

THEOREM 6. *Also known as entropy triangle inequality, the theorem states that*

$$S(A, B) \geq |S(A) - S(B)|. \quad (59)$$

The proof is given in the original work by Araki and Lieb [6].

Its greatest benefit for us dealing with Matrix Product States will be that we can extract significant knowledge from observations of entropies of subsystems, which allows us to measure the entropy of small blocks of the system instead of the whole system at once, thus sparing the costly task of restoring the complete density matrix.

8.3. Monogamy of entanglement

Until now we defined entropy as a measure of information about a system. While this proposition will be sustainable throughout this thesis, we now will highlight that the implication that non-zero entropy necessarily means factual *lack of knowledge* is, in fact, not correct. The reason is, of course, quantum entanglement, and more specifically, its so-called monogamy [132]:

THEOREM 7 (Coffman, Kundu, Wothers). *Given three qubits A, B, C , one may quantify the correlations between the subsystems with some continuous entanglement measure $C_{U,V} \in [0, 1]$ that behaves like an entropy. For maximally entangled qubits A, B we have that*

$$C_{A,B}^2 + C_{A,C}^2 \leq C_{A,(BC)}^2. \quad (60)$$

The rigorous proof of the statement can be found in [25].

In other words, if two subsystems are maximally entangled, a third system can not share any more entanglement with the entangled systems. This is important because it clearly states that entanglement can be understood as a limited property of a system in its entirety, but also has to be considered for the subsystems at hand.

9. Spin

Despite its various intricacies, Quantum Spin is a simple natural toy model for dealing with logical qubits. We will first explain its basic properties and then explore how we can use it as a means to instigate somewhat practical Quantum Information.

When Otto Stern and Walther Gerlach found that (electrically neutral) silver atoms show a bipartite distribution after going through a specially prepared magnetic field [61, 62] that would only act on the atom's magnetic moments, it was one of the most surprising observations of 1922 and the then-young Quantum Theory. While it is widely considered impossible to directly undertake a Stern-Gerlach-like experiment with charged particles, it was subsequently deduced that the observed angular momentum could not be credited to the macroscopic momentum components of the silver atoms but established instead that there exist quantum particles bearing intrinsic momentum, called spin for discrimination. Some opinions have likened this to a current running in a loop, but although this seems like a good way to visualize angular momentum, spin does not have any electrical properties apart from magnetic coupling and shall thus, for the remainder of this work, be treated as a property of particles that behave like labels and act only on couplings, when they are engineered in that way.

This intrinsic quantized spin is one of the fundamental properties of elementary particles (albeit some of them bearing spin “0”, it is a property every particle has) and one of the most interesting degrees of freedom to explore, since its very particular coupling properties make it the perfect candidate for a logical qubit. There can be no doubt that spin itself is a profoundly interesting concept, but in this work we will humbly concentrate on its impact on Quantum Information. Before we can discuss applications, we have to learn about Lie algebras and the structure spins gives rise to.

First of all we will look at the most simplistic case – a spin- $\frac{1}{2}$ -system. Such a system, known as a *Fermion*, follows very peculiar rules. Its internal Hilbert space $\mathcal{H}_{\frac{1}{2}}$ is two-dimensional, because there are two basis vectors only, $|1/2\rangle$ and $|-1/2\rangle$, i.e. the measurement outcomes of the Pauli-z-matrix $\sigma_z = \begin{pmatrix} 1 & 0 \\ 0 & -1 \end{pmatrix}$. If we remember the Stern-Gerlach experiment, it seems opportune to repeat measurements in all three spatial directions. If one were to, say, perform *successive* measurements in both x - and z -direction, one would find that the spin property measurement cannot be performed with full precision – it is subject to the so-called **Heisenberg uncertainty relation** [181, 98]:

PROPOSITION 1. *Suppose there is a quantum state $|\Psi\rangle$ and two observables X and Y that have non-zero commutator $[X, Y]$. Then the deviations $\sigma_X = \sqrt{\langle X^2 \rangle - \langle X \rangle^2}$ and $\sigma_Y = \sqrt{\langle Y^2 \rangle - \langle Y \rangle^2}$ fulfill an inequality of the form*

$$\sigma_X \sigma_Y \geq \frac{|\langle \Psi | [X, Y] | \Psi \rangle|}{2}, \quad (61)$$

known as their uncertainty relation, where $\langle X \rangle^2 = |\langle \Psi | X | \Psi \rangle|^2$ refers to the evaluation with regard to $|\Psi\rangle$, thus uncertainty of observables is a relative measure depending on the state. Furthermore, it seems worthwhile to remind ourselves that we set $\hbar \equiv 1$, otherwise obscuring the usual way of presenting the lower bound of the inequality as $\frac{\hbar}{2}$.

Being one of the most well-known results of quantum mechanics, there exists an operational misconception about the uncertainty relation that mixes up uncertainty and “disturbance”. While we will not discuss the philosophical implications of the question whether there *is* such a thing as a (non-)disturb-able wave function,

we still feel the need to note that Heisenberg’s uncertainty principle itself actually makes no such claims. Without additional interpretational overhead, only a statistical interpretation, namely that for repeated measurements of X and a respective number of measurements on Y the ensemble average will satisfy the inequality, makes proper sense of the statement with regard to the present work.

Coming back to spin systems, we can check that indeed the set of Pauli matrices from Eq. (41) share mutually non-vanishing commutators:

$$[\sigma_0, \sigma_z] = 2\mathbf{i}\sigma_y; [\sigma_x, \sigma_y] = 2\mathbf{i}\sigma_z \Rightarrow [\sigma_i, \sigma_j] = 2\mathbf{i}\epsilon_{ijk}\sigma_k. \quad (63)$$

A basis of the vector space of 2×2 -matrices over \mathbb{C} , the Pauli matrices are most useful as we will see in all kinds of representations of spin systems. Note that σ_0 is not considered a Pauli matrix throughout most of the literature. Though, it is the missing piece in the orthogonal basis of the matrix vector space. The vector space they span is homomorphic to the group representation of $SU(2)$, which has a nice visualization: the Bloch sphere we already introduced.

10. Spins as logical qubits

We are now ready to explore the algebraic and operational properties of the spin. Whenever a physical system is two-dimensional, i.e. it is of the form $\mathcal{H} = \mathbb{C}^2$, whatever the physical realization, it can be mapped to a spin-1/2 and vice versa. The fundamentally invariant postulates of quantum mechanics allow to treat all two-dimensional systems alike, be it a vibration-coupled ion in a trap [17, 134, 14], a charge in one (or possibly more) quantum dot(s) [93, 106] or the spin of a laser-cooled molecule [139, 7]. For each of these realizations, all that matters is to find the suitable implementation of three operators: σ_z and the **ladder operators** S^+ and S^- . The ladder operators are defined by their action on the basis states, that will be explicitly denoted by $|+\rangle$ and $|-\rangle$ for spin systems. Depending on the implementation they might be identical to the logical states $|0\rangle$ and $|1\rangle$, but do not need to be:

$$S^+ |+\rangle = 0, \quad (64)$$

$$S^+ |-\rangle = |+\rangle, \quad (65)$$

$$S^- |+\rangle = |-\rangle, \quad (66)$$

$$S^- |-\rangle = 0. \quad (67)$$

As you can see they either “flip” the state of the spin or annihilate the state, which stems from the fact that “adding” a positive quantized momentum to a system where it already is maximal will result in no state at all – you cannot change the spin value beyond $-1/2$ and $1/2$. Note that although spin is quantized, we can speak of superpositions of basis states $|+\rangle$ and $|-\rangle$; of course it is feasible to write down a state of the form $|\Psi\rangle = \alpha|+\rangle + \beta|-\rangle$, and furthermore useful to adopt the ensemble interpretation that $\sigma_z |\Psi\rangle \in [-1/2, 1/2]$, where measuring a mixed state ensemble would result in values *between* the quantized basis states. Reciprocating from the interpretational intermission in Proposition 1, of course, this does not mean we will ever be able to see a spin with value -0.231 – but *on average* this is the outcome of the σ_z -measurement.

One can now argue that coupling two such spins is the minimal requirement to see actual physics happening, but we will skip this exercise and continue with the introduction of chains after taking a sidestep toward the second quantization formulation of quantum mechanics.

11. Second Quantization

While the investigation of spin ladder operators already sneakily introduced second-quantized operators, we wish to keep the bigger picture in scope and give a more thorough introduction to a concept foreign even to many physicists, although, contrary to somewhat popular belief, it is, of course, a tool to make things easier rather than more complicated. In the case of second quantization, Paul Dirac and his contemporaries were looking for a way to improve on the concept of particle exchange: Whereas in classical mechanics every particle has “a label” that identifies it with certainty, there are a priori indistinguishable particles in quantum mechanics, thereby giving rise to particle exchange symmetry. That is, if particles are identical, the physics must not change if we are to exchange particles. But in turn that means wave functions must be identical too:

$$|\Psi_B(\cdots, r_i, \cdots, r_j, \cdots)\rangle = + |\Psi_B(\cdots, r_j, \cdots, r_i, \cdots)\rangle \quad (68)$$

and

$$|\Psi_F(\cdots, r_i, \cdots, r_j, \cdots)\rangle = - |\Psi_F(\cdots, r_j, \cdots, r_i, \cdots)\rangle, \quad (69)$$

where the labels B/F mark bosonic and fermionic particles respectively. This is no problem as long as we act on a system without change of particles, but, in essence, this means that whenever a particle *is* created or annihilated, the wave function must be symmetrized or antisymmetrized to satisfy the constraint. Second Quantization offers a way out by adopting a different perspective: When asking for the number of particles, we can realize that this is a (both macroscopically and microscopically) measurable quantity, thus giving rise to a proper observable, for which we can, of course, pose the question what its Eigenstates are. It should be noted that this way of phrasing the fundamental observation of symmetry in quantum mechanics somewhat implicitly states the famous **Pauli exclusion principle** [135]:

DEFINITION 4. *It is impossible for two electrons of a poly-electron atom to have the same values of the four quantum numbers (n, l, m_l and m_s). For two electrons residing in the same orbital, n, l , and m_l are the same, so m_s must be different and the electrons have opposite spins.*

While stated for atomic occupation numbers, this was the basis for the many-body statistics later derived (independently) by E. Fermi and P. Dirac [50, 39]. It turned out [53] that the concept of Fock space is a very elegant answer. V. Fock defined it as a direct sum of tensor products of single-particle-spaces H such that

$$F_\alpha(H) = \bigoplus_{n=0}^{\infty} S_\alpha H^{\otimes n} = \mathbb{C} \oplus H \oplus (S_\alpha(H \otimes H)) \oplus (S_\alpha(H \otimes H \otimes H)) \oplus \cdots, \quad (70)$$

where F stands for the Fock space and S_α denotes the symmetrized or antisymmetrized states of two or more identical particles, α denoting whether we are dealing with bosons or fermions. Fock could subsequently prove for the completion of the direct sum that inner products of states on this space converge:

$$\langle \Psi_n | \Psi_n \rangle_\alpha = \sum_{i_1, \dots, i_n, j_1, \dots, j_n} a_{i_1, \dots, i_n}^* a_{j_1, \dots, j_n} \langle \psi_{i_1} | \psi_{j_1} \rangle \cdots \langle \psi_{i_n} | \psi_{j_n} \rangle, \quad (71)$$

$$|\Psi_\alpha|^2 = \sum_{n=1}^{\infty} \langle \Psi_n | \Psi_n \rangle_\alpha < \infty. \quad (72)$$

Returning to this hypothetical number operator, we can now write down its properties:

Given a pure state of n particles, a “good” way of parametrization seems to be to write down the decomposition into a product of states on the respective factors:

$$|\Psi\rangle_\alpha = |\phi_1, \phi_2, \dots, \phi_n\rangle_\alpha = |\phi_1\rangle |\phi_2\rangle \cdots |\phi_n\rangle. \quad (73)$$

It seems opportune to omit non-occurring states and instead of writing down a list of infinitely many zeros, decompose the state into a set of occupation numbers:

$$|[n_\alpha]\rangle \equiv |n_1, n_2, \dots, n_\alpha, \dots\rangle, \quad (74)$$

where the notion $[n_\alpha]$ naturally defines that there are n_α particles in the state $|\alpha\rangle$. A most educated question would be to ask whether this decomposition has to be of product form since we saw before that quantum mechanics allows for entanglement of pure states. Indeed, even for second quantization there can be found Fock-entangled states like the famous Schrödinger cat states [68], which should act as an operational hint that second quantization is a worthwhile concept, although naturally, for a theoretician the definitions suffice. It is still most fascinating that these predictions have already been implemented in the lab, up to ten-photon-entanglement [113] as recent as 2010. Furthermore we note that due to the aforementioned Pauli exclusion principle, no two Fermions can share the exact same state, such that

$$n_\alpha = \begin{cases} 0, 1 & \text{fermions,} \\ 0, 1, 2, 3, \dots & \text{bosons.} \end{cases} \quad (75)$$

We shall denote the case of no particles by $|0\rangle \in \mathbb{C}$, and is called the *vacuum state*. For completion of the space, it acts as the unit of the tensor product, i.e. $|0\rangle \equiv 1$.

11.1. Creation and Annihilation operators

Of course, changing perspective is not enough to justify the use of second quantization. It must resolve to practical use. This is given by the creation and annihilation operators, that automatically inhibit the symmetrization properties in demand.

Starting from the vacuum state $|0\rangle$, we demand that for all $n > 0$, applying a certain operator a^\dagger should add a particle to the state:

$$a^\dagger |n\rangle = \sqrt{n+1} |n+1\rangle, \quad (76)$$

whereas its adjoint a should remove it:

$$a |n\rangle = \sqrt{n} |n-1\rangle. \quad (77)$$

Repeated application allows to reach arbitrary particle numbers:

$$a^{\dagger n} |0\rangle = \sqrt{n!} |n\rangle. \quad (78)$$

We furthermore observe that for (identical) bosons there is a *canonical commutation relation*

$$[a^\dagger, a] = 1, \quad (79)$$

while for (identical) fermions, we have the *canonical anti-commutation relation*

$$\{a^\dagger, a\} = 1. \quad (80)$$

For different particles α, β we always have that $[a^\dagger_\alpha, a_\beta] = 0$.

Since every subspace of occupation numbers is finite, the states $|n\rangle, |m\rangle$ can be normalized such that $\langle n, n \rangle = 1, \langle n, m \rangle = 0 \forall n \neq m$ and

$$a^\dagger a |n\rangle = n |n\rangle, \quad (81)$$

where we call $\hat{n} = a^\dagger a$ the number or particle count operator.

Note that while some publications consequently denote operators by the hat symbol $\hat{\cdot}$, we will only denote operators in such a way where confusion is likely.

It is precisely the relation in Eq. (81) that also proves that indeed the Fock states are eigenvalues of the number operator but is a both semantically and didactically moot point whether one should introduce the Eigenvalue relation as the basic assumption of second quantization or consequence of the exchange principle. In the end, it should be clear that this is an elegant way to rephrase many-body systems, i.e. pragmatically speaking, if it is of use, we shall not bother too much about its genesis.

Correlated Spin Systems and its Dynamics

Supposed we could control quantum systems individually, such that each of them had a logical representation $|+\rangle/|-\rangle$ that could be treated as a single spin. Although a historic perspective on this question will tell you that it indeed is *difficult* to achieve this, small chains of dozens of spins can be addressed with today's experimental realizations [63, 40]. The natural question is, how the theoretical treatment of such systems looks like. While this thesis will become more detailed in the following chapters, we aim to give an overview of spin chains here such that the jump to the results sections will not be overly discontinuous.

1. Spin Lattices

When it comes to the question of highlighting suitable toy models, physicists never tire to come up with simpler, yet more generic systems. However, one can hardly argue that in terms of accessibility the spin chain can be matched. Moreover, spin lattices are a well-established testbed for quantum computational approaches [117, 155] as well as being realizable in the lab with relative ease – if one can ever speak of such a thing regarding the manipulation of single quantum particles at all. We may now familiarize ourselves with the notion of a lattice. Most abstractly spoken, a lattice is any collection of quantum systems that can be ordered by some geometric or graph-theoretic rule. As such, although we will limit ourselves to chains and their Cartesian products, one can easily imagine more intricately structured systems. Figure 3 shows some basic examples of lattice configurations. But how can one describe those systems mathematically?

First of all note that we can take a naive, albeit constructive approach and notice that for each individual system we can describe an individual Hilbert space \mathcal{H}_n . Note furthermore that while the total number of elements of the lattice might be infinite, we demand that it be still countable in the set-theoretic sense. One can give all kinds of theoretical reasons for this, but at the heart of a numerical method lies the fact that we want to make predictions about some fraction of the physical world, thus accepting that using classical computers for this endeavor, both our representation and knowledge will necessarily remain finite. There is a point to be made about allowing infinite local Hilbert spaces, but we want to keep in mind that in principle everything we are about to explore should one day be replicated in a lab, every experimentalist will concur that, although academically existent, infinite local dimensions are of little practical relevance unless someone manages to create tools of infinite precision – a thing we already ruled out in Chapter 1. Thus, we will be speaking of lattices with possibly infinite spatial extension, but finite local dimension.

The most abstract description is probably that of a **direct sum** of the local Hilbert spaces, or mathematically more precise: a co-product of vector spaces for that matter: The Hilbert space of a quantum lattice can be given as

$$\mathcal{H}_{lattice} = \bigoplus_{n=1}^N \mathcal{H}_n, \quad (82)$$

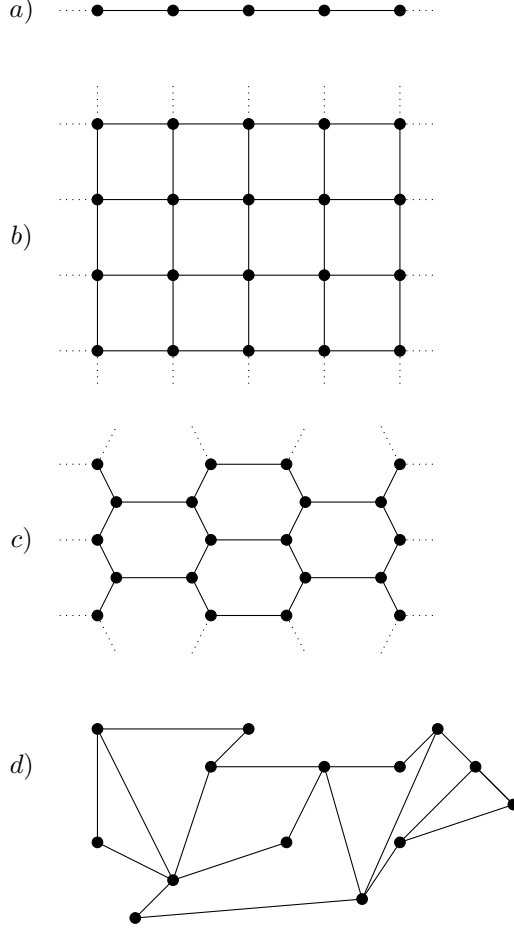


FIGURE 3. **Exemplary lattice configurations.** a) One-dimensional lattice with next-neighbor edges. b) (Two-dimensional) square lattice. c) Honeycomb lattice: vertices are connected in a hexagonal pattern. d) Irregular lattice: without translation invariance, this example is that of an arbitrary graph.

where the generating operation of the co-product $\mathcal{H}_{full} = \mathcal{H}_1 \oplus \mathcal{H}_2$ is

$$|\Psi\rangle \oplus |\Phi\rangle, \quad (83)$$

where $|\Psi\rangle \in \mathcal{H}_1$ and $|\Phi\rangle \in \mathcal{H}_2$ are vectors on their respective spaces “glued together” by writing their components as one large vector:

$$|\Psi\rangle = \begin{pmatrix} \Psi_1 \\ \Psi_2 \\ \vdots \\ \Psi_N \end{pmatrix}, |\Phi\rangle = \begin{pmatrix} \Phi_1 \\ \Phi_2 \\ \vdots \\ \Phi_M \end{pmatrix} \Rightarrow |\Psi\rangle \oplus |\Phi\rangle = \begin{pmatrix} \Psi_1 \\ \Psi_2 \\ \vdots \\ \Psi_N \\ \Phi_1 \\ \Phi_2 \\ \vdots \\ \Phi_M \end{pmatrix}, \quad (84)$$

where $\dim \mathcal{H}_1 = N$ and $\dim \mathcal{H}_2 = M$.

Note the structural difference to the tensor product: While $\dim(\mathcal{H}_1 \otimes \mathcal{H}_2) = \dim \mathcal{H}_1 \cdot \dim \mathcal{H}_2$, for the direct sum the dimension of the resulting space is the sum of the dimensions of its factors: $\dim(\mathcal{H}_1 \oplus \mathcal{H}_2) = \dim \mathcal{H}_1 + \dim \mathcal{H}_2$.

It is vital to understand that in contrast to the tensor product, which is the correct physical representation $\bigotimes_n \mathcal{H}_n$ of the coupled system, the direct sum merely acts as an abstraction layer to allow for orderly treatment of *local* operations of sites that are independent – whenever we perform physics on more than one lattice site, the dynamics governing coupling of lattice subsets follow the tensor structure and operators acting on more than one site are of the form $O = O_1 \otimes O_2 \otimes \cdots \otimes O_N$ as introduced in Eq. (3) on page 9. Since the numerical treatment of the exponentially growing dimensions of the tensor product is complicated, we will have to use methods suited to this challenge and shall start by introducing Finitely Correlated States to see how Matrix Product States came to life and can be of use.

2. Finitely Correlated States

One particular ansatz for this seemingly self-contradictory task has been invented by Fannes, Nachtergaele and Werner [48, 49] in 1992 and 1994 respectively. Their approach basically aimed at an efficient representation of valence bond states, but as we will see, its use ultimately extends far beyond that initial scope.

Since the original definitions are proposed in the language of C*-algebras of (possibly) infinite systems, we refer to the well-known textbook [15] by Bratteli and Robinson for the basic definitions. Deep understanding of this section is not necessary for the following work, but will subsequently highlight the emergence of the Matrix Product Formalism that we use extensively.

Throughout their work on Finitely Correlated States (FCS), Fannes, Nachtergaele and Werner base their approach on the chain algebra $\mathcal{A}_{\mathbb{Z}} = \bigotimes_i \mathcal{A}_i \in \mathbb{Z}$, with identical C*-algebras on each site. Note that there is no geometry “present” at this stage of the definition. Their idea then basically resolves to the concept of an ancillary vector space \mathcal{B} that is used to model the correlations between all the different bonds of the chain.

Together with the definition of $\mathcal{A}_{\mathbb{Z}}$ a state can subsequently be reconstructed by a map $e : \mathcal{A} \otimes \mathcal{B} \rightarrow \mathcal{B}$ and two elements (notation by FNW) $\rho \in \mathcal{B}^*$ and $e \in \mathcal{B}$. They make a point that for spin chains this can be restricted to a finite vector space and the proposition that e, ρ, e be positive in the C*-algebraic sense. They already prove that the class of C*-finitely correlated states is a **weakly dense convex subset of the set of translation invariant states*, pointing out that this will make it a useful tool for translation invariant states. They subsequently use their class of states for the calculation and construction of ground states of translation invariant systems, but do not pursue the idea of time evolution. Before introducing ways of efficient approximate time evolution, we will have to see how to transform a family of states with finite correlation into a truly variational class.

2.1. Entanglement and Correlations

We briefly introduced the notion of entanglement in Chapter 1, but to really grasp its implications we need to apply the quantum information tools to composite systems, like spin chains. With the research on lattice systems, physicists are always eager to test the quantum nature of single particles. While this is, without a doubt, interesting in its own regard, it seems even more worthwhile to ask for genuine quantum properties of the systems, not its constituents. Apart from the von Neumann entropy there are other measures of entanglement, such as the **concurrence** [141]. While they are intrinsically different, the qualitative statements are equal. How can we tell that entanglement is more than a random correlation? The answer lies in the differentiation of correlations into classical and explicitly quantum parts. Of

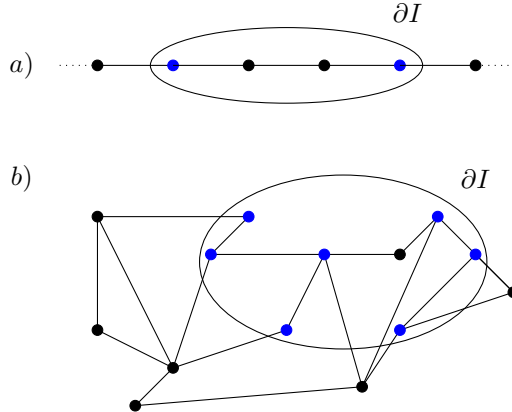


FIGURE 4. **Boundary of a sublattice.** ∂I is given by the blue nodes of the graph, because they share edges with nodes from *outside* the sublattice. a) One-dimensional lattice. b) Two-dimensional, non-regular example. Note that only one of the sites in the set I does not belong to its boundary, because of the geometry of the set.

course quantum systems can (and for the most part, do) exhibit classical correlations, but the subtleties and wonders of this construction are quantum in nature. To see this, we will quickly look at correlation inequalities of the Bell-type.

2.1.1. *Bell Inequality.* John Bell’s seminal work [91] addressing the famous Einstein-Podolski-Rosen paradox [43] essentially proved that quantum mechanics indeed is complete in the sense that neither are there (local) hidden variables necessary to describe “reality”, nor does the wave function necessarily represent a physically “real” object. While we note, again, that it is not the scope of this work to address the philosophical implications of this observation, it lies very well in our interest what the mathematical implications are. To this end, we will straightaway concern ourselves with the generalization of Bell’s argument, commonly known as CHSH inequalities referring to John Clauser, Michael Horne, Abner Shimony, and Richard Holt’s work from 1969 [24]. In it, they devise the following gedankenexperiment: Given a bipartite quantum system $\mathcal{H}_A \otimes \mathcal{H}_B$ with bipartite measurement outcomes, i.e. measurement of A results in either a or a' with equal probability and measurement of B results in either b or b' , they propose the following measure of correlation:

$$-2 \leq S \leq 2, \quad (85)$$

where

$$S = E(a, b) - E(a, b') + E(a', b) + E(a', b') \quad (86)$$

and of course, $E(a, b) = \delta_{ab}$ for a single measurement. Like Bell for his version of the proposition, they also show that there are sets of events where this bound can be violated by quantum mechanics, but by no means by classical probability theories. We will not give a derivation of the proof because it is not the central theme of this work, but nevertheless the finding that quantum mechanics, i.e. specifically quantum entanglement, give rise to a unique form of fundamentally different correlations is what sparks our interest. We have seen before how entanglement can be expressed as linear combinations of non-separable states of composite systems. Since entanglement is such a fundamental quantity of quantum mechanics, we need to be able to understand its impact on many-body systems, if we are to subject them to dissipation that potentially changes the correlation behavior of the system.

2.1.2. *Area laws.* One of the deeper insights into quantum spin systems comes from the understanding of entanglement and its limitations, namely of the fact that it is subject to monogamy. The fact that two maximally entangled states do, under no circumstances, share entanglement with another system, is the foundation of area laws. Heuristically, we consider the following situation: Assume a set of qubits on a plane, for simplicity, each interacting with neighboring spins only, i.e. an unordered many-body system. Equipped with nothing else but the knowledge about entanglement monogamy, we conclude that if the number of spins is finite, so must be the total amount of entanglement on the graph that is formed by mapping qubits to vertices and next-neighbor-interactions to edges. Indeed, we can see that this is true iteratively (see Fig. 4): Moving along the graph, we attribute maximal entanglement to any pair we encounter. Now, while depending on the graph geometry there might be vertices that cannot be maximally entangled with their neighbors because all of them already have a partner, we can *count* the number of maximally entangled pairs in a finite region of dimension d and, following [44], observe that the entropy of that set L must be

$$\overline{S(\rho_I)} = |I| \log(d) - \frac{d^{|I|-|O|}}{2 \log(2)} \quad (87)$$

for an arbitrary inner set $I \subset L$ and its outer complement $O = L \setminus I$, which is a *volume law* really, because it is linear in the number of particles. This is what one would expect from a set of (thermal) random states because there is no a priori ordering applied. The boundary of a one-dimensional subset of a one-dimensional system necessarily consists of only the sites that define the boundary, i.e. w.l.o.g., we can assume that the boundary consists of exactly one or two site(s), depending on the fact whether we look at periodic or open boundary conditions of the lattice:

$$\partial I = i \in I : \exists j \in L \setminus I \quad \text{with} \quad \|i, j\| = 1, \quad (88)$$

where i and j denote the position of the vertices. An area law for this region then clearly must have the form

$$S(\rho_I) = \mathcal{O}(1). \quad (89)$$

It has been shown (see e.g. [130, 175, 174]) that this is the case for many of the spin systems we are interested in, if they have a gapped Hamiltonian (see Section 3.7 for remarks about criticality). It seems opportune to stress some nomenclature at this point: Different publications do have different terms for the two things addressed here as boundary and inner structure. Although the mathematical term boundary (or surface) is usually more precise in the topological sense, we will also speak of the edges and the bulk of a system whenever practical considerations are to be included. The reason for this is that physical systems do not care about set-theoretic properties. You cannot observe the part of the system that is in the ε -ball of the surface. All we can see in the lab is whether the behavior is different when there are approximately the same order of neighboring sites in both directions of the observed spatial dimension versus the case where there are not.

This property is of vital importance for numerical methods in order to be able to understand the time scales on which (dissipative) processes happen. Area laws bound the correlation transport between particles that do not directly interact, i.e. especially for extended systems we have to keep in mind that not only interaction strength plays a role, but also the question how fast information propagates through the bulk of the lattice.

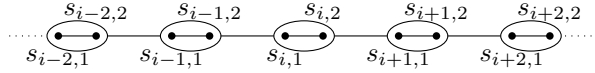


FIGURE 5. **Valence bond theory.** One virtual lattice site consists of two atoms with one unpaired electron each. Either one of the two spins in such a bond then interacts with one of the spatial nearest neighbors, such that the resulting lattice has alternating pairs of spins connected physically and virtually.

3. From FCS to MPS

While Finitely Correlated States have proven their ability to model spin-lattice ground states, the aim of this work, and much that came before it, was to allow for a more intricate look at the physical properties of such systems, like phase transitions and approximate dynamics. FCS are a powerful and general tool, but lack a straightforward way of restricting oneself to finite systems with very specific demands – simply because their purpose lies in the thorough treatment of infinite systems.

If we are to model actual physical models, it will prove to be hard, if not outright impossible, to tell an effortfully engineered logical qubit to unify all correlation properties of an infinite C*-algebra in its behavior – which is not to say that the FCS constructions does not have its merits – albeit, for real systems with real caveats we will need to be able to look at finite systems with finite boundary conditions.

First of all, note that there are different ways of motivating Matrix Product States. We will try to give a coherent picture with FCS in mind but might refer to additional material where a general survey seems appropriate. Indeed, it seems remarkable from a mathematician’s point of view that the way Matrix Product States came into fruition was *not* through generalization, but rather a reduced application of it – in [137], Cirac et. al. use the FCS theory as a basis to construct a specific, *finite* structure out of it. We shall see how they approached this:

They consider N spins on a “ring”, i.e. a one-dimensional lattice with periodic boundary conditions. Then one can adopt what is called the valence-bond construction: With each site we identify *two* (virtual) spins of momentum quantization $1/2$, i.e. internal dimension $d = 2$. This theory is based on the observation [31] that certain molecules form bonds based on overlapping atomic orbitals, thus pairing the effective wave functions of their respective electrons.

Looking at Fig. 5, we can identify one of each site’s two parts as a *bond* with their respective neighboring site, coupled by a tensor product, turning the product of dimension d^2 into an entangled bond:

$$|I\rangle = \sum_{\alpha=1}^d |\alpha, \alpha\rangle. \quad (90)$$

Instead, analogously to the FCS, a map is applied to every site of the lattice:

$$\mathcal{F} = \sum_{i=1}^N \sum_{\alpha, \beta=1}^d A_{i, \alpha, \beta} |i\rangle \langle \alpha, \beta|, \quad (91)$$

where α and β correspond to the virtual systems. Cirac et. al. then write A_i for the whole tensor $A_{i, \alpha, \beta}$ by contracting around the virtual indices and subsequently observe that in terms of a product basis, the components of the lattice state are

given by the matrix product

$$\text{tr}(A_{i_1} A_{i_2} \cdots A_{i_N}). \quad (92)$$

It is straightforward to see how to obtain the complete state, again following [137] in the convention that with the introduction of $A_i^{[k]}$, these being matrices of dimension $d_m \times d_{m+1}$ with $d_1 = d_{N+1} = 1$, we can write

$$|\Psi\rangle = \sum_{i_1, \dots, i_N=1}^d \text{tr} [A_{i_1}^{[1]} A_{i_2}^{[2]} \cdots A_{i_N}^{[N]}] |i_1, i_2, \dots, i_N\rangle. \quad (93)$$

This construction is called a **Matrix Product State** (MPS) and we shall notice that it is neither normalized nor unique and subsequently proceed to illustrate basic properties and applications.

3.1. Explicit MPS examples

Before being able to present the systems we investigated, let us briefly familiarize ourselves with the formalism of Matrix Product States.

3.1.1. *GHZ state.* One of the most prominent, yet sufficiently simple examples is the famed **Green-Horne-Zeilinger state** [67]

$$|\text{GHZ}\rangle = \frac{1}{\sqrt{2}} (|000 \dots 0\rangle + |111 \dots 1\rangle), \quad (94)$$

i.e. a system of length N and internal dimension $d = 2$ in the computational basis $\{|0\rangle, |1\rangle\}$. The natural choice of bond dimension is $D = 2$, since it can be easily seen that the Schmidt rank of every bipartition is bounded by 2 and the matrices of the product are

$$A_i^{[0]} = \begin{pmatrix} 1 & 0 \\ 0 & 0 \end{pmatrix}, A_i^{[1]} = \begin{pmatrix} 0 & 0 \\ 0 & 1 \end{pmatrix}. \quad (95)$$

It seems opportune to note that although the state is maximally entangled according to most entanglement measures, the MPS representation is strikingly simple.

3.1.2. *W state.* In the zoo of useful toy states, the **W state** [41] $|W\rangle = |100\rangle + |010\rangle + |001\rangle$ is kind of an antagonist of the GHZ state $|000\rangle + |111\rangle$. While the latter will decay into nonentangled pure states $|00\rangle$ or $|11\rangle$ upon measurement of one of its subsystems in the computational basis, the W state will leave its bipartite entanglements undisturbed. This more complex correlation structure is somewhat mirrored in the MPS representation: For an exact representation we have to choose $D \geq 2$ and find

$$\begin{aligned} A_1^{[0]} &= \begin{pmatrix} 1 & 0 \\ 0 & 1 \end{pmatrix} & A_1^{[1]} &= \begin{pmatrix} 0 & 0 \\ 1 & 0 \end{pmatrix} \\ A_2^{[0]} &= \begin{pmatrix} 1 & 1 \\ 1 & -1 \end{pmatrix} & A_2^{[1]} &= \begin{pmatrix} \frac{1}{2} & 0 \\ 0 & \frac{1}{2} \end{pmatrix} \\ A_3^{[0]} &= \begin{pmatrix} 1 & 0 \\ 0 & 1 \end{pmatrix} & A_3^{[1]} &= \begin{pmatrix} 0 & 0 \\ 1 & 0 \end{pmatrix} \end{aligned} \quad (96)$$

In this representation, we can see very clearly the entanglement structure: Each set of decompositions has one matrix with only one entry (thus entangling two subsystems) and one with two entries, that entangles all three subsystems. With this structure in mind, we can understand that a single measurement does not collapse the entanglement between non-measured subsystems, but will decrease the total entanglement of the system: If, for example, we look at the density operator

of the system before and after measurement, we can see that

$$\begin{aligned}
\text{tr}_3(|W\rangle\langle W|) &= \text{tr}_3(|100\rangle\langle 100| + |100\rangle\langle 010| + |100\rangle\langle 001| \\
&\quad + |010\rangle\langle 100| + |010\rangle\langle 010| + |010\rangle\langle 001| \\
&\quad + |001\rangle\langle 100| + |001\rangle\langle 010| + |001\rangle\langle 001|) \\
&= |10\rangle\langle 01| + |10\rangle\langle 10| + |01\rangle\langle 10| + |01\rangle\langle 01| + |00\rangle\langle 00| \\
&= 2[(|10\rangle + |01\rangle)(\langle 10| + \langle 01|)] + |00\rangle\langle 00|,
\end{aligned} \tag{97}$$

no matter the outcome of the measurement. It is precisely this robustness against *particle loss* that makes $|W\rangle$ one of the most interesting prototypes for Quantum Computation and Quantum Communication, whenever the entanglement is to be used as a resource, e.g. in entanglement distillation schemes [69, 70].

Lifting this argument to larger systems, we can understand why it is important not to limit the bond dimension of an MPS too much: Multipartite entanglement will result in higher Schmidt rank than bipartite entanglement. Thus, we would lose out on important physical correlation properties, if the variational class of the MPS is too narrowly chosen. (For this property, see Section 4.1 of Chapter 3.)

3.2. Properties and applications of MPS

First of all notice that we can realize *any state* in the way Eq. (93) details, if only the bond dimensions D are sufficiently large. Cirac et. al. thus correctly note that this is only then a useful characterization of a class of states once one bounds the bond dimension from above. It is also clear that MPS will only ever be useful in a computational perspective if we can ensure that such a truncation does not destroy too much information.

3.2.1. *Expectation values.* In order to illustrate the advantage of the MPS construction, we first explain how to calculate expectation values.

For an operator in product form, say, $O = \otimes_{n=1}^N O_n$, where O_n acts on a single site only, i.e. locally, expectation values are efficiently computable:

$$\overline{\langle \Psi[A] | O | \Psi[A] \rangle} = \text{tr} [E_{O_1}(1) E_{O_1}(1) \cdots E_{O_N}(N)], \tag{98}$$

where the superoperators $E_{O_i}(i)$ are, following Haegemann et.al. [73], defined like this:

$$E_O(i) = \sum_{\alpha, \beta=1}^D \langle \alpha | O | \beta \rangle \left(A^\beta(i) \otimes \overline{A^\alpha(i)} \right). \tag{99}$$

The operator O can be understood as acting on the virtual (ancillary) indices of the MPS, contracting the ancilla space of $\mathbb{C}^{D_n} \otimes \mathbb{C}^{D_n}$ with effective range $n - 1$. The superoperator in turn is a second-order tensor in A , thus inhabiting dimensions $\mathbb{C}^{D_{n-1}^2} \otimes \mathbb{C}^{D_n^2}$. When we speak of “efficiency” though, you have to keep in mind that the whole expectation evaluates in $\mathcal{O}(D^6)$, although Haegemann et. al. have demonstrated optimizations to $\mathcal{O}(D^5)$ by exploiting the tensor structure. The correct figure of comparison, of course, is inverting the density matrix of the complete product space, which scales, as we know, exponentially in D . We will see in Theorem 8 how we can calculate expectations even more efficiently depending on the boundary type of the system.

3.2.2. *MPS from slightly entangled states.* Another way of introducing MPS has been established by G. Vidal in his work on *Slightly Entangled States* [176], i.e. many-body systems with limited quantum correlations. We will not discuss the relation to finitely correlated states in detail and instead point the reader to the fact that this particular ansatz comes from computational considerations: The aim of Vidal’s research was to prove that pure states with restrictively bounded entanglement can be simulated efficiently. Yet, it is remarkable that the construction he proposes can

be easily rephrased in terms of an MPS as follows: Consider a system of qubits with states $|0\rangle$ and $|1\rangle$. Invoking the Schmidt decomposition again, we can see that one such state $|\Psi\rangle \in \mathcal{H} = \mathbb{C}^{2^N}$ can be written as

$$|\Psi\rangle = \sum_{i_1=1}^1 \sum_{i_2=1}^1 \cdots \sum_{i_N=0}^1 c_{i_1 \dots i_N} \bigotimes_{j=1}^N |i_j\rangle, \quad (100)$$

where the coefficients are defined as

$$c_{i_1 \dots i_N} = \sum_{\alpha_1, \dots, \alpha_{N-1}} \Gamma[1]_{\alpha_1}^{i_1} \lambda[1]_{\alpha_1} \Gamma[2]_{\alpha_1 \alpha_2}^{i_2} \lambda[2]_{\alpha_2} \cdots \Gamma[N]_{\alpha_{N-1}}^{i_N}. \quad (101)$$

Here, $\lambda[l]$ contains the Schmidt coefficients of the bipartition $[1l] : [(l+1)n]$. By contraction in either direction over the virtual indices, i.e. $\lambda \leftrightarrow \Gamma$ or $\Gamma \leftrightarrow \lambda$ one obtains Eq. (93). This also nicely illustrates that there is some freedom in the choice of matrices, a thought we briefly mentioned before. We will explore the *gauge freedom* of the MPS formalism more detailed in Chapter 3.

Vidal subsequently showed that this construction can be found for all pure states, although it is not always an *efficient representation*. We shall see why this is the case.

If we look at the definition of $c_{i_1 \dots i_N}$ and the fact that there is a sequence of N sums in the definition of the state, it should become apparent that Vidal makes a Schmidt decomposition at every bond of the chain, sweeping from one side to the other this way. Starting at site 1, he sets

$$|\Psi\rangle = \sum_{\alpha_1} \lambda[1]_{\alpha_1} |\phi[1]_{\alpha_1}\rangle |\phi[2 \dots n]_{\alpha_n}\rangle, \quad (102)$$

such that every Schmidt vector for site 1 is now expanded in some computational basis $\{|\phi\rangle\}$. Iterating this scheme $N-1$ times yields the MPS of Eq. (100). To understand the computational complexity, we can check each decomposition's Schmidt rank. We calculate the maximal Schmidt rank

$$S_\chi = \log_2(\max \text{rank}(\Gamma)) \quad (103)$$

and infer that if and only if this quantity is bounded by $\mathcal{O}(\log N)$ the representation scales polynomially in N , making this a viable computational scheme. Also, notice that we just used the Schmidt rank as an entanglement witness in the sense that observing Schmidt rank larger than one means the state is non-separable. We will later see why this is important when we try to represent mixed states, where this circumstance is particularly annoying.

3.2.3. Connection to DMRG. One of the most striking advantages of the MPS picture is that it can explain the success of the **density matrix renormalization group (DMRG)** better than its original conception was able to explain. A scheme for studying one-dimensional many-body systems (much like we will do in the following chapters, albeit without dissipation) [183, 182], for a long time its practical use was apparent [138], while a solid and complete theoretical justification could not be given, until it became clear that it can be considered a variational method in the realm of MPS representations.

As an aside, it is one of the more ironic instances of science, that the sheer realization of how the two methods are interconnected conjured up unrest among DMRG-inclined people – since DMRG was there “before”, they feel that traditionally speaking the MPS formalism should be subsumed under the DMRG framework, albeit generalizing it to some extent. We will not burden ourselves with the politics of nomenclature and simply explain how things fit together. It is our hope that

although sometimes hurt by the incongruence of seemingly contradictory nomenclature and definitions it will be possible to find a comprehensive view about the matter of numerical variational methods in Quantum Information.

Created for finding ground states of systems with zero temperature, DMRG at its heart is a variational method that works by iteratively putting sites together to “blocks” that can be diagonalized for certain conditions. Using deliberate reduction of the state space truncating less probable degrees of freedom, one can show [156] that this method is more useful for ground state problems than it is for time evolution. As we proceed to explain this in detail, we will also directly notice the limitations.

Consider a lattice of N sites again. The idea is to constructively generate the “full” Hilbert space by adding sites to an initial block in the following way: We start with a block $[B]$ comprised of $n \ll N$ sites. For this block, we can readily give its ground state by diagonalization of the Hamiltonian H . For the first iteration step, the basis is explicitly known and we can proceed to add sites. This is performed by taking a similar block $[B']$ at the other side of the chain and adding two sites in between, such that the resulting scheme is $[B \ a \ B']$. While in principle the total state space would be the tensor product of its factors, DMRG imposes additional conditions to reduce the state space, like demanding total spin equal to zero if the spin in the previous iteration step was zero, thus truncating all states with non-zero spin components. Although it is clear that we have to be careful about this, especially if the system could have phase transitions regarding spin, in general, we observe that this is a reasonable ansatz. Next step in one iteration process is to diagonalize again using Lanczos [110] or Davidson [35] sparse algorithms. It is crucial to decide how many basis vectors are kept, e.g. the ground state for sure and several excited states might prove to be better than the ground state alone. Then the density matrix for the block $[B \ a]$ is reconstructed and $[a \ B']$ is considered as a thermal heat bath for this matter. Again, we keep the largest, thus most probable eigenvectors and truncate the rest. With the reconstructed density matrix we have effectively calculated the new block $[B_{\text{new}}] \hat{=} [B \ a]$ and can start the next iteration. A pictorial explanation of this process is given in Fig. 6.

This scheme is explained in much more detail in, e.g. [156] and we shall see how this compares to matrix product states. First of all note that while the construction above is the most common way of formulating DMRG, one can indeed replace the two intermediate vectors $[aa']$ and replace them by one: $[\tilde{a}]$. When following this path one can show that for ground states this is exactly equivalent to a (variational) MPS method, as long as there are no excitations involved, in this particular case the fixed truncation error of DMRG costs dearly, while an MPS will simply have higher Schmidt rank and, albeit being computationally less efficient due to higher bond dimensions, can at least represent an excited state. For a comprehensive treatment of the comparison at hand, see again [156]. What this section should emphasize, however, is that for any problem there might be different methods with different benefits and drawbacks. We will later discuss the intricacies of dissipative dynamics in certain methods, and for that matter it will prove useful to have some basic understanding of the tools at hand. To this end, we shall discuss one more such tool.

3.3. The canonical form

When we mentioned that the state in Eq. (93) is not unique, this comment was in anticipation of this section because it is one of the greatest strengths of the MPS formalism.

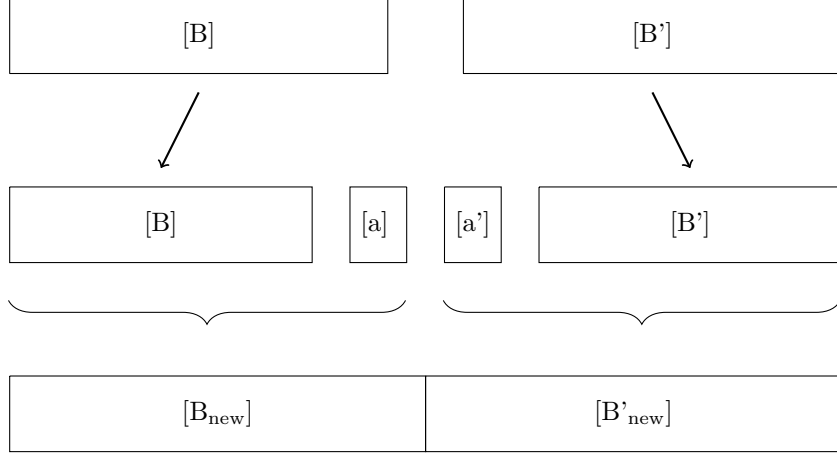


FIGURE 6. **DMRG iteration scheme.** In the first step, the half-chain block [B] is diagonalized to find its approximate ground state. Afterward, a smaller block [a], comprised of one site (and possibly, but rarely more sites), is added at the center of the total chain. The superblock [B a] then is treated as the new block [B_{new}]. The dual [B'] is used to either model a heat bath coupling or for providing proper boundary conditions in case of finite length.

The usual way of showing this is by example: If we consider the transformation

$$A[i]^{s_i} \longrightarrow X[i]A[i]^{s_i}X[i+1]^{-1}, \quad (104)$$

we can easily see that it does not alter the state if A is normal and X is non-singular. Following [176] again, we recall that Eq. (93) can be considered in terms of open boundary conditions (OBC) if the outermost matrices are vectors, i.e. $D_1 = D_{N+1} = 1$. Vidal then proved the following set of statements, that are more comprehensively stated in [137]:

THEOREM 8 (Completeness and canonical form). *Any state $\Psi \in \mathbb{C}^{d^{\otimes N}}$ has an OBC-MPS representation of the form*

$$|\Psi\rangle = \sum_{i_1, \dots, i_N} A_{i_1}^{[1]} A_{i_2}^{[2]} \dots A_{i_{N-1}}^{[N-1]} A_{i_N}^{[N]} |i_1 \dots i_N\rangle \quad (105)$$

with bond dimension $D \leq d^{\lfloor N/2 \rfloor}$ and the following holds:

- (1) $\sum_i A_i^{[m]} A_i^{[m]\dagger} = \mathbb{1}_{D_m} \quad \forall 1 \leq m \leq N$,
- (2) $\sum_i A_i^{[m]\dagger} \Lambda^{[m-1]} A_i^{[m]} = \Lambda^{[m]} \quad \forall 1 \leq m \leq N$,
- (3) $\Lambda^{[0]} = \Lambda^{[N]} = 1$ and each $\Lambda^{[m]}$ is a $D_{m+1} \times D_{m+1}$ diagonal matrix which is positive, full rank and satisfies $\text{tr} \Lambda^{[m]} = 1$.

Although we will not replicate the full proof, we may sketch the reasoning: Considering Eq. (104), we can see that we can reorganize the statement such that it reads as

$$A_i^{[m]} A_j^{[m+1]} = \left(A_i^{[m]} X \right) \left(X^{-1} A_j^{[m+1]} \right). \quad (106)$$

Iterating Schmidt decompositions as we are already familiar with, we can start from either the left or the right to end up with a state that is unique up to permutations

and degeneracies in the Schmidt decomposition, while the $\Lambda^{[m]}$ are now diagonal and contain the Eigenvalues of the reduced density operator $\rho_m = \text{tr}_{m+1, \dots, N}(|\Psi\rangle\langle\Psi|)$.

To wrap this section up, we will give the full conditions on the canonical form depending on whether we sweep from left or right. For the right-canonical form, we demand that

$$\sum_{s_i} A[i]^{s_i} (A[i]^{s_i})^\dagger = \mathbb{1}, \quad (107)$$

$$\sum_{s_i} (A[i]^{s_i}) \Lambda[i] (A[i]^{s_i})^\dagger = \Lambda[i-1], \quad (108)$$

while the left-canonical form imposes

$$\sum_{s_i} (A[i]^{s_i})^\dagger A[i]^{s_i} = \mathbb{1}, \quad (109)$$

$$\sum_{s_i} (A[i]^{s_i})^\dagger \Lambda[i-1] A[i]^{s_i} = \Lambda[i]. \quad (110)$$

As a last note to this section, we did not mention periodic boundary conditions so far. While technically very similar to open boundary conditions, bearing one extra term, we will see in Section 4.1 of Chapter 3 that this will make it hard to simply apply a sweep-through algorithm that acts on one site (or two neighboring sites, for that matter), because we might get a recursion conflict at the edge of the chain.

3.4. Translation invariance

While being close to finitely correlated states, it sometimes seems strange to first narrow our view such that we can understand the concept of open boundary conditions, implicitly concerned with finite lattices, before we can generalize the concept back to periodic boundary conditions again – in short, systems that are similar to FCS, albeit also finite in representation and simulation.

Also, the difference from the algebraic point of view is indeed very simple – just make every operator act translation-invariantly – but complicated from a computational perspective: It is not a priori clear whether we can lift the canonical form to this case, but we shall see how we can solve this.

First of all, it is a priori clear that a state Ψ given as an MPS with identical Schmidt decompositions for all bipartitions, i.e. the $A[i]$ s being equal, $A[i] = A[1] \forall i$, exhibits translation invariance. But neither does it prove whether the converse is true, nor, equally interesting from a computational perspective, how to obtain such a form, and whether it is canonical or at least comparable to the canonical form. To make a statement about this, we refer to [137], specifically their Theorem 3:

THEOREM 9. *Every translation-invariant pure state with periodic boundary conditions (PBC) on a finite chain has an MPS representation with site-independent matrices $A_i^{[m]} = A_i$, i.e.,*

$$|\Psi\rangle = \sum_{i_1, \dots, i_N} \text{tr}(A_{i_1} \dots A_{i_N}) |i_1 \dots i_N\rangle. \quad (111)$$

If we start from an OBC MPS representation, to get site-independent matrices one has (in general) to increase the bond dimension from D to ND (note the N -dependence).

Proof. Since the proof is both constructive and instructive, we will replicate it. We start from an MPS with open boundary conditions as defined in Eq. (93)

and define matrices of dimension $N \cdot D$ for $0 < i < d - 1$:

$$B_i = N^{-\frac{1}{N}} \begin{pmatrix} 0 & A_i^{[1]} & & & & \\ & 0 & A_i^{[2]} & & & \\ & & \ddots & \ddots & & \\ & & & 0 & A_i^{[N-1]} & \\ A_i^{[N]} & & & & & 0 \end{pmatrix}. \quad (112)$$

We can now answer what MPS this is equal to:

$$\begin{aligned} & \sum_{i_1, \dots, i_N=0}^{d-1} \text{tr}(B_{i_1} \dots B_{i_N}) |i_1, \dots, i_N\rangle & (113) \\ &= \frac{1}{N} \sum_{j=0}^{N-1} \sum_{i_1, \dots, i_N=0}^{d-1} \text{tr}(A_{i_{1+j}}^{[1]} \dots A_{i_{N+j}}^{[N]}) |i_1, \dots, i_N\rangle, & (114) \end{aligned}$$

where $i_j = i_{j-N}$ if $j > N$ – which in turn states, using the fact that the latter is by construction translation-invariant, it is equal to Eq. (111). ■

As an easy example we can again use the N -dimensional W state $|W\rangle = \frac{1}{\sqrt{N}} (|1 \dots 0\rangle + |01 \dots 0\rangle + \dots + |0 \dots 1\rangle)$. We recall that for open boundary conditions the optimal bond dimension is $D = 2$, but this is of course, not sufficient to represent a translation-invariant MPS. Appendix 1 of the aforementioned work by Perez-Garcia et.al. also proves that there is no TI representation with smaller bond dimension than $(N \cdot D)$.

3.5. Gapless and frustration-free Hamiltonians

Before starting the investigation of more complex many-body models, some more preparations are in place. In ?? we briefly mentioned the observation that for infinite systems the Hamiltonian will have (in one or the other way) an infinite amount of Eigenvalues. Of course, in a mathematical sense these are rather points in a continuous spectrum. Depending on the question whether this bulk of states arises, like for an atom, above some excitation threshold or, worse, near the ground state, the analysis of a system can become much more complicated, culminating in the observation that a system can be *gapless* altogether, i.e. without energy gap between ground state and first excited state.

There are two important points to mention here. First, we have to understand that, since we want to work on finite chains, the arguments given by Fannes, Nachtergaele and Werner in [48] for the existence of a uniquely determined finitely-correlated ground state do not apply anymore. Still, understanding systems without a gap is important because, as we will see, in reality many systems of practical importance are gapped, but the energy threshold is so small that with numerical accuracy of approximate systems (i.e., apart from direct diagonalization) it looks (and hence, behaves) gapped. This point was first observed by Perez-Garcia, Verstraete, Wolf and Cirac in [137] and solved by the concept of parent Hamiltonians.

A parent Hamiltonian is a Hamiltonian that is constructed to be gapped as well as close to the original Hamiltonian – it basically tries to capture the physics of the gapless system without sacrificing too much of its intricacies. While certainly perceived as “reverse engineering”, the fact that one always has the option to look at the result and refuse it can be seen as a first, albeit formally crude way of variational ansatz. But before discussing its implications, we shall see what the construction looks like.

First of all we observe the *inverse problem*: for any given MPS $|\Psi\rangle$ we can construct a Hamiltonian that has $|\Psi\rangle$ as its ground state, simply because we can create the trivial case of engineering a matrix in a canonically extended basis containing $|\Psi\rangle$ as Eigenvector with the lowest Eigenvalue in its diagonalization. Of course, this does not necessarily capture physical systems, and so have to come up with a non-trivial scheme that perturbs the original Hamiltonian in a way that does not change its properties *much*. Perez-Garcia et.al. use the property of block-injectivity for this matter, a proposition that can as well be traced back to the seminal papers already known: [48, 137]. We first informally state that an MPS can be brought into standard form when blocking sites together: Suppose we have that $A_{j_k} \equiv A_{i_{2k-1}} A_{i_{2k}}$. Then we can quote the following theorem from [51]:

THEOREM 10. *After blocking, any MPS can be written in a standard form where the matrices A_i have the following properties:*

- (1) *The A_i are block-diagonal: $A_i = \bigoplus_{j=1}^D A_i^j \otimes \Gamma_j$ where $A_i^j \in \mathcal{M}_{l_j}$ (the space of $l_j \times l_j$ matrices) and the Γ_j are positive diagonal matrices from Eq. (101).*
- (2) *The A_i span the space of block-diagonal matrices: $\text{span}_i A_i = \bigoplus_{j=1}^D \mathcal{M}_{l_j} \otimes \Gamma_j$.*
- (3) *For all j and for all A^j denoting the MPS tensor defined by the submatrices A_i^j , the map $\varepsilon_j := E_{A^j}$ has spectral radius one, with 1 as the unique eigenvalue of modulus 1, and with eigenvectors $\varepsilon_j(\mathbf{1}) = \mathbf{1}$ and $\varepsilon_j^*(\Lambda_A^j) = \Lambda_A^j$, where $\Lambda_A^j > 0$, $\text{tr}(\Lambda_A^j) = 1$, where $E_A^B : X \mapsto \sum_i A_i X B_i^\dagger$ is a map from left to right indices and vice versa.*

*Property 2 with every $\Gamma_j = 1$ is called **block-injectivity**; in particular, if $D = 1$, and $\Gamma_1 = 1$, A is called *injective*.*

Given a tensor $(T_i)_{\alpha\beta}$ with virtual indices α, β and a physical index i , we define the span of T as

$$\text{span}\{T\} := \text{span} \left\{ \sum_i \text{tr}[T_i X] |i\rangle |X \in \mathcal{M}_D \right\},$$

with another projector corresponding to T , $\Pi[T]$ being the orthogonal projector onto $\text{span}\{T\}^\perp$.

Regarding one or more tensors as a block, the authors of [51] write $T = A \overset{\circ}{\leftarrow} A$, such that

$$\text{span}\{A \overset{\circ}{\leftarrow} A\} = \text{span} \left\{ \sum_{i,j} \text{tr}(A_i A_j X) |i, j\rangle |X \in \mathcal{M}_D \right\}.$$

Note that the tensors need not be next neighbors from the right hand side of the relation alone, but will nevertheless be by virtue of the plausibility of the physical indices where we want neighbors to be neighbors, avoiding problematic unraveling conditions for e.g. higher spatial dimensions. This helps us to define the actual property we are looking for:

DEFINITION 5. *Let $|\Psi(A)\rangle$ be a block-injective MPS and let*

$$h_{i,i+1} = \Pi[A \overset{\circ}{\leftarrow} A]$$

be a block representation. Then we call $H = \sum_i^N h_{i,i+1}$ the parent Hamiltonian.

The authors also show that this construction is robust enough to ensure the gap is not closed in the thermodynamic limit.

3.6. AKLT model

While the previous examples are illuminating from an abstract point of view, we want to increasingly concentrate on many-body systems as our main subject. One of the most important and easily accessible models is the so-called **Affleck-Kennedy-Lieb-Tasaki state**, which is the unique ground state of the AKLT Hamiltonian [1, 2, 47]

$$H = \sum_i S_i S_{i+1} + \frac{1}{3} (S_i S_{i+1})^2. \quad (115)$$

The model deals with spin-1 particles, but that statement is misleading in the sense that we will show that the AKLT state is constructed from composed spin-1/2 systems. The idea is then to use the symmetrized triplet states

$$\begin{aligned} |+\rangle &= |\uparrow\uparrow\rangle, \\ |1\rangle &= \frac{|\uparrow\downarrow\rangle + |\downarrow\uparrow\rangle}{\sqrt{2}}, \\ |-\rangle &= |\downarrow\downarrow\rangle \end{aligned} \quad (116)$$

with total spin $S = 1$ for the internal degrees of freedom while the bonds are described by the singlet state

$$|0\rangle = \frac{|\uparrow\downarrow\rangle - |\downarrow\uparrow\rangle}{\sqrt{2}}. \quad (117)$$

We shall now proceed to see how the AKLT model can be encoded into a $D = 2$ -MPS. For this matter we define two vectors, $|\varphi\rangle = |\varphi_1, \dots, \varphi_N\rangle$ and $|\mu\rangle = |\mu_1, \dots, \mu_N\rangle$ representing the two spins per site. Together with a matrix K that mediates the interaction between neighboring sites,

$$K = \begin{pmatrix} 0 & \frac{1}{\sqrt{2}} \\ -\frac{1}{\sqrt{2}} & 0 \end{pmatrix},$$

we can now compose this a state

$$|\Psi_K\rangle = \sum_{\varphi} \sum_{\mu} K_{\mu_1 \varphi_2} K_{\mu_2 \varphi_3} \dots K_{\mu_N \varphi_1} |\varphi \mu\rangle \quad (118)$$

that has periodic boundary conditions. If we want to cut the chain open, we just remove the first matrix of the expression. While this is not the formal expression in “AKLT-language”, it should sufficiently illuminate the fact that it can indeed be expressed as an MPS. It will be interesting to see the similarities with the Heisenberg model, which we introduce in Section 3.8. Although not identical, we can formulate the hypothesis that Heisenberg chains, unless frustrated, can be approximated well by Matrix Product States.

3.7. Criticality

The second objection to the applicability of generic FCS is in its semantic nature similar to the argument brought up in Section 3.5, but different in the sense that it arises from a variational argument based in Quantum Complexity Theory called **criticality**. It is not an uncommon observation that critical systems are in general not gapped (and the question whether they are is even undecidable [32]), but we will approach the subject from a different angle: In a classical Heisenberg chain of spins that are either up- or downward oriented, we can observe situations where a site can become frustrated, which can e.g. be described by an ansatz like this:

$$\mathcal{H} = \sum_G -t_{i,j} S_i \cdot S_j, \quad (119)$$

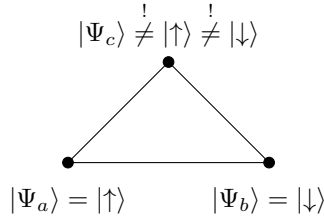


FIGURE 7. **Frustrated system.** Given a system of three mutually connected sites of qubit dimension representing spin orientation, it is easy to show how to geometrically frustrate that system. With the proposition that neighboring spins should, by action of the system Hamiltonian H , align anti-parallel, this can obviously not lead to a self-consistent ground state for the depicted graph.

where G is the graph topology of the lattice under consideration, t is the coupling strength between to sites i and j and $S_{i/j}$ representing the inner product of the spin algebra in question, which can be of Pauli-type $\{\sigma_x, \sigma_y, \sigma_z\}$, if the spin values are $|1/2\rangle$ and more complex angular momentum operators for more complex systems.

Also, see Fig. 7 for a pictorial explanation how we can easily create very basic systems that already possess geometrically frustrated spin configurations.

Different conditions demand mutually exclusive spin configurations. Starting from a randomly ordered lattice configuration we would like to undergo dynamics that subsequently place the lattice in its ground state, whether at zero temperature or above. One can show [161] that depending on the parameters of coupling and magnetic field term adiabatic cooling [164, 82] and other dynamics may converge to energies not at all near the ground state. It was particularly the realization that this effect can occur in reasonably interesting systems that led to the exploration of robust methods to circumvent this numerical challenge.

It seems particularly noteworthy that this very effect seems to be interconnected with all kinds of computational problems [90]: Without invoking exotic epistemic arguments it is already interesting to see that the emergence of frustrated systems in nature goes along with strikingly simple ways of mathematically describing their structure (albeit not their solutions, obviously). In other words: If a thing as simple as a 2-dimensional Heisenberg chain can be frustrated, it seems also opportune to imagine much more complicated systems in chemistry, biology or of even more macroscopic scale frustrated in certain logical degrees of freedom. However, recent research indicates that noise represented as perturbations [3] can lead to regularizing effects on Hamiltonians. Although the ansatz presented in the cited article above is not directly connected to our research, it acts as a firm hint that noise acts as a computational resource in the sense that it can be used to actually increase the amount of certainty in critical systems, i.e. decrease its entropy.

In fact, recently it was shown [66] that indeed frustrated and non-frustrated Hamiltonians show stark differences in their scaling behavior: Somewhat expectable, the aforementioned reference establishes that the correlation length of a system is bounded as a function of the spectral gap.

3.8. Heisenberg model

Systems of Heisenberg-type are arguably among the most well-studied models in the world of physics, yet exhibit a so rich variety of phenomena, that research can hardly be categorized as finished – it is a simple truth that its structure allows for both simplistic ansatzes that describe basic quantum mechanics as well as very

complex systems depending on the focus of research. Studying basic magnetic properties, they can be used to abstract many-body localization, magnetic properties of semiconductors and their phase transitions and even rudimentary ansatzes of molecule-folding.

The overarching assumption is that neighboring spins (of value $1/2$) minimize the energy by aligning anti-parallel, thus giving rise to Hamiltonians of the form

$$H = -J \sum_{j=1}^N \sigma_j \sigma_{j+1} - h \sum_{j=1}^N \sigma_j, \quad (120)$$

where J is the interaction strength of the spins and h is the (constant) magnetic field. Despite the naïve interpretation of strictly momentum-coupled spins, in an experimental realization of the model the couplings J need not strictly be 1, for example in optical lattices. Also, it can, of course, be different when the dynamics of a different, albeit closely related system are to be mapped onto a Heisenberg-type model.

As is widely known, systems of this type are solved in one dimension by the Bethe ansatz [11]. Since the Time-Dependent Variational Principle can solve it as well this is more of a historical marginalia: We will use analytics where available to verify numerical procedures but will also notice where we venture into the uncharted territory of non-integrable systems. Before introducing the variational methods at our disposal, we shall proceed to explain the general Heisenberg model. In three spatial dimensions, it takes the form

$$H = -\frac{1}{2} \sum_{j=1}^N (J_x \sigma_j^x \sigma_{j+1}^x + J_y \sigma_j^y \sigma_{j+1}^y + J_z \sigma_j^z \sigma_{j+1}^z + h \sigma_j^z), \quad (121)$$

where the couplings J_x, J_y, J_z can be mutually different, which gives rise to the number of complex phenomena this model allows to study. Also, since the Hamiltonian acts on the Hilbert space given by $(\mathbb{C}^2)^{\otimes N}$, it exhibits $2^N - 1$ degrees of freedom – a scaling that we know becomes hard to simulate with exact methods for as little as 4 sites.

There are two important special cases worth mentioning. On the one hand, we can simplify the Hamiltonian to a form like

$$H = -J_z \sum_{j=1}^N \sigma_j^z \sigma_{j+1}^z - g J_x \sum_{j=1}^N \sigma_j^x \quad (122)$$

that is called the **one-dimensional Ising model**. Among the first spin systems studied, it was solved in 1921 by Ernst Ising in his dissertation after Wilhelm Lenz proposed it as a suitable topic [86]. Ising (somewhat implicitly) showed that there is no phase transition, although the thermodynamic theory of criticality was in its infancy at best and it took twenty more years until Lars Onsager solved the two-dimensional case [129, 12], in which a phase transition can be found. Despite its seemingly simple structure, the Ising model certainly inspired physicists to sharpen their theoretical tools to be able to solve more complex variations of its theme. It was later shown that the three-dimensional Ising model does not exhibit an analytical solutions [46], but can be tackled with numerical methods only, like molecular field approximations in the Landau theory [111, 154] or Monte Carlo simulations [142, 115].

In the case that $J = J_x = J_y \neq J_z$, on the other hand, the system is called an **XXZ-Heisenberg chain**. It is considerably less complex than the case $J_\alpha \neq J_\beta \forall \alpha, \beta \in \{x, y, z\}$ but still features many more properties worth exploring in

comparison to Ising-type systems. In Section 1 of Chapter 6 we will study such an XXZ ansatz as well.

If the couplings J_α are positive, we expect ferromagnetic behavior, whereas negative coupling privileges anti-ferromagnetic behavior in more than one dimension. Research of this particular ground states gave rise to another adaption of the model, namely the models by Hubbard et al., as we present in the next section.

3.9. Hubbard model

Proposed by John Hubbard in 1963 [83], this model of second quantized particles is the most influential abstraction in solid state physics dealing with phase transitions between conducting and insulating phases.

$$H = -t \sum_{\langle i,j \rangle, \sigma} (c_{i,\sigma}^\dagger c_{j,\sigma} + c_{j,\sigma}^\dagger c_{i,\sigma}) + U \sum_{i=1}^N n_{i\uparrow} n_{i\downarrow}, \quad (123)$$

where the sum consequently is over neighboring sites and the c s are the second-quantized creation and annihilation operators as shown in Section 11 of Chapter 1.

3.9.1. *Jordan-Wigner transformation.* In the next chapter, we will review and expand the Time-Dependent Variational Principle acting on Matrix Product States, usually stated for spin lattices. Since we want to treat Fermi-Hubbard models as well in Chapter 7, it seems opportune not to try and reinvent the wheel for this kind of structure. An observation from Eugene Wigner and Pascual Jordan from the 1920's proposed a transformation between spin-1/2-lattices and its second quantization [92] – obviously not with the way we utilize it in mind because it was three decades prior to the formulation of the Hubbard model. Nevertheless, it proves robust enough to allow effortless conversion of models whenever the tools or numerics demand it. Suppose we look at a chain of spin 1/2 particles, then we already know that they obey the canonical anti-commutation relation in Eq. (79):

$$\{\sigma_i^+, \sigma_i^-\} = 1, \quad \{\sigma_i^+, \sigma_i^+\} = 0 = \{\sigma_i^-, \sigma_i^-\}. \quad (124)$$

It seems opportune to try and presume whether they also obey these relations for *different* lattice sites $i \neq j$, but in fact we easily check that they do not:

$$[\sigma_i^+, \sigma_j^-] = 0 = [\sigma_i^+, \sigma_j^+] = [\sigma_i^-, \sigma_j^-]. \quad (125)$$

However, Jordan and Wigner have shown how to restore the commutation relation by adding a phase factor depending on the previous lattice sites:

Suppose that

$$c_i = e^{i\phi_i} \sigma_i^- \quad \text{with} \quad \phi_i = \pi \sum_{j<i} \sigma_j^+ \sigma_j^-, \quad (126)$$

then we can check the commutators again:

$$\{c_i, c_j^\dagger\} = \delta_{ij}, \quad \{c_i^\dagger, c_j^\dagger\} = 0 = \{c_i, c_j\}, \quad (127)$$

because we observe that

$$e^{i\pi \sigma_i^+ \sigma_i^-} = e^{i\pi n_i} = 1 - 2n_i, \quad (128)$$

where $n_i = \sigma_i^+ \sigma_i^-$, directly analogous to Eq. (81) from Chapter 1. That means that within the scope of the Jordan-Wigner transformation next-neighbor-interacting spins can indeed be treated as fermions.

Before putting this useful armory of second-quantized knowledge to use in Chapter 7 about applications of the Fermi-Hubbard model, we finally can explain how variational methods help in numerically calculating approximate solutions to computationally difficult problems.

Variational Ansatzes in numerical Many-body Physics

Ever since realizing that Matrix Product States prove to be efficient representations of certain classes of quantum states, it has been an obvious question how one could exploit the representational symmetry not only to find ground states but for questions regarding dynamics (i.e., time evolution) as well. This chapter aims to give an overview of the state of the art both regarding the method of choice in this thesis (the Time-Dependent Variational principle) as well as highlighting benefits and drawbacks of comparable methods, among them tools we already mentioned, such as DMRG and Matrix Product Operators as well as methods specifically suited for the simulation of dynamics, such as Variational Monte Carlo.

1. The variational principle

While we, among many physicists alike, will imply that the time-independent variational method is a specific, albeit general, method of finding solutions to a number of physical and mathematical problems alike, in truth it is not so much a method but the basic mathematical observation that extremizing a suitable function that encodes the relevant information about the problem at hand can yield insights to that problem, sometimes even solving it straightaway, i.e.

$$\delta I(x, \delta x) = 0, \tag{129}$$

where we can observe that for $I = \int \mathcal{L} dt$ we obtain a classical Lagrangian.

Of course, we are not the first to observe this property [118, 45, 89]. Much earlier, Fermat's principle both variationally solves a specific problem as well as it is an application of 'the' variational principle, just like the principle of least action in classical mechanics is.

In quantum mechanics there is an important distinction between the time-independent [89] and time-dependent version [60], as we will see. That is for two reasons. First of all, time does not behave like a standard observable [180, 153], thus it cannot (easily) be subject of variation as a degree of freedom. Secondly, and due to the first, physicists over and over find that static problems are easier to solve most of the time. Historically, the variational method was known from the very beginnings of quantum mechanics, while the *Time-Dependent* Variational Principle took some 50 years to become of interest. It seems wrong to imply that 'it was not there' before, since quantum mechanics did not change to allow the principle to emerge, but rather directions of research, in particular Quantum Information, needed to evolve into a state where questions would be raised that could not be answered without generalizing the Variational Principle to include time. That is, questions of time evolution as well as the observation that including time into static variational calculations can be beneficial were not addressed as detailed as the TDVP allows before powerful computers became the common tool of research. Although the main part of this dissertation solely relies on the time-dependent variational principle, it seems prudent to treat its ancestor in detail as well. We

will also see how the time-independent variational principle gives rise to DMRG and its derivatives.

1.1. Derivation

While the most general perspective on variational methods would be to really start from the original principle of least action and how it ties in with Lagrangian mechanics, we will not address this part of science history, but focus on quantum mechanics instead. Regarding notation, we will follow a nomenclature close to [72].

Here, we have basically only one option, i.e. using basic spectral theory that assures that for every physical system (i.e. one that can be treated using a Hamiltonian operator), we have a ground state, and as such, a lower bound on the energy expectation:

$$E^{(0)} \leq \frac{\langle \Psi | H | \Psi \rangle}{\langle \Psi | \Psi \rangle}, \quad (130)$$

where $E^{(0)}$ is the ground state energy corresponding to the smallest Eigenvalue. For some variational ansatz $|\Psi(z)\rangle$ with variational parameters z , we can directly see that

$$H(\bar{z}, z) = \frac{\langle \Psi(\bar{z}) | H | \Psi(z) \rangle}{\langle \Psi(\bar{z}) | \Psi(z) \rangle} \quad (131)$$

serves as a template for variational minimization of the ground state energy within some variational manifold \mathcal{M} , i.e. the linear span of $\Psi(\bar{z}, z)$ for all $\bar{z}, z \in \mathbb{C}$. We can clearly see that a priori this need neither be the whole Hilbert space, nor a particularly physically sound class, albeit being valid in the sense that we can check its normalization and existence in the respective Hilbert space. If we so choose, it is certainly easy to find variational classes that do not approximate the ground state in question at all. As with all variational methods it will be inevitable to spend some time on an educated guess before blindly applying the method.

As a side-remark we shall generally assume throughout this thesis that any variational class be holomorphic in \bar{z} and z or whatever the variational parameters are called. Note that this assumption does not change any result w.l.o.g., but will prevent complicated terms of mixed dependency to show up.

Returning to the time-independent variational method, we can now ask the question what kind of condition can be imposed such that we can certify a “good” approximation. We observe that certainly

$$\begin{aligned} \frac{\partial}{\partial z_i} H(\bar{z}, z) &= 0, \\ \frac{\partial}{\partial \bar{z}_i} H(\bar{z}, z) &= 0 \end{aligned} \quad (132)$$

characterizes an optimum regarding the derivative of the variational class, this being close to a gradient method. Whether the solution one finds is robust with regards to *other* physical properties however remains to be seen. Also, we will make use of the shortcut $\partial_i = \frac{\partial}{\partial z_i}$ and declare use of Einstein’s summation convention $a_i b^i \equiv \sum_i a_i b^i$ unless otherwise noted.

Once a ground state candidate is obtained with satisfying accuracy, it is not uncommon to chose a new ansatz orthogonal to that state to gain knowledge about low-lying excitations. However, with the set of conditions at hand it is not possible to study the bulk of higher excitations or even band structure. But this is no general limitation – if we are given a set of other conditions (e.g. incorporating more spectral properties), we might very well find ourselves equipped with tools to gain knowledge about physics far from the ground state.

Still, among others, [145, 151] suggested – albeit for classical mechanics – as early as 1870 that restriction to a finite set of state vectors $\{|\Psi_i\rangle \forall i = 1, 2, \dots, N\}$ is

a worthwhile ansatz. Although intuitively one could conclude that for problems on high-dimensional spaces this is a futile endeavor, it turns out that due to the fact that ground states (and low-lying excitations to a lesser extent) usually have the least correlation with states outside the variational manifold, if chosen “correctly”, i.e. in such a way that some approximation to the ground state can be found in

$$\mathcal{M} = \text{span}\{|\Psi_i\rangle\}. \quad (133)$$

Consequently, known as the **Rayleigh-Ritz method**, one can obtain flow equations of the form

$$H_{\Psi}z = EN_{\Psi}z, \quad [H_{\Psi}]_{\bar{i},j} = \langle\Psi_{\bar{i}}|H|\Psi_j\rangle, \quad [N_{\Psi}]_{\bar{i},j} = \langle\Psi_{\bar{i}}|\Psi_j\rangle. \quad (134)$$

with the expansion $|\Psi(z)\rangle = z^i |\Psi_i\rangle$.

In conjunction with parent Hamiltonians, this method can easily be applied to quantum many-body systems. Of course there are problems with the scaling behavior when increasing the number of sites (i.e. particles), but this is the case for all methods, since we know that the limit of such systems is an infinite-dimensional case with (likely) infinite correlations.

Coming back to the more abstract time-independent variational principle, one can raise the question whether the variational manifold \mathcal{M} has to be a proper vector space. The answer is no, as long as we have other means to certify that approximations on (or tangential to) the variational plane capture relevant physical degrees of freedom. In this way it is sometimes possible to find variational classes that seem odd as a constructive approach, but converge very fast even with low-order methods. Furthermore, physicists using the variational principle never tire to explain how it does not exhibit the sign problem [116, 100, 166] many Monte Carlo-methods suffer from.

It is vastly successful as the foundation of Hartree-Fock ansatzes to mean-field theories [77, 78, 54, 158] as well as density functional theory [85, 81, 104] and of course density matrix normalization group.

2. DMRG

Along the path that led to the seminal works on DMRG by S. White [183, 182], among others especially the studies on **Numerical Renormalization Group (NRG)** [186, 108, 18] proved vital for both its success as well as spread and use.

NRG directly lends its ansatz from a slightly adapted time-independent variational principle to explain impurities in metals with non-monotonic resistivity behavior. While the scope sounds very special, the method Wilson et al. derive would still have been generic if it would not be for the logarithmic discretization scheme they use: They found that describing band gaps becomes necessarily exponentially complicated the closer the method converges to the Fermi energy of the conducting phase. Their solution is to discretize the band into segments that become logarithmically smaller converging to the Fermi energy.

Although not historically sound, NRG can be recognized as an evolutionary link between early variational methods and DMRG itself, since DMRG was able to fill both conceptual and numerical shortcomings when applying NRG to Hubbard or Heisenberg systems, as explained in e.g. [156, 178]. We already learned in Section 3.2.3 that DMRG is well-suited to finding ground states [138].

As successful as DMRG was when finding ground states, both convergence and efficiency in simulating time-evolution was not its main scope. An extension that aims to remedy these shortcomings has been found in the **Time-Evolving Block Decimation (TEBD)** [191]. Given the time propagator e^{-iHdt} , per-site treatment by the DMRG fails if the Hamiltonian does not exhibit locality properties. It can be argued that for next-neighbor interactions the DMRG can be adapted in

the following way: The aforementioned propagator is subjected to the Lie-Trotter decomposition [165] and decomposed into a product of local unitaries, if possible. This procedure basically returns an MPO (see next section) that can subsequently be truncated back to lower-dimensional Schmidt rank. While the process itself is flexible enough to treat a multitude of systems and interactions, drawbacks include the fact that the truncation accuracy is hard to quantify as well as the observation that usually energy conservation cannot be guaranteed. Additionally, symmetries like translation invariance may be broken. The basic problem, as was pointed out by [73], is that the Trotter-step leaves the variational manifold. While not a priori unsolvable, incorporating the necessary conditions into the Trotter step is, as we will argue in Section 4.1, not the optimal treatment of the problem.

After all, by learning about TEBD, we understand that DMRG indeed *is* a variational method, since the way of finding ground states basically optimizes over an MPS representation. It is important to note however, that although all micro-configurations are upper bounds to the ground state energy, the iteration itself need not be monotonous, because the specific truncation imposed by the respective Schmidt decompositions is not. In 2013, Wouters et al. proved [188] a Thouless-like theorem for the MPS manifold that shows how to parametrize it without redundant degrees of freedom, subsequently showing that it is identical if one was to use it as the basis for a DMRG algorithm of the same bond dimension, apart from the fact that for DMRG-based methods there is no straightforward answer on how to make sure to project infinitesimal time steps back to the manifold in an optimal way.

This, together with works by Stoudemire et al. [159] showing that for almost-orthogonal representations the bond-dimension can be radically reduced, makes DMRG outright equivalent to MPS ansatzes using the time-dependent variational principle, basically reducing the pragmatic difference to using different parametrizations. Granted, practitioners will object that this is only true insofar as formal equivalence is concerned – actual implementations and their skillful handling of symmetries and gauge-freedom will make one or the other implementation preferable depending on the problem at hand. For the finer details we however refer to Section 4 of the derivation of the time-independent variational principle for MPS.

3. Matrix Product Operators

Following the likes of [156], to understand the scope of the MPO formulation, we would like to consider a single MPS coefficient $\langle \sigma | \Psi \rangle$. It can be calculated explicitly as

$$\begin{aligned} \langle \sigma | \Psi \rangle &= \Gamma^{\sigma_1} \lambda[1] \Gamma^{\sigma_2} \dots \lambda[N-1] \Gamma^{\sigma_N} \\ &= M^{\sigma_1} M^{\sigma_2} \dots M^{\sigma_{N-1}} M^{\sigma_N}, \end{aligned} \quad (135)$$

where we set $M^{\sigma_i} = A^{\sigma_i} V \lambda[i]$, where V is a matrix with orthonormal columns such that the local basis can be written as $|a_i\rangle = \sum_{\sigma_{i+1}, \dots} V_{a_i, \sigma_{i+1} \dots} |\sigma_{i+1} \dots\rangle$, which in turn implies that the whole expression consists of valid Schmidt decompositions only. Moreover, we can consider using this formula to express coefficients of operators:

$$\langle \sigma | O | \sigma \rangle = W^{\sigma_1 \sigma'_1} W^{\sigma_2 \sigma'_2} \dots W^{\sigma_{N-1} \sigma'_{N-1}} W^{\sigma_N \sigma'_N}, \quad (136)$$

where we need to add a second physical index to accommodate the second 'leg' of the operator. Compared to DMRG visualizations, it seems imperative to note that they differ only by means of focus. While DMRG is mainly concerned with the unraveling of the physical indices, an MPO can in principle act on all indices.

The rule of MPS that ingoing and outgoing legs must be equal is thus lifted to MPOs as well. By studying the relevant literature of MPOs, we can conclude that

any operator can be decomposed into an MPO like this:

$$\begin{aligned} O &= \sum_{\sigma_1, \dots, \sigma_N, \sigma'_1, \dots, \sigma'_N} c_{(\sigma_1 \dots \sigma_N)(\sigma'_1 \dots \sigma'_N)} |\sigma_1, \dots, \sigma_N\rangle \langle \sigma'_1, \dots, \sigma'_N| \\ &= \sum_{\sigma, \sigma'} W^{\sigma_1 \sigma'_1} W^{\sigma_2 \sigma'_2} \dots W^{\sigma_{N-1} \sigma'_{N-1}} W^{\sigma_N \sigma'_N} |\sigma\rangle \langle \sigma'|. \end{aligned} \quad (137)$$

If we were to unravel the index pair (σ, σ') , we can see that indeed the form is identical to a simple MPS expansion. Of course, one has to be careful in actually performing the decomposition into an MPO, since, much like with MPS, it could be exponentially complex with a faulty choice of basis or bond dimension, but can be as good as $Nd^2D^2D_W^2$, where D_W is the total MPO dimension. Still, the added benefit of MPOs lies simply in the fact that they can safely be applied to an MPS and will return an MPS – albeit at the dimension of the product of the MPS and MPO dimensions. The argument is as follows. Using $N_{(b_{i-1}, a_{i-1}), (b_i, a_i)}^{\sigma_i} = \sum_{\sigma'_i} W_{b_{i-1} b_i}^{\sigma_i \sigma'_i} M_{a_{i-1} a_i}^{\sigma'_i}$, we can show

$$\begin{aligned} O|\Psi\rangle &= \sum_{\sigma, \sigma'} \sum_{a, b} \left(W_{b_0, b_1}^{\sigma_1, \sigma'_1} W_{b_1, b_2}^{\sigma_2, \sigma'_2} \dots \right) \left(M_{a_0, a_1}^{\sigma'_1} M_{a_1, a_2}^{\sigma'_2} \dots \right) |\sigma\rangle \\ &= \sum_{\sigma, \sigma'} \sum_{a, b} \left(W_{b_0, b_1}^{\sigma_1, \sigma'_1} M_{a_0, a_1}^{\sigma'_1} \right) \left(M_{a_1, a_2}^{\sigma'_2} W_{b_1, b_2}^{\sigma_2, \sigma'_2} \right) \dots |\sigma\rangle \\ &= \sum_{\sigma, \sigma'} \sum_{a, b} N_{(b_0, a_0), (b_1, a_1)}^{\sigma_1} N_{(b_1, a_1), (b_2, a_2)}^{\sigma_2} \dots |\sigma\rangle \\ &= \sum_{\sigma_i} N^{\sigma_1} N^{\sigma_2} \dots |\sigma\rangle, \end{aligned} \quad (138)$$

where we include dummy indices $a_0 \equiv 1 \equiv b_0$.

Put into perspective, Matrix Product Operators are useful whenever we have long-range interactions that cannot be addressed in an otherwise elegant manner, like absorbing them into periodic boundary conditions. We shall proceed to explain how MPOs can be used in variational calculations.

The typical way of looking at variational calculations is also true for Matrix Product Operators: We want to find a ground state for our problem, be it a Hamiltonian, a time-dependent Hamiltonian or a dissipative superoperator. In the case of MPOs, the most common ansatz [172], that can still be traced back to proceedings like [138], is to directly minimize $\frac{\langle \Psi | H | \Psi \rangle}{\langle \Psi, \Psi \rangle}$ using an alternating least squares (ALS) method.

In difference to “pure” DMRG-based approaches, the minimization need not be happening one block after the other, but can, in case of local terms, be done for whole parts of the chain at once. If this is the case, the bond dimension of the MPS resulting from application of the MPO can be controlled much better than for iterative schemes in DMRG.

Throughout the evolution, a general approach would be to start from a small bond dimension to subsequently take this as a starting point for a variation with larger bond dimension. Although practical experience tells us that more often than not ground states do not exhibit large bond dimensions, variational optimizations toward them very well do. That is the crucial point here: Just like for DMRG and the Time-Dependent Variational Principle, the computational complexity proposes a tradeoff with regard to accuracy. Moreover, MPOs impose a more complicated unraveling, because the contraction tensor network is larger by at least one auxiliary dimension, if not more.

Working toward the ground state, one can then produce an MPS approximation like above, minimizing $\|H|\Psi_0\rangle\|$ with respect to e.g. the Euclidean norm, where $|\Psi_0\rangle$ is a first guess for the ground state after some convergence assertion to the MPO evolution. As you can see, this is not very far from the Time-Dependent Principle acting on the MPS variational manifold, but this scheme has other problems, namely the fact that with an MPO we can not guarantee that the ansatz state will represent a physical state [102], because the variational manifold does not restrict to physically realizable states, i.e. being positive and inhibiting $\text{tr}(|\Psi_0\rangle\langle\Psi_0|) = 1$. In the case of unitary evolution with a Hermitian Hamiltonian, this would only be a problem for cases where one would introduce non-zero temperature through means that do not resolve to using an auxiliary system, but it has been shown [33, 179, 191, 170] that this poses an increasingly difficult challenge, the more general the introduced dissipation is, like we review in Chapter 5.

4. The Time-Dependent Variational Principle

Although the basis for the deep understanding of time-dependent usage of the variational principle we possess today can be traced back to research of Dirac [38], Frenkel [56] and others in the early beginnings of quantum theory, it took half a century until its implications to simulation of quantum systems was fully appreciated [112]. Real-time evolution of systems, that could be considered both close to laboratory conditions as well as theoretically accessible, could be treated numerically only after the emergence of scalable computing power beginning in the 1980's and later, when DMRG gave rise to schemes of time-evolving block decimation [191] as a first glimpse at the power of the TDVP. Although it is our aim to not only simulate real-time evolution, but moreover generalize it to dissipative applications, we will need to understand quantum dynamics in a broader sense and will thus have to verbosely derive the TDVP flow equations.

As a side-note, for readers not interested in the detailed derivation, a concise, evolved insight of state of the art TDVP algorithms and applications, that developed over the last few years, can be obtained from, e.g. [71, 8].

4.1. Derivation

First of all, we observe that in contrast to standard quantum mechanical problems (and the time-independent variational principle), we need to start from a time-dependent equation of motion.

While it seems obvious that such an equation of motion can be found by implying time-dependence to a Hamiltonian, its impact regarding interpretations of quantum mechanics, physics and the universe itself cannot be understated. For the matter of this thesis however, it is no more but the linear partial differential equation that gives rise to wave functions as solutions of quantum mechanical problems. Although this is an understatement of political correctness (of course there are “interpretations” of any of the three things mentioned above that can safely be ignored), we will leave it at this and proceed with the precise, indisputable definition of that equation of motion:

$$i\hbar\frac{\partial}{\partial t}|\Psi(t)\rangle = H(t)|\Psi(t)\rangle. \quad (139)$$

Again, in this equation the \hbar is there for brevity and familiarity, but for the remainder of the thesis we assert that $\hbar \equiv 1$. If the variational class does not span the whole Hilbert space – as is most often the case – even infinitesimal time evolution (i.e. applying the operator $e^{-iH(t)dt}$ to the initial state $|\Psi(0)\rangle$) will generally leave the variational manifold \mathcal{M} . The time-dependent variational principle will enable

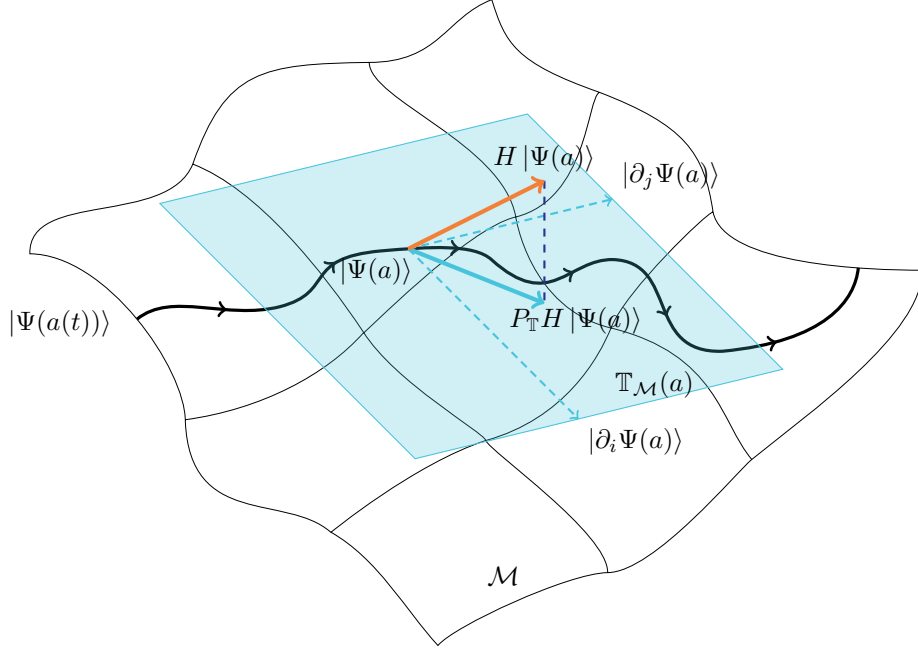


FIGURE 8. **Pictorial illustration of the variational manifold \mathcal{M} and its tangent plane \mathbb{T} .** The path of the variational flow, represented by the Matrix Product State $|\Psi(a(t))\rangle$, on the variational manifold $\mathcal{M}(a)$, is shown together with its derivatives $\partial_i |\Psi(a)\rangle$ and $\partial_j |\Psi(a)\rangle$ with respect to variational parameters a_i, a_j at time t . The shaded area below depicts the tangent plane $\mathbb{T}_{\mathcal{M}}(a)$, to which the discretely with respect to time propagated state $H |\Psi(a)\rangle$ is projected, resulting in the expression $P_{\mathbb{T}} H |\Psi(a)\rangle$.

us to create an approximation to the infinitesimally evolved state vector that stays in the variational manifold by projecting in an optimal way.

Following notation from [73] by Haegeman et al., we begin with a geometric argument and later return to the action principle. Given a wave function $|\Psi(a(t))\rangle$, we can input it into the TDSE in Eq. (139) to obtain the expression

$$\dot{a}^i |\partial^i \Psi(a(t))\rangle = -iH |\Psi(a(t))\rangle, \quad (140)$$

where $|\Psi(a(t))\rangle$ is an MPS on an infinite spin-1/2 lattice of the form

$$|\Psi(a(t))\rangle = \sum_{\{s_k\}=1}^d v_L^\dagger (\prod_{n \in \mathbb{Z}} a^{s_n}) v_R |s\rangle, \quad (141)$$

with $|s\rangle \equiv |\dots s_1 s_2 \dots\rangle$ and v_L/v_R are two D -dimensional vectors. The variational parameters form a set of $D \times D$ -matrices A^s and can be subsumed under a collective index i , such that $a_i = A_{\alpha,\beta}^s$ is a dD^2 -dimensional vector – a format we know from Chapter 2. The derivation does not depend on the specific form of lattice – it can without trouble be adapted to finite cases.

Looking at the format of Eq. (140), we identify a linear combination of tangent vectors to the variational manifold \mathcal{M} on the left hand side, while the right hand side $-iH |\Psi(a(t))\rangle$ is simply a general vector in Hilbert space. Osborne et al. thus correctly conclude that the equation cannot have an exact solution for the variational parameters a^i .

Instead, an approximation has to be performed. The logical candidate for this is an orthogonal projection minimizing

$$\|\dot{a}^i |\partial^i \Psi(a(t))\rangle + \mathbf{i}H |\Psi(a(t))\rangle\|, \quad (142)$$

which can be identified as

$$\langle \partial_j \Psi(\bar{a}(t)) | \partial_i \Psi(a(t)) \rangle \dot{a}^i = -\mathbf{i} \langle \partial_j \Psi(\bar{a}(t)) | H | \Psi(a(t)) \rangle. \quad (143)$$

Notice that the expression on the left hand side now contains the Gram matrix of the tangent vectors:

$$g_{\bar{i},j}(\bar{a}, a) = \langle \partial_{\bar{i}} \Psi(\bar{a}(t)) | \partial_j \Psi(a(t)) \rangle. \quad (144)$$

We define the transfer matrix $E = \sum_{s=1}^d A^s \otimes \bar{A}^s$ and assume that it has exactly one eigenvalue 1 with left and right eigenvectors $\langle l|$ and $|r\rangle$. They are of dimension $D \times D$, Hermitian and full rank when reshaped to quadratic matrix form. Also, we demand that they obey normalization such that

$$\langle l|r\rangle = \text{tr}(lr) = 1. \quad (145)$$

Osborne et al. furthermore assume that all other eigenvalues of E lie within the unit circle such that the spectral radius of $E - |r\rangle\langle l|$ is smaller than one.

With these additional conditions we can now propose what it would mean to have an operator O acting on neighboring sites:

$$\begin{aligned} O(\bar{a}, a) &= \frac{\langle \Psi(\bar{a}) | O | \Psi(a) \rangle}{\langle \Psi(\bar{a}) | \Psi(a) \rangle} \\ &= \langle l | \sum_{s,t=1}^d O_{t_1 \dots t_n, s_1 \dots s_n} (a^{s_1} \dots a^{s_n}) \otimes (\bar{a}^{t_1} \dots \bar{a}^{t_n}) | r \rangle. \end{aligned} \quad (146)$$

It seems possible that this operation is efficient, but we have yet to verify this. The explicit discussion of computational complexity is performed in the next section.

We now approach the lengthy endeavor to specify the explicit form of the tangent vector: For a translation invariant Hamiltonian $H = \sum_{N \in \mathbb{Z}} T^n h^n T^{-n}$ in nearest-neighbor form, where h acts on sites zero and one only, T denoting the shift operator, we find that the tangent vector B_i can be given as

$$B_i |\partial_i \Psi(a(t))\rangle = \sum_{n \in \mathbb{Z}} T^n \sum_{s_k=1}^d v_L^\dagger (\dots A^{s-1} B^{s_0} A^{s_1} \dots) v_R |s\rangle. \quad (147)$$

We observe that for an infinite one-dimensional lattice

$$\begin{aligned} \bar{b}^{\bar{i}} g_{\bar{i},j} b^j &= |\mathbb{Z}| \left[\langle l | E_{b'}^b | r \rangle + \langle l | E_{b'}^a (1-E)^{-1} E_b^a | r \rangle \right. \\ &\quad \left. + \langle l | E_a^b (1-E)^{-1} E_{b'}^a | r \rangle + |\mathbb{Z} - 1| \langle l | E_{b'}^a | r \rangle \langle l | E_a^b | r \rangle \right], \end{aligned} \quad (148)$$

$$\begin{aligned} \bar{b}^{\bar{i}} \langle \partial_{\bar{i}} \Psi(\bar{a}) | H | \Psi(a) \rangle &= |\mathbb{Z}| \left[\langle l | H_{bb}^{aa} | r \rangle + \langle l | H_{ba}^{aa} | r \rangle + \langle l | H_{aa}^{aa} (1-E)^{-1} E_b^a | r \rangle \right. \\ &\quad \left. + \langle l | E_b^a (1-E)^{-1} H_{aa}^{aa} | r \rangle + (|\mathbb{Z} - 2|) \langle l | E_b^a | r \rangle \langle l | H_{aa}^{aa} | r \rangle \right], \end{aligned} \quad (149)$$

with the shortcuts $H_{cd}^{ab} = \sum_{s,t,u,v=1}^d \langle s, t | h | u, v \rangle (a^u b^v) \otimes (\bar{c}^s \bar{d}^t)$ and $E_b^a = \sum_{s=1}^d a^s \otimes \bar{b}^s$, where $E \equiv E_a^a$. Note that $(1-E)^{-1}$ is the pseudo-inverse of $(1-E)$:

$$\langle l | (1-E)^{-1} = 0 = (1-E)^{-1} | r \rangle, \quad (150)$$

i.e. acting on the left or right Eigenvector of E gives zero. The cardinality factors of order $\mathcal{O}(|\mathbb{Z}|)$ are due to the infinite chain length and cancel out. For a system of finite size N this works mutatis mutandis, but does not solve the problem that the last term of the right hand side of Eq. (148) diverges anyway. Indeed, Osborne

et al. show that they disappear once one restricts the evolution to tangent vectors orthogonal to the state vector such that

$$\langle \Psi(a) | \partial_i \Psi(a) \rangle b^i = |\mathbb{Z}| \langle l | E_a^b | r \rangle = 0 \quad (151)$$

and that it is globally optimal in \mathcal{M} . In fact the tangent plane contains the state itself. That means, while we could perform an infinitesimal change in that direction, we should not do it, because it would only result in a change in norm or phase, which is not what we want.

4.2. Properties

Looking at Eq. (148), we can see that only expectations occur within the equations of motions, i.e. the TDVP is a symplectic method that preserves (all) constants of motion and the variational parameters can be decomposed into generators of the respective system symmetries. This is a profound advantage compared to Monte Carlo methods, where symplectic structure can only be retrieved for special cases of very simple symmetries and also helps with the exploration of translation-invariant systems. Just like for DMRG, we find that if the system has translation-invariant blocks, we can further increase the computational efficiency.

Moreover, the symplectic structure gives rise to full time-reversal symmetry, useful for real-time evolution applications where one can use real-valued Hamiltonians, see [167] for an approach that uses “trotterized” evolution to achieve this.

It is important to bear in mind that the absence of a Trotter error as a matter of principle means that there is no need for a inevitable decrease in dt for accuracy reasons. While we will concern ourselves with dissipative systems that are precisely *not* time-reversible and have, due to their inherently decorrelating nature, not much symmetry – if at all – it is important to keep in mind that the method in principle is, i.e. if a specific symmetry presents itself to us, the TDVP toolkit is equipped to exploit it.

4.3. Examples and algorithms: evoMPS

Finding schemes for computational work in science is a noble endeavor, albeit not the whole work. Implementing algorithms to check and prove and extend the scope of mankind’s understanding is a likewise humble task. In case of the TDVP, there are two implementations of particular noteworthiness. First and foremost, Jutho Haegemann implemented a great deal of the propositions in [73] and his PhD thesis [72]. The influence of his work on the development of MPS-based numerical schemes cannot be understated. Still, for the matter of this thesis we make use of the **evoMPS** framework, written and maintained by A. Milsted et al. [120], furthermore in the spirit of open access science published under the free GPL license and thus freely extendable.

Originally started as part of A. Milsted’s MSc project, it has over the last years become a mature implementation of the TDVP that will form the basis of our extension regarding dissipation. In this section we give a basic overview of inner workings, features and applications.

Based on [73] and [122] in particular, evoMPS is implemented using the **Python programming language** using the **SciPy** [29] modules with advanced optimized linear algebra solver libraries **LAPACK** [27] and **BLAS** [26].

Out of the box it handles states on a finite chain with open boundary conditions, block translation invariant states on an infinite chain (with adjustable block size) and furthermore block translation invariant states with a localized nonuniformity on an infinite chain. Also, later additions include experimental implementations of arbitrary interactions using an MPO extension. We shall now see how the implementation works **en detail**. One iteration basically takes four steps, that are

repeatedly performed until the desired result is obtained to some accuracy – this can either mean that the ground state is found, the error measure has grown so much that you cannot certify a good approximation result or the scaling parameters of the system are chosen such that we miscalculated the runtime and now have to wait until the universe falls dark until the operation is complete – obviously this is part of the mathematical physicist’s work and should not be regarded as capital punishment, since most of the time one can change the variational class (e.g. by adapting the bond dimension) to get fast calculations at the cost of reduced accuracy. But before discussing computational complexity, we will introduce the actual work to be done.

Before calculating the tangent vector the the variational manifold, we have to evaluate two auxiliary quantities. First of all we need to incorporate the property of pseudo-invertibility of $(1 - E)$ into the flow equations, so suppose that

$$(K| = (l|H_{aa}^{aa}(1 - E)^{-1}, \quad (152)$$

where $(l|H_{aa}^{aa}$ is replaced by $(l|H_{aa}^{aa} - h|l$ since $(l|(1 - E)^{-1} = 0$. We furthermore make $(1 - E)$ non-singular by substituting

$$(1 - E) \rightarrow (1 - E) + |r)(l|$$

and now can solve

$$K - \sum_{s=1}^d a^{s\dagger} K a^s + \text{tr}[K r] l = [(l|H_{aa}^{aa}] - h l, \quad (153)$$

$$\text{with } [(l|H_{aa}^{aa}] = \sum_{stuv} \langle st|h|uv \rangle (\bar{a}^s \bar{a}^t)^\dagger l (a^u a^v) \quad (154)$$

for the unknown $D \times D$ -matrix K with an iterative solver. In evoMPS, this is part of the `update()` routine. `update()` is the wrapper for the basic iteration step of the TDVP implementation. It explicitly obeys the relation $\text{tr}(K r) = (K|r) = 0$. After calculating the K matrices by calling `calc_K()`, we need to calculate an additional auxiliary variable before we can treat the tangent vectors, i.e. we have to perform the calculation `calc_C()`:

$$C^{st} = \sum_{uv} \langle st|h|uv \rangle a^u a^v, \quad (155)$$

such that we can finally obtain

$$F = \sum_{s,t=1}^d (V_L^s)^\dagger l^{1/2} C^{st} r (a^t) r^{1/2} + \sum_{s=1}^d (V_L^s)^\dagger l^{-1/2} \left(\sum_{t=1}^d a^{t\dagger} l C^{ts} + K a^s \right) r^{1/2}. \quad (156)$$

The flow F now can be identified with the quantity x we need to minimize:

$$\|b^i(x) |\partial_i \Psi\rangle - H |\Psi\rangle\|^2 = |\mathbb{Z}| \text{tr} [x^\dagger x - x^\dagger F - F^\dagger x + \text{constant}]. \quad (157)$$

With $F \hat{=} x = x^\dagger$ we conclude that

$$\dot{a}^i = -i b(x^*), \quad (158)$$

an operation that is performed by the evoMPS function `calc_B()`. To wrap up, lets look at the whole algorithm again:

- (1) Calculate the tangent vector’s projection b^i back onto \mathcal{M} by
 - (a) Calculate K from Eq. (153).
 - (b) Calculate C from Eq. (155).
 - (c) Calculate $x^* = F$ from Eq. (157).
- (2) Set $a(t + dt) = a(t) - i dt b(x^*)$.
- (3) Fix the gauge such that the canonical form is retained and renormalize the state.

- (4) Calculate observables, increment the time by one step dt .

Notice that in principle the complexity is $\mathcal{O}(D^6)$, but unraveling the most critical part – inverting $(1 - E) + |r\rangle\langle l|$ – into an iterative solution that sweeps through the sites, Osborne et al. showed that it can be done with $\mathcal{O}(D^3)$, although one has to give up arbitrary interactions and be content with nearest-neighbor and next-nearest-neighbor terms of the Hamiltonian. For a detailed treatment of this matter, see the supplementary material of [73].

To put the whole scheme to use, we now review the two kinds of time evolution one can apply.

4.3.1. *Imaginary time evolution.* Setting $dt = i d\tau$, one obtains **imaginary time evolution**, technically a Wick rotation by $\pi/2$ [184], i.e. a way of adiabatically observing quantum statistical properties that evolve along phase space trajectories corresponding to the imaginary time that has passed. It is obvious that one can access observables like energy expectation this way, but not real-time dynamics, and for sure not, as we will see in Chapter 5, dissipative dynamics. A minimal working example of imaginary time evolution is included in the evoMPS distribution and resolves to using an Euler integration scheme on Heisenberg anti-ferromagnetic spin-1 lattices. The TDVP algorithm runs until the energy expectation is minimal:

$$\langle \partial_i \Psi | H | \Psi \rangle = 0. \quad (159)$$

In practical implementations this means that one has to set some energy threshold for more complicated systems, unless we want to wait until the approximation is on the level of the numerical accuracy of the implemented floating point precision, which is completely unnecessary and will take uneconomically long.

4.3.2. *Real time evolution.* In contrast to the previous section, **real time evolution** is a more ferocious beast.

In RTE, we want to find out what happens to a system under successive infinitesimal application of e^{iHdt} , e.g. to find out about entanglement behavior, Rabi-like dynamics, anyonic chains [52], molecule dynamics [57] or evolution of time-dependent observables. Unfortunately, Euler integration is not enough to capture the dynamics to sufficient accuracy, but instead using a time-reversal invariant numerical integrator is preferable, as can be seen from [73], because the relation $H(\bar{a}(t), a(t)) = \langle \Psi(\bar{a}(t)) | H | \Psi(a(t)) \rangle$ drifts more and more the longer we simulate its evolution, although it should be a constant of motion for an exact calculation. Due to the non-linear structure of the flow equations (157), $H(\bar{a}(t), a(t))$ is in general non-separable. Osborne et al. also argue that for real-valued Hamiltonians there is time-reversal symmetry that is inherited by the TDVP flow. Thus, using a (second-order) integration scheme that accounts for this, one can obtain stable long-time behavior, linearly-bounded global error and near-preservation of first integrals [76]. Haegemann [72] has given an explicit mid-point construction for an adapted backward Euler scheme that can solve most of the mentioned problems, and is correct up to $\mathcal{O}(dt^4)$. This can be further improved by using higher-order Runge-Kutta algorithms [152, 109, 19, 75], albeit one observes that for most practical purposes backwards Euler is sufficient. It can be shown that this method outperforms most other approaches regarding accuracy, especially time-evolving block decimation – which is the main concern for real-time evolution, since the dispersion error basically governs how long of a time one can simulate. We will discuss more intricacies of RTE when we begin our treatment of dissipative systems.

5. Variational Monte Carlo

The variational Monte Carlo (VMC) method aims, just like the previously discussed ansatzes, to approximate the ground state of many-body systems. The method of choice hereby is Monte Carlo sampling of suitable parameters [124, 23].

Usually, the variational Monte Carlo is defined in this way: Given a variational class $|\Psi(a)\rangle$, we can write down the energy configuration as

$$E(a) = \frac{\langle \Psi(a) | \mathcal{H} | \Psi(a) \rangle}{\langle \Psi(a) | \Psi(a) \rangle}. \quad (160)$$

The right-hand side can be expanded:

$$\frac{\langle \Psi(a) | \mathcal{H} | \Psi(a) \rangle}{\langle \Psi(a) | \Psi(a) \rangle} = \frac{\int |\Psi(X, a)|^2 \frac{\mathcal{H}\Psi(X, a)}{\Psi(X, a)} dX}{\int |\Psi(X, a)|^2 dX} \quad (161)$$

and we subsequently identify $\frac{|\Psi(X, a)|^2}{\int |\Psi(X, a)|^2 dX}$ as a stochastic integral over an unknown probability distribution, that can be treated as tuples of random variables – i.e. the variational parameters. Variational Monte Carlo then aims to minimize the property

$$\mathcal{E}_{\text{loc}}(X) = \frac{\mathcal{H}\Psi(X, a)}{\Psi(X, a)}, \quad (162)$$

called **local energy**. Of course, the Hilbert space dimension grows exponentially, just like for every other method previously discussed. One benefit of stochastically evaluating the probability distribution is though, that it can be done in parallel: While the evaluation of the exact instance has $d^2 - 1$ parameters (keep in mind that the constraint of normalization as a single separate side condition does not effectively decrease complexity), stochastic integration of lower-dimensional variational instances still take a long time, but scales as low as $\mathcal{O}(N^{2-4})$, compared to $\mathcal{O}(d^N)$ for exact solvers. Still, depending on the complexity of the problem and whether the variational class is constrained by other conditions, such as additional (e.g. chemical) symmetries [146, 189], VMC also suffers from the fact that for large particle numbers, higher order correlations become more significant, thereby increasing the complexity of the sampling necessary for accurate results [125]. Using stochastic methods, it is often too easy to shove off the question about errors toward the simple declaration that it scales with $e_s \approx \frac{1}{\sqrt{N}}$.

However, a variational method, we must consider the conceptual errors as well [99], i.e. while minimizing over the variance only has the added benefit that its value can be bounded from below and constructively be calculated, the question remains whether this is variationally optimal. Of course useful as a measure of uncertainty about the acquired solution, it has its merits. However, when we consider the fact that the variation itself can depend on the variance (if some weight is given to the variance bound and some kind of gradient estimate is taken), it can no longer function as an unbiased error estimate since it becomes a random variable of the minimization as well, thus being potentially subject to self-sampling bias. For example, there are certain publications that have shown that directly using energy or linear combinations of energy and variance cost functions can increase accuracy for some systems [162] and that different measures of accuracy have to be taken into account in this case.

Finally, as a last and fundamental caveat to Monte Carlo Sampling of any kind acts the well-known sign-problem [116, 100, 166], as already mentioned in the introduction of this chapter.

5.1. Time-Dependent Variational Monte Carlo

While VMC is well suited to solving ground state problems, we have yet to see how the numerical calculation of time-evolving dynamics can be performed. One such ansatz [22, 21], developed by G. Carleo et al., tries to generalize it using the Time-Dependent Variational Principle.

The variational class is built upon ansatz wave functions of the form

$$\Psi(X, t) = \exp\left(\sum_k a_k(t) O_k(X)\right), \quad (163)$$

where over a many-body configuration X with operators $O(X)$ the (complex) variational parameters $a(t)$ are optimized, thus giving rise to the following infinitesimal step of time evolution:

$$\Psi(X, a(t + \epsilon)) = \Psi(X, a(t)) \left[1 + \epsilon \sum_k \dot{a}_k O_k(X)\right]. \quad (164)$$

The variational approach consists of the observation that one can estimate the difference to the exact state by the following argument[20]:

Given the quantities

$$Z_1^R(X, t) = \sum_k \dot{a}_k^R O_k(X) - \mathcal{E}^I(X, a(t)), \quad (165)$$

$$Z_1^I(X, t) = \sum_k \dot{a}_k^I O_k(X) + \mathcal{E}^R(X, a(t)), \quad (166)$$

one can calculate the norm difference as

$$\Delta_1^2(t) = \sum_X |\Psi(X, a(t))|^2 [Z_1^R(X, t)^2 + Z_1^I(X, a(t))^2]. \quad (167)$$

Minimizing the gradient components $Z_1^{R/I} \frac{\partial}{\partial \dot{a}_k^R}$, we find that the flow equations read

$$\sum_{k'} \dot{a}_{k'}^R \langle O_k O_{k'} \rangle = \langle \mathcal{E}^I O_k \rangle, \quad (168)$$

$$\sum_{k'} \dot{a}_{k'}^I \langle O_k O_{k'} \rangle = -\langle \mathcal{E}^R O_k \rangle. \quad (169)$$

The subsequent implementation makes use of the Metropolis-Hastings algorithm [119, 80] by sampling the acceptance probabilities P for the transition

$$T_{x \rightarrow x'} = \frac{1}{w(X, t)} \frac{|\Psi(X', t)|}{|\Psi(X, t)|}, \quad (170)$$

as $P = \min\{1, \frac{w(X')}{w(X)}\}$, where $w(x, t)$ is normalization factor, the X 's are chosen in a way that guarantees $H_{X, X'} \neq 0$, which effectively leads to the situation where wave functions with greater modulus are more often accepted than less likely ones, the standard treatment using Metropolis sampling. It is however in its current form limited to closed systems and as such only mentioned out of academic interest. It remains to be seen whether this could be extended by methods like the one we are about to present.

CHAPTER 4

Stochastic Calculus

Dealing with stochastic models, variables and processes, the main application of stochastic calculus is to answer questions that arise when integrating stochastic processes - a question that emerged as soon as 1905, when Albert Einstein explained Brownian Motion as a stochastic process of randomly bouncing particles [42]. This not only firmly established the existence of atoms, but also helped pave the way for statistical mechanics as a branch of physics. More than a century later we know that applications of this field are vast and versatile. In fact, we will see that in studying dissipation there is a connection to the physical process the scientific discipline of Stochastic Calculus originates – from Brownian Motion itself.

1. Markov Processes

Before tackling stochastic integration, at least one even more basic ingredient must be treated. Understanding random variables as random processes is vital to all branches of statistical mechanics, even more so in quantum mechanics, because, as we know, the theory is inherently probabilistic. It is thus somewhat consequential to resort to a fully stochastic treatment of quantum dynamics as not a mere method to some ends (understanding time evolution), but rather a necessity given by nature itself.

In the following we will try to confine the used notation to the likes of [58], a fine textbook and reference to all classical stochastic propositions presented in this chapter.

In particular, we have to identify systems where measurements yield statistical results, i.e. where observables are random variables $X(t)$ according to some distribution $p(X(t))$, with a set of probability densities, such that for values $x_1, x_2, x_3 \dots$ there exists an identification

$$p(x_1, t_1; x_2, t_2, \dots) \quad (171)$$

that describes the system in question completely. The tuples (x_i, t_i) are an identification of outcomes x_i with some parameter t_i in a way that $\dots t_{i-1} \geq t_i \geq t_{i+1} \dots$ is a well-defined partially ordered set. If the realization of that order is of temporal nature, we call the dimension of t time, but since there is no strictly necessary notion to follow here, it could also be identified with some other quantity as long as it facilitates a proper ordering that is needed for the definition of a process as a concept that *evolves along* the axis of the ordering parameter, e.g. time. Obviously we did also omit to explain what a proper probability distribution would be. For the matter of this investigation, we make use of the following convention:

Throughout the dissertation, p_X denotes a **probability distribution** of a random variable X , such that the relation

$$\Pr[a \leq X \leq b] = \int_a^b p_X(x) dx \quad (172)$$

gives the information about the respective probability of the interval $[a, b]$ of the distribution p_X for an event x to be happening. Whenever it is clear what random

variable the probability is associated to, we may drop the subscript x for notational tidiness.

Note that while this can be extended to quantum mechanics in a branch of stochastics called *Quantum Stochastic Calculus* [84, 59], up to now this chapter is an investigation about classical systems and will suffice to derive all necessary tools for this thesis.

Also, based on Eq. (171), one can of course define the notion of conditional probabilities for an additional random variable $Y(t)$:

$$p(x_1, t_1; x_2, t_2; \dots | y_1, \tau_1, y_2, \tau_2; \dots) = \frac{p(x_1, t_1; x_2, t_2; \dots; y_1, \tau_1, y_2, \tau_2; \dots)}{p(y_1, \tau_1, y_2, \tau_2; \dots)}. \quad (173)$$

For a complete description of the evolution of the system including the random variables $X(t), Y(t)$, one in principle has to have knowledge about the complete history to be able to make predictions, including all joint probabilities. Such a process, where the predictions depend on joint probability history, is called *separable*, i.e. if we know all *possible* joint probabilities. Note that this notion of separability is different from quantum state separability. This is not a problem though because apart from defining stochastic processes we don't need this version.

Going forward, we can start to classify $p(x_1, t_1; x_2, t_2; \dots)$ based on its properties. First observe that for completely independent events we obtain Bernoulli trials:

$$p(x_1, t_1; x_2, t_2; \dots) \equiv \prod_i p(x_i, t_i), \quad (174)$$

where an identical process is repeated at all times t_i . Now we are left with two cases: either the past of the process is taken into account, or only the present.

In the latter case, this proposition is called **Markov assumption**. It requires that in order to calculate conditional probabilities, only the current instance is to be taken into account:

$$p(x_1, t_1; x_2, t_2; \dots | y_1, \tau_1, y_2, \tau_2; \dots) = p(x_1, t_1; x_2, t_2; \dots | y_1, \tau_1). \quad (175)$$

This is precisely the statement made by Einstein explaining Brownian motion: after microscopic particles have interacted with one another, they obtain a new velocity vector that is irrespective of their entire history. Likewise, we find that indeed

$$p(x_1, t_1; x_2, t_2; \dots; x_n, t_n) = p(x_1, t_1 | x_2, t_2) p(x_2, t_2 | x_3, t_3) \dots \\ \dots p(x_{n-1}, t_{n-1} | x_n, t_n) p(x_n, t_n) \quad (176)$$

for an ordering of events $t_1 \geq t_2 \geq \dots \geq t_{n-1} \geq t_n$. Summing over all mutually exclusive events, one can eliminate that variable. This important insight has been found by Chapman and Kolmogorov (see e.g. [101]) and formally reads

$$p(x_1, t_1 | x_3, t_3) = \int dx_2 p(x_1, t_1; x_2, t_2 | x_3, t_3). \quad (177)$$

For discrete vector spaces, x can be considered a vector. Without making an effort in this work to explain similarities in structure to matrix product states, we note that something like this has been approached [10], where instead of transfer operators the induction of refined (i.e. lower-dimensional) Master equations is studied. It seems worthwhile to see and explore whether Markov chains can indeed be formulated in the language of matrix product states, a question that the aforementioned citation sadly does not answer exhaustively.

Returning to the derivation of Markov processes, one realizes that the dx should, formally, of course, be a measure $d\mu(x)$, although we have to explain what measure exactly we want to use. Incidentally, this is the precise question of stochastic integration in the following Section 2. Before introducing integration, though, we need to discuss continuity of the model process p at hand. Returning to the

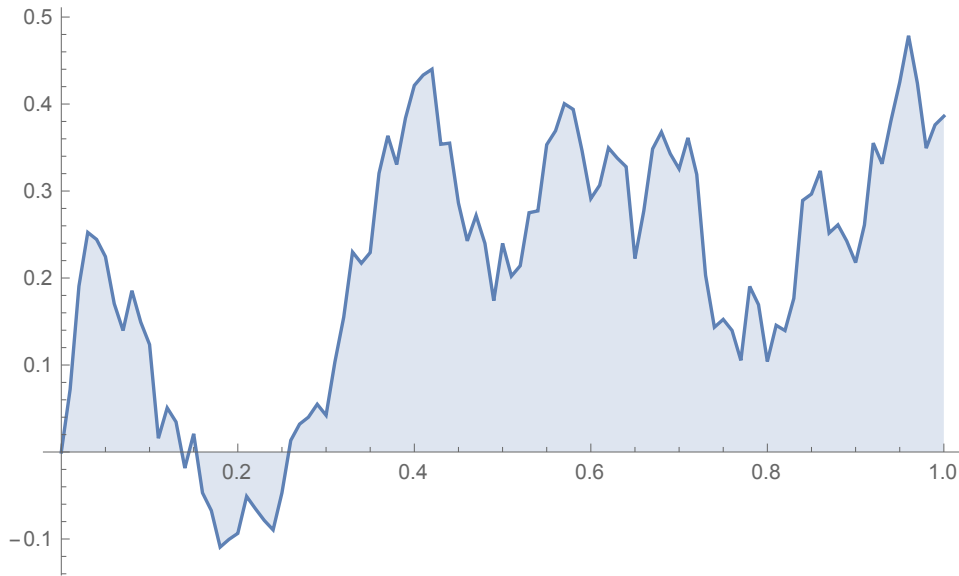


FIGURE 9. **Example of Brownian motion.** Simulated Markov process with drift coefficient $\mu = 0.5$, volatility $\sigma = 0.3$ and time discretization of 0.01 as given in Eq. (186).

Brownian Motion hypothesis of Einstein that, at the time of its publication, could not be experimentally verified, we realize that in a hard core gas with elastic bouncing all particles can in principle realize all phase space configurations. This does not produce continuous sample paths since their velocity changes in an instant if a bounce occurs. Still, the position path still needs to appear continuous, because the axioms of classical mechanics require it to be. The fast and in-vitro correct conclusion is that in nature there are no true Markov processes because its approximations are too restrictive. However, the solution to this seeming paradox of trajectory continuity is that it depends on the coarse-graining scale of the system, whether one can make this assumption. In the case of Brownian motion, it is obvious that since the description is macroscopic, so must be the treatment of continuity, i.e. we check that the *memory time* of the process in question is so small that continuity is not a practical, but rather a theoretical question that can be treated constructively.

With that in mind, we can look at visualizations of Brownian motion like Fig. 9 and realize that in this way of accessing the system, the sample paths are continuous. But if this is the case, we can start talking about differential treatment. Non-differentiability of Brownian motion is a known and even prominent property, but we will see that this does not interfere with the application we have in mind.

More concretely this means that in stochastic calculus one divides the considerations of differentiability between the concept of continuously represented points and the (discontinuously reciprocating) instant of motion, or, more abstractly, *expectation change*. Introducing the class of stochastic differential equations, we need to treat, what C. Gardiner [58] proposed to call the *differential Chapman-Kolmogorow*

equation:

$$\begin{aligned} \partial_t p(x, t|y, \tau) = & - \sum_i \frac{\partial}{\partial z_i} [A_i(z, t)p(z, t|y, \tau)] \\ & + \sum_{i,j} \frac{1}{2} \frac{\partial^2}{\partial z_j \partial z_i} [B_{ij}(z, t)p(z, t, y, \tau)] \\ & + \int dx [W(z|x, t)p(x, t|y, \tau) - W(x|z, t)p(z, t|y, \tau)], \end{aligned} \quad (178)$$

where the quantities A_i, B_{ij} are connected continuously, while $W(z|x, t) = 0$ for all $x \neq z$. W represents the distribution of (non-contiguous) jumps and hence will be called jump term or Wiener process. Please note that τ does not stand for imaginary time, but rather the set of times for the event tuples given by the random variable Y . A priori, it is not clear whether solutions of Eq. (178) are solutions of Eq. (177), or to what extent they exist. Still, C. Gardiner shows that under the conditions that A, B are positive semi-definite and W is non-negative, there exists a solution of the differential CK equation and that *this* solution indeed is a solution to the standard CK equation. Additional conditions include the initial configuration

$$p(z, t|y, \tau) = \delta(y - z) \quad (179)$$

and appropriate boundary conditions. This is complicated to specify in general, but will be possible in the case of the Fokker-Planck equation.

1.1. The Fokker-Planck Equation

If the jump terms $W(x, t)$ of Eq. (178) are zero, we end up with the class of *Deterministic (partial) Differential equations* called Fokker-Planck equations, that have the form

$$\begin{aligned} \partial_t p(x, t|y, \tau) = & - \sum_i \frac{\partial}{\partial z_i} [A_i(z, t)p(z, t|y, \tau)] \\ & + \sum_{i,j} \frac{1}{2} \frac{\partial^2}{\partial z_j \partial z_i} [B_{ij}p(z, t, y, \tau)]. \end{aligned} \quad (180)$$

It models a diffusion process [87] *without* jumps. $A_i(t)$ is the so-called drift vector while B_{ij} is called the diffusion matrix. It must be positive and symmetric because all moments of order higher than 2 vanish. In quantum mechanics, symmetry of the diffusion process means that, since the evolution is definitely continuous (in expectation values, not state vectors) without any contribution from W , it is in principle time-reversible, although for real dissipative systems this is not the case, as we will see.

We will make use of the Fokker-Planck equation in Chapter 5 and continue to introduce the stochastic integral through the use of the Wiener process we need to derive. To this end, we may ask what a solution of this particular stochastic differential equation would look like. As with most meaningful differential equations, they are hard to solve. If however the drift term A_i vanishes and we set $B_{ij} = \mathbb{1}$, the corresponding Fokker-Planck equation reads

$$\partial_t p(x, t|y, \tau) = \frac{\partial^2}{\partial z_j \partial z_i} p(z, t, y, \tau). \quad (181)$$

In this case, there is a both elegant as well as fundamentally interesting exact solution available: Applying the initial condition to the condition probability, we can state the conditional function

$$\phi(\sigma, t) = \int dwp(w, t|w_0, t_0) e^{i\sigma w}, \quad (182)$$

satisfying

$$\frac{\partial \phi}{\partial t} = -\frac{1}{2}\sigma^2 \phi. \quad (183)$$

Obviously, entering the initial condition from Eq. (179), we obtain

$$\phi(\sigma_0, t_0) = e^{i\sigma w_0} \quad (184)$$

such that

$$\phi(\sigma, t) = e^{[i\sigma w_0 - \frac{1}{2}\sigma^2(t-t_0)]}. \quad (185)$$

We check that the Fourier inversion (see e.g. [55]) is well-defined and feasible and find that the sought-after solution

$$p(w, t|w_0, t_0) = \frac{1}{\sqrt{2\pi(t-t_0)}} e^{-\frac{(w-w_0)^2}{2(t-t_0)}} \quad (186)$$

is obviously a diffusing Gaussian with mean w_0 and variance $(t-t_0)$. The solution of the univariate case indeed *is* the Brownian motion and has a few important properties [148].

First of all, as already mentioned, sample paths are, though continuous in the perspective we put it before, non-differentiable. Physically, this means that particles under the effect of Brownian motion behave highly irregular. Secondly, sample paths are irregular, i.e. although the mean value of $W(t)$ is zero, the mean square becomes infinite for $t \rightarrow \infty$. Although it is true for any random process that results are non-reproducible, this is even true for the *scale* of an individual Wiener realization (i.e. a so-called sample path) – while on average it will stay “close” to its mean value, there are instances, where it diverges – a most troubling behavior when identified with classical particles. Where necessary, a more realistic treatment can be obtained using the Ornstein-Uhlenbeck process [168, 64, 13], that will neither be applied nor discussed in this thesis. Moreover, it is the next property that is of most interest. Since the Wiener process is a Markov process, it inherits statistical independence, i.e. events ΔW_i are independent of each other and of the initial condition $W(t_0)$. This basically defines again that from the history of the process we can in no way guess its future. Independence plays a pivotal role in the definition of stochastic integration.

1.2. Itô's Lemma

Of particular importance in stochastic calculus obviously is the ability to actually perform calculus. Apart from evaluating integrals, which we will introduce in the next section, the derivatives of stochastic processes are among the most basic operations to perform.

As already mentioned, we can, in general, not certify variance finiteness and even continuity of stochastic processes. Still, approximating the gradient of such a process is very useful and thus its evaluation desirable. It is due to Itô Kiyosi [87] that we can derive the differential from the following argument, known as Itô's Lemma:

Assuming $X(t)$ to be a drift-diffusion process with drift $A(t)$ and diffusion matrix $B(t)$, then we can find a stochastic differential equation of the form

$$dX(t) = A(t)dt + B(t)dW(t), \quad (187)$$

where W_t is a Wiener process. For any at least 2-times differentiable test function $f(x, t)$, we can write down its Taylor expansion up to second order:

$$df = \frac{\partial f}{\partial t} dt + \frac{\partial f}{\partial x} dx + \frac{1}{2} \frac{\partial^2 f}{\partial x^2} dx^2 + \mathcal{O}(dx^3) + \mathcal{O}(dt^3). \quad (188)$$

If we now perform the substitutions $x \rightarrow X(t)$ and $dX(t) \rightarrow A(t)dt + B(t)dW(t)$, we obtain

$$\begin{aligned} df &= \frac{\partial f}{\partial t} dt + \frac{\partial f}{\partial x} (A(t) dt + B(t) dW(t)) \\ &+ \frac{1}{2} \frac{\partial^2 f}{\partial x^2} (A(t)^2 dt^2 + 2A(t)B(t) dt dW(t) + B(t)^2 dW(t)^2) \\ &+ \mathcal{O}(dx^3) + \mathcal{O}(dt^3) + \mathcal{O}(dW(t)^3), \end{aligned} \quad (189)$$

which has a somewhat intricate asymptotic behavior: For $dt \rightarrow 0$, we find that dt^2 and $dt dW(t)$ go to zero faster than $dW(t)^2$, which is $\mathcal{O}(dt)$. Ordering Eq. (189) by these propositions, the differential now reads

$$df = \left(\frac{\partial f}{\partial t} + A(t) \frac{\partial f}{\partial x} + \frac{B(t)^2}{2} \frac{\partial^2 f}{\partial x^2} \right) dt + B(t) \frac{\partial f}{\partial x} dW(t), \quad (190)$$

which is obviously different from the chain rule of standard calculus. However, it is often more convenient to follow adapted derivation rules than updating the even more complicated rules for integration, as we will see now by introducing the stochastic integral.

2. The Stochastic Integral

There are many ways to motivate the stochastic integral, but one very illuminating is this: In principle, we do not know how to integrate a non-predictable, irregular random process that is Markovian because a Riemann-like deconstruction into partial sums must fail because of the infinite mean-square behavior. Still, suppose we have an arbitrary time-dependent function $f(t)$, we can give the formally correct proposition, independent from the question of its existence, i.e.

$$\int_{t_0}^t f(t) dW(t) = S_n = \sum_{i=1}^n f(\tau_i) [W(t_i) - W(t_{i-1})]. \quad (191)$$

Obviously, the value of S_n depends on the choice of intermediate points τ_i and is not constant – on the contrary, its mean value is between 0 and $(t - t_0)$. To formulate a meaningful resolution, an auxiliary tool will be necessary.

Regarding $X(\omega)$ as functions of ω , we check for any value $X_n(\omega)$ that

$$\lim_{n \rightarrow \infty} \int d\omega p(\omega) [X_n(\omega) - X(\omega)]^2 \equiv \lim_{n \rightarrow \infty} \langle (X_n - X)^2 \rangle = 0. \quad (192)$$

In this case we call $X(w)$ convergent in the **mean square limit**, written as **ms-lim**. Going forth, we can define the stochastic integral in Itô form:

$$\int_{t_0}^t f(t) dW(t') = \text{ms-lim}_{n \rightarrow \infty} \left\{ \sum_{i=1}^n f(t_{i-1}) [W(t_i) - W(t_{i-1})] \right\}. \quad (193)$$

3. The Glivenko-Cantelli theorem

The theorem we are about to present is so fundamental to statistical mathematics that it is sometimes even called the fundamental theorem of statistics, but more formally is known as **Glivenko-Cantelli Theorem**:

THEOREM 11. *Assume that X_1, X_2, \dots are independent and identically distributed (i.i.d.) random variables in \mathbb{R} with common cumulative distribution function $F(x)$. The so-called empirical distribution function for X_1, \dots, X_n is defined*

by

$$F_n(x) = \frac{1}{n} \sum_{i=1}^n I_{(-\infty, x]}(X_i), \quad (194)$$

I_C denoting the indicator function of some set C . $F_n(x)$ is a sequence of random variables which converge to $F(x)$ almost surely for every (fixed) x by the strong law of large numbers, that is, F_n converges to F pointwise.

Note that Glivenko and Cantelli later improved this result further by also proving uniform convergence of F_n to F . While we don't need the rigor of the latter generalization, it is of importance to us that we can use expectation values where averages show up in the TDVP expressions, like in Section 3.2.

4. The Quantum Master Equation

The final building block for treating dissipative quantum systems is the Master equation [114, 105]. Giving an equation of motion for the stochastic treatment of the density matrix of open systems, it masters interaction with heat baths or, more colloquially, the environment, and is the generalization of the quantum Liouville equation

$$\frac{\partial \rho}{\partial t} = \frac{1}{i\hbar} [H, \rho], \quad (195)$$

hence the name. It can (rather lengthily) be inferred from the Born-Markov equation [4, 136, 96] and has the form

$$\dot{\rho} = -\frac{i}{\hbar} [H, \rho] + \sum_{\alpha, \beta} h_{\alpha, \beta} \left(L_{\alpha} \rho L_{\beta}^{\dagger} - \frac{1}{2} \left(\rho L_{\beta}^{\dagger} L_{\alpha} + L_{\beta}^{\dagger} L_{\alpha} \rho \right) \right), \quad (196)$$

where the reference to Markov approximation implies that the (external) heat bath does not have memory and the Born approximation refers to the assumption that the energy capacity of the heat bath be much larger than the energy threshold of the internal system, such that we can safely assume that the bath does not change with time. Equation (196) is the most general form of a time-homogenous master equation governing the real-time evolution for any starting state ρ that is trace-preserving and completely positive.

Since Eq. (196) is so central to this work, we will now derive it explicitly. Beginning with an ansatz $\rho(0) = \rho_S(0) \otimes \rho_B(0)$, we assume that the system, represented by the density operator $\rho_S \in \mathcal{H}_S$ of the system is in a product state with the external heat bath $\rho_B \in \mathcal{H}_B$. Assuming no memory in the external heat bath whatsoever, we can infer that the time evolution of the internal system ρ_S must look like

$$\rho_S(t) = V(t)_{\rho_S(0)} \equiv \text{tr}_B \{ U(t, 0) [\rho_S(0) \otimes \rho_B(0)] U^{\dagger}(t, 0) \}, \quad (197)$$

where $V(t)_{\rho_S(0)} : B(\mathcal{H}_S) \rightarrow B(\mathcal{H}_S)$ is a one-parameter dynamical map that can be characterized by its action on \mathcal{H}_S alone. Recalling that

$$\rho_B = \sum_{\alpha} \lambda_{\alpha} |\Psi_{\alpha}\rangle \langle \Psi_{\alpha}|, \quad \sum_{\alpha} \lambda_{\alpha} = 1$$

we can express it as

$$V(t)_{\rho_S} = \sum_{\alpha, \beta} W_{\alpha\beta}(t) \rho_S W_{\alpha\beta}^{\dagger}(t), \quad \mathcal{H}_S \ni W_{\alpha\beta} = \sqrt{\lambda_{\beta}} \langle \Psi_{\alpha} | U(t, 0) | \Psi_{\beta} \rangle. \quad (198)$$

Also note that we find for the $W_{\alpha\beta}$

$$\sum_{\alpha, \beta} W_{\alpha\beta}^{\dagger}(t) W_{\alpha\beta}(t) = \mathbb{1}_S \Rightarrow \text{tr}_S \{ V(t)_{\rho_S} \} = \text{tr}_S \rho_S = 1, \quad (199)$$

such that for the continuous time variable t we obtain a one-parameter family of dynamical maps $\{V(t)|t \geq 0\}$, where $V(0) = \mathbf{1}_S$, that satisfies the semigroup property

$$(V(s) \circ V(t))(\rho) = V(t+s)(\rho), \quad t, s \geq 0. \quad (200)$$

We can now make the superoperator ansatz to solve the equation of motion in the following way:

$$V(t) = e^{\mathcal{L}t} \Rightarrow \frac{d}{dt}\rho_S(t) = \mathcal{L}\rho_S(t), \quad (201)$$

where we have to explain how to obtain \mathcal{L} .

For an N -dimensional system, we have $N^2 - 1$ degrees of freedom in the density operator, hence we chose N^2 orthogonal operators $\{\tilde{L}_i | i = 1, 2, \dots, N^2\}$, where we set $\tilde{L}_{N^2} = \frac{1}{\sqrt{N^2}}\mathbf{1}_S$ for convenience such that $\tilde{L}_1, \dots, \tilde{L}_{N^2-1}$ are traceless and find

$$(\tilde{L}_i, \tilde{L}_j) \equiv \text{tr}_S \left\{ \tilde{L}_i^\dagger \tilde{L}_j \right\} = \delta_{ij}, \quad (202)$$

which in turn gives us completeness of the basis with regard to the operators W :

$$W_{\alpha\beta}(t) = \sum_{i=1}^{N^2} \tilde{L}_i \left(\tilde{L}_i, (W_{\alpha\beta}(t)) \right). \quad (203)$$

Using Eq. (198), we can subsequently write

$$V(t)\rho_S = \sum_{i,j=1}^{N^2} h_{ij}(t) \tilde{L}_i \rho_S \tilde{L}_j^\dagger, \quad (204)$$

where $h_{ij}(t) = \sum_{\alpha,\beta} \left(\tilde{L}_i, W_{\alpha\beta}(t) \right) \left(\tilde{L}_j, W_{\alpha\beta}(t) \right)^*$, which implies both hermiticity and positivity for h_{ij} , as can be seen from

$$\sum_{ij} h_{ij} v_i * v_j = \sum_{\alpha\beta} \left| \left(\sum_i v_i \tilde{L}_i W_{\alpha\beta}(t) \right) \right|^2 \geq 0 \quad \forall N^2\text{-dim. complex vectors } v \quad (205)$$

Inserting Eq. (204) into Eq. (201), we obtain

$$\begin{aligned} \mathcal{L}\rho_S &= \lim_{\varepsilon \rightarrow 0} \frac{1}{\varepsilon} (V(\varepsilon)\rho_S - \rho_S) \\ &= \lim_{\varepsilon \rightarrow 0} \left\{ \frac{1}{N} \frac{h_{N^2 N^2}(\varepsilon) - N}{\varepsilon} \rho_S + \frac{1}{\sqrt{N}} \sum_{i=1}^{N^2-1} \left(\frac{h_{i N^2}(\varepsilon)}{\varepsilon} \tilde{L}_i \rho_S + \frac{h_{N^2 i}(\varepsilon)}{\varepsilon} \rho_S \tilde{L}_i^\dagger \right) + \sum_{i,j=1}^{N^2-1} \frac{c_{ij}(\varepsilon)}{\varepsilon} \tilde{L}_i \rho_S \tilde{L}_j^\dagger \right\} \end{aligned} \quad (206)$$

If we now define and substitute the quantities

$$\begin{aligned} a_{N^2 N^2} &= \lim_{\varepsilon \rightarrow 0} \frac{h_{N^2 N^2}(\varepsilon) - N}{\varepsilon}, \\ a_{i N^2} &= \lim_{\varepsilon \rightarrow 0} \frac{h_{i N^2}(\varepsilon)}{\varepsilon}, \\ a_{ij} &= \lim_{\varepsilon \rightarrow 0} \frac{h_{ij}(\varepsilon)}{\varepsilon}, \quad i, j = 1, \dots, N^2 - 1, \\ \tilde{L} &= \frac{1}{\sqrt{N}} \sum_{i=1}^{N^2-1} a_{i N^2} \tilde{L}_i, \\ G &= \frac{1}{2N} a_{N^2 N^2} \mathbf{1}_S + \frac{1}{2} (\tilde{L}^\dagger - \tilde{L}), \\ H &= \frac{1}{2i} (\tilde{L}^\dagger - \tilde{L}) \end{aligned}$$

into Eq. (206), it has the form

$$\mathcal{L}_{\rho_S} = -\mathbf{i}[H, \rho_S] + \{G, \rho_S\} + \sum_{i,j=1}^{N^2-1} a_{ij} \tilde{L}_i \rho_S \tilde{L}_j^\dagger. \quad (207)$$

Now using the trace-preservation property again, we find that

$$0 = \text{tr}_S(\mathcal{L}_{\rho_S}) = \text{tr}_S \left\{ \left(2G + \sum_{i,j=1}^{N^2-1} a_{ij} \tilde{L}_j^\dagger \tilde{L}_i \right) \rho_S \right\} \Rightarrow G = -\frac{1}{2} \sum_{i,j=1}^{N^2-1} a_{ij} \tilde{L}_j^\dagger \tilde{L}_i, \quad (208)$$

which gives the **first standard form of the generator**:

$$L_{\rho_S} = -\mathbf{i}[H, \rho_S] + \sum_{i,j=1}^{N^2-1} a_{ij} \left(\tilde{L}_i \rho_S \tilde{L}_j^\dagger - \frac{1}{2} \{ \tilde{L}_j^\dagger \tilde{L}_i, \rho_S \} \right). \quad (209)$$

Since the coefficient matrix $(a)_{ij}$ is positive, we can diagonalize it using some unitary U :

$$U a U^\dagger = \begin{pmatrix} \gamma_1 & & & \\ & \gamma_2 & & \\ & & \ddots & \\ & & & \gamma_{N^2-1} \end{pmatrix}, \quad (210)$$

where the Eigenvalues γ_i are non-negative. We then set $\tilde{L}_i = \sum_{k=1}^{N^2-1} U_{ki} L_k$ and obtain the Lindblad Master Equation from Eq. (196) with the simplification that $\alpha = \beta$:

$$\dot{\rho} = -\frac{\mathbf{i}}{\hbar}[H, \rho] + \sum_{i=1}^{N^2-1} \gamma_i \left(L_i \rho L_i^\dagger - \frac{1}{2} (\rho L_i^\dagger L_i + L_i^\dagger L_i \rho) \right). \quad (211)$$

In order to model dynamics following a master equation, there are in general two things we can do: Either solve the Master Equation for the generator, such that the propagation is merely the application of a matrix multiplication, which is, in general, impossible for all practical purposes because of the exponential growth of the state space of composite systems and cannot be performed for systems with more than eight qubits. On the other hand, it may be possible to find a suitable, iterative computational scheme integrating Eq. (196) for small time steps (i.e., controlling the truncation error) as we will present in Chapter 5 about the Monte Carlo Time-Dependent Variational Principle.

Part 2

Monte Carlo Dissipation Models

A Monte Carlo Time-Dependent Variational Principle

1. Motivation

We put it as bluntly as it is stated in the research paper [163] this chapter is based on: Quantum many-body systems are hard to solve. In the preliminary chapters we have seen that one of the most fundamental features quantum mechanics exhibits is that – in stark contrast to classical systems – its state space grows exponentially in degrees of freedom when particles are added.

This might seem exaggerated at first, but in fact the interaction of the sheer number of degrees of (quantum) freedom a many-body system possesses, together with the observations of entanglement monogamy and the fact that quantum systems can be easily frustrated, gives rise to a very peculiar conclusion: Macroscopic behavior emerges from the fact that quantum coherence of 10^{23} particles is, for all practical purposes, impossible. Put into the perspective of quantum information physicists who aim to work with open systems, this seems daunting at first: Even relatively small systems of $\mathcal{O}(10)$ particles cannot be treated coherently in classical computers. But it is precisely this domain of scale that still lies in the quantum regime, although it seems that one would already expect classical, macroscopic effects.

While research of entanglement behavior and area laws [79] has shown that most highly entangled states are not of physical relevance [44, 131], for computational physics they are a hindrance nevertheless: without understanding in excruciating detail *which* precise degrees of freedom are relevant to the comprehension of a system and its behavior, we have to crunch through an exponential number of parameters.

However, physicists never enjoy brute force. The Time-Dependent Variational Principle and the extension we are about to propose highlight this in striking elegance: they allow nothing less than to declare beforehand how many degrees of freedom the experiment will include. Albeit, always with the underlying agenda that the tradeoff between accuracy of the approximation and computational cost should turn in our favor.

As such, this chapter derives and benchmarks an extension to the TDVP to allow the treatment of dissipative dynamics. Though, dissipative systems, due to the fact that they necessitate the use and simulation of mixed quantum states, are even harder to treat numerically because of the same reasons stated above, albeit exaggerated by nature itself: From previous research it is totally clear that dissipation either lacks a clear way to define the information distance [107] if treated with variational methods like the TDVP, or worse, cannot be treated in the necessary detail for a large number of particles, e.g. when using Quantum state diffusion [65] or Monte Carlo sampling [21] – whereby “large” refers to the fact that exact numerical treatment cannot ever hope to examine more than $\mathcal{O}(10)$ particles, because the number of parameters of a density operator for only ten qubits is already $2^{2 \times 10} \approx 10^6$.

The principal complication of mixed state treatment will be circumvented by not aiming to store the entire density matrix of the many-body systems in question, but rely on the already presented framework of Matrix Product States in the following way: Adding dissipation to a system that is represented as an MPS seems contradictory, because product states are of course given in a product basis, and consequently, cannot be mixed. This means that, whenever something “interesting” happens to the system, we are confronted with the choice to either restore the canonical form (see Theorem 8 of Chapter 2) or inflate the variational parameter space. We show that one can derive a numerical scheme that allows to trace the behavior of the tangent vector on the variational manifold for dissipative actions and that it furthermore can be projected in a way similar to the standard TDVP.

After the derivation, we discuss the performed implementation of the method and explain the benchmarks to verify its working accuracy by treating XXZ-Heisenberg chains, quasi-homogenous models and a KX-Heisenberg chain with particle numbers of order $\mathcal{O}(100)$ in Chapter 6. In order to highlight the significant improvement that can keep up with the advancing approaches of experimentalists to scale the number of directly accessible quantum degrees of freedom in controlled lab experiments [40], we show how to adapt the method for the treatment of spinless Fermi-Hubbard models in Chapter 7.

2. Derivation of the method

Before starting with the derivation of the dissipative Time-Dependent Variational Principle, let us find an intuition first: What we are trying to do seems counterintuitive at best, if not outright impossible. Matrix product States are, as the name says, product states. But if the action we impose on the system is non-unitary, there will inevitably be *some* product states that are mapped to mixed states via the time evolution of the dissipation. Put the other way around: Product states in general will not capture the dynamics governed by the Quantum Master Equation (see Eq. (196)) and we shall quickly see why. Choosing a substitution of the form

$$Q = -iH - \frac{1}{2} \sum_{\alpha} L_{\alpha}^{\dagger} L_{\alpha}, \quad (212)$$

we can subsequently write the Master Eq. (196) as

$$\partial_t \rho = Q\rho + \rho Q^{\dagger} + \sum_{\alpha} L_{\alpha} \rho L_{\alpha}^{\dagger}. \quad (213)$$

We hereby restrict ourselves to cases where $\alpha = \beta$, i.e. the Lindblad operators do not mix with each other. The solution of Eq. (213) can then, by invoking the time evolution propagator $e^{t\mathcal{L}}$ certainly be stated as

$$\dot{\rho}(t) = e^{t\mathcal{L}} \rho(t), \quad (214)$$

if only we know the generator (or superoperator) \mathcal{L} – a task that is the particular challenge of dissipative dynamics, since it involves diagonalizing a matrix with $\dim(\mathcal{H})^2$ elements – which is completely hopeless for systems of practical relevance, even if the dissipative part would vanish. Nevertheless, exact diagonalization can serve both as a benchmark and certificate of the correctness of the method we are about to present.

By now we can already rule out the possibility to just use the Time-Dependent Variational Principle as a tool to solve this equation, because the truncation error we make by fixing a bond dimension, i.e. the number of Schmidt coefficients, will grow exponentially fast, just like the degrees of freedom of the density matrix [107].

Now, while we realize that the standard solution to this equation of motion cannot be computed right away, we *can* give at least the form of it. Given that

$p(\bar{a}, a)$ represents the probability distribution of some (holomorphic) variational parameters \bar{a}, a of the hypothetical solution $|\Psi(\bar{a}, a)\rangle$, we write

$$\rho = \int_{\mathcal{M}} p_t(\bar{a}, a) |\Psi(\bar{a}, a)\rangle \langle \Psi(\bar{a}, a)| d\bar{a} da \quad (215)$$

and hence

$$\partial_t \rho = \int_{\mathcal{M}} \partial_t p_t(\bar{a}, a) |\Psi(\bar{a}, a)\rangle \langle \Psi(\bar{a}, a)| d\bar{a} da \quad (216)$$

to get a full expression for the solution. Although one can formally demand that p be a proper probability distribution, $\int_{\mathcal{M}} p_t(a, \bar{a}) da d\bar{a} = 1$, it cannot be computed explicitly for the same reasons $\dot{\rho}$ cannot be obtained as stated above. We can, however, take samples from it using the TDVP as is explained in the following paragraphs. In fact, if we substitute the Master Equation into the integrand, we can see that we can solve terms of the form ρA^\dagger and $A\rho$ with the ansatz

$$Q\rho = \int p_t Q |\Psi\rangle \langle \Psi| d\bar{a} da, \quad (217)$$

because that is precisely the integration performed in the standard TDVP. We substitute Eq. (140) from Chapter 3 and find that

$$Q\rho \doteq \int p_t \sum_j Q_j |\partial_j \Psi\rangle \langle \Psi| d\bar{a} da \quad (218)$$

$$= \int \frac{\partial}{\partial a^j} (p_t Q_j) |\Psi\rangle \langle \Psi| d\bar{a} da, \quad (219)$$

and accordingly for ρQ^\dagger :

$$\rho Q^\dagger \doteq \int \frac{\partial}{\partial \bar{a}^j} (p_t \bar{Q}_j) |\Psi\rangle \langle \Psi| d\bar{a} da, \quad (220)$$

This is all fine, since the terms are linear in A and give the desired expressions for the TDVP tangent vectors from Eq. (147). However, there is no sufficient integration scheme according to the TDVP for the $Q\rho Q^\dagger$ part of the Master equation, because we need to differentiate twice:

$$Q\rho Q^\dagger \doteq \int \frac{\partial}{\partial a^j} \frac{\partial}{\partial \bar{a}^k} (Q^j \bar{Q}^k p_t) |\Psi\rangle \langle \Psi| d\bar{a} da \quad (221)$$

A priori, we can only make general observations about the integral. It is obviously well-defined if the variational manifold we are talking about is isomorphic to the full Hilbert space, because that would make it identical to direct diagonalization. If we however want to restrict the variational manifold \mathcal{M} to a certain bond dimension, this is no longer clear.

At this point it becomes a bit tricky to explain the inference step that had to be taken to be able to solve the problem. Let us take the following perspective: The ensemble consisting of $|\Psi(\bar{a}, a)\rangle \langle \Psi(\bar{a}, a)|$ consists of pure states for all possible values of a and \bar{a} , but can be understood as a mixed state representation if one considers convex combinations of them. Sampled from the underlying probability distribution p_t that explicitly shows up in Eq. (216), this can be integrated implicitly by assuming a well-defined measure over the probability distribution. If the variational manifold is smaller than the Hilbert space dimension, this measure is undefined, hence the integration cannot be performed. In fact, the situation technically is even worse: Not only do we not know the measure of the probability distribution p_t for a given bond dimension $d < \dim(\mathcal{H})$, we do not even know the distribution itself. If we knew it, there would be a straightforward solution: Take samples from it and integrate using a Monte Carlo integrator. Actually, this

technique has been applied by Overbeck et al. in [133] to some effect. The clear downside of this ansatz stays however: One has to endure particularly hard analytics to get an estimate for p_t , and even then it is still hard to bound the error. Obviously, guessing the probability distribution in order to sample from it does not work in general if we do not want to give up the primary aim of this endeavor, reducing computational complexity by reducing the variational parameters.

What we did instead was to step back one step further. Treating unknown probability distributions is daunting, but can lead to new insights, like the following. Instead of guessing the distribution ourselves, in some sense we can have nature do the hard work for us: If we consider the probability distribution to be a random variable, we can answer what principal distribution it ought to have: Invoking the Glivenko-Cantelli theorem from Chapter 4, we know that the distribution of distributions is normal. As such, we do not have to concern ourselves with the derivative distribution we sample from, but instead identify the random variable $p_t \approx |\Psi(\bar{a}, a)\rangle \langle \Psi(\bar{a}, a)|$ with the variational parameters a and \bar{a} .

Before giving the exact ansatz we will finally use, let us briefly review the expectation value of a function of a random variable described by Ito's Lemma:

$$\begin{aligned} \frac{d}{dt} \langle f[x(t)] \rangle &= \left\langle \frac{df[x(t)]}{dt} \right\rangle \\ &= \left\langle A[x(t), t] \partial_x f + \frac{1}{2} B[x(t), t]^2 \partial_x^2 f \right\rangle, \end{aligned} \quad (222)$$

where now $x(t)$ is a random variable, while again $A(x, t)$ models the drift and finally $B(x, t)$ represents the diffusion coefficient. If we evaluate $x(t)$ according to the conditional probability density $p(x, t|x_0, t_0)$ with initial conditions (x_0, t_0) , then

$$\begin{aligned} \frac{d}{dt} \langle f(x[t]) \rangle &= \int dx f(x) \partial_t p(x, t|x_0, t_0) \\ &= \int dx \left[A[x(t), t] \partial_x f + \frac{1}{2} B[x(t), t]^2 \partial_x^2 f \right] p(x, t|x_0, t_0). \end{aligned} \quad (223)$$

The expression from Eq. (221) now has to be evaluated as a stochastic integral. For this purpose $f(x)$ has to be differentiable twice and $p(x, t)$ has to be differentiable at least one time. We give practical justifications at the end of the argument. Now, in order to evaluate Eq. (223), we use continuity of f to write down the principal value integral

$$\lim_{x_0 \rightarrow x} \int_{|x-x_0| > \varepsilon} dx f(x, x_0) \equiv \int dx f(x, x_0). \quad (224)$$

But then, Eq. (223) is well-defined so long as $p(x, t|x_0, t_0)$ is a proper probability distribution and once differentiable. This can safely be assumed because the quantum state space is convex and continuously connected. But since that is the case, we can use the reasoning we already mentioned in the derivation of eq. Eq. (178) and integrate by parts over f :

$$\begin{aligned} \int dx f(x) \partial_t p(x, t|x_0, t_0) &= \int dx f(x) \left\{ -\partial_x [A(x_0, t) p(x, t|x_0, t_0)] \right. \\ &\quad \left. + \frac{1}{2} \partial_x^2 [B(x_0, t)^2 p(x, t|x_0, t_0)] \right\} \\ &\quad + \text{surface terms.} \end{aligned} \quad (225)$$

This is almost the desired solution, but we have to give an argument why one can discard the surface terms that arise from partial integration. It is precisely the fact that $p(x, t)$ is a probability distribution that helps us again: For any non-singular, finite range R of $\int dx f(x) \partial_t p(x, t|x_0, t_0)$, it is thus clear that the

conditional expression $p(x, t|x_0, t_0)$ vanishes unless both $x \in R$ and $x_0 \in R$. But we can choose f such that this is the case.

Heuristically, this models the fact that the conditional probability $p(x, t|x_0, t_0)$ could change discontinuously if x_0 crossed the boundary of the sampling region R . But since we will in general choose R to be the quantum state space itself (or a subset thereof), any states outside are either unphysical or not part of the variational class, such that we can indeed safely ignore them. As such, no transitions will occur over the boundary of R and the surface terms can be discarded as proposed.

Comparing this to Eq. (180) we can immediately see that they are equal:

$$\partial_t p = -\partial_x[A(x, t)p] + \frac{1}{2}\partial_x^2[B(x, t)^2 p], \quad (226)$$

which is precisely the Fokker-Planck equation from Chapter 4 and can be treated accordingly: The evolution of p is governed by drift A and diffusion B . The intuition of this is that, compared to the standard solution of the Fokker-Planck equation Eq. (181), the hermitian part $H - \mathbf{i}L_\alpha^\dagger L_\alpha$ is constituting the drift coefficient, whereas the action of the Lindblad operators L_α governs the coefficients of diffusion and Wiener process.

We now know that the problem has a solution, but we still need to derive the new form of the TDVP flow equations. First of all, we need to adapt the language of a multivariate process: we treat complex variables $x^j \in \mathbb{C}$, such that the respective solution takes the form

$$dx^j = r^j(\bar{x}, x, t)dt + U_\alpha^j(\bar{x}, x, t)dw_\alpha, \quad (227)$$

with $dw_\alpha = \frac{1}{\sqrt{2}}(du_\alpha + idv_\alpha)$ being complex Wiener processes constructed by complex linear combination from two real Wiener processes du_α, dv_α such that

$$\langle dw_\alpha \overline{dw_\beta} \rangle = \delta_{\alpha\beta} dt \quad \text{and} \quad \langle dw_\alpha dw_\beta \rangle = 0. \quad (228)$$

Now we can put in the variational ansatz for p_t into Eq. (225), to see whether the TDVP can produce the correct drift and diffusion quantities. In fact, the vectors $Q|\Psi(a)\rangle$ and $L_\alpha|\Psi(a)\rangle$ are expressed as $b_Q^j \partial_{a^j} |\Psi(a)\rangle$ and $b_\alpha^j \partial_{a^j} |\Psi(a)\rangle$ by use of Eq. (140) and give the desired result:

$$\partial_t \rho_t = \int_{\mathcal{M}} [-\partial_{a^j}(p_t b_Q^j) - \text{c.c.} + \partial_{a^k} \partial_{\bar{a}^l} (b_\alpha^k \overline{b_\alpha^l} p_t)] \times |\Psi\rangle \langle \Psi| d\bar{a} da. \quad (229)$$

We check that the RHS of Eq. (229) has the same form as Eq. (225). We can thus read off the corresponding Fokker-Planck equation for p_t :

$$\partial_t p_t = -\partial_{a^j}(p_t b_Q^j) - \text{c.c.} + \partial_{a^k} \partial_{\bar{a}^l} (b_\alpha^k \overline{b_\alpha^l} p_t). \quad (230)$$

and obtain for the variational parameters a

$$da^j(t) = (b_Q^j + \langle \bar{L}_\alpha \rangle b_\alpha^j) dt + b_\alpha^j dw_\alpha(t), \quad (231)$$

where, again, we are interpreting a as a random, stochastic variable.

It is also of particular noteworthiness how one could have naïvely chosen an ansatz of the form $a = b_Q dt + b_\alpha d\omega_\alpha$, where $d\omega_\alpha(t)$ is a complex Wiener process (white noise), corresponding to the linear expression $d(|\psi\rangle) = Q|\psi\rangle dt + L_\alpha|\psi\rangle d\omega_\alpha$, but it would fail to produce correct results, because it treats the variation on the level of pure states (i.e. wave functions) only. Instead, we need to evaluate the differential for the density operator $d(|\Psi(\bar{a})\rangle \langle \Psi(a)|)$, essentially a *product of two random variables*, and therefore again subject to Itô's Lemma:

$$d(|\psi\rangle \langle \psi|) = |d\psi\rangle \langle \psi| + |\psi\rangle \langle d\psi| + L_\alpha |\psi\rangle \langle \psi| \bar{L}_\alpha dt. \quad (232)$$

The derivation of the “magic” term $\langle \bar{L}_\alpha \rangle b_\alpha^j$ can also be found in the Quantum State Diffusion [65] method by Gisin and Percival that aims to use the same stochastic

differential equation, albeit in full Hilbert space instead of a variational manifold. This has the benefit of maximal accuracy, but of course scales unfavorably with the number of particles.

By numerically integrating Eq. (231) we can evolve a pure state component $|\Psi(a)\rangle$ of some initial ρ such that it samples the evolution of the full mixed state. Using M such samples, properties of ρ_t can be approximated with an error (variance) that scales as $1/\sqrt{M}$, multiplied by the truncation error of the MPS ansatz, both of which can be controlled: While the stochastic error in practice can be made arbitrary small by using enough (parallel) processes, the MPS error can be bounded like in [72, 73].

In Fig. 10 we show the adapted TDVP scheme: instead of only propagating the unitary time evolution step $H|\Psi(a)\rangle$, additional tangent components are calculated from the evaluation of the Lindblad tangent vectors $L_\alpha|\Psi(a)\rangle$, weighted by a random process of Wiener form. This gives rise to a different perspective altogether: One can understand the random process underlying the Lindblad actions as a resource that drives the system into equilibrium. We also can be sure that this does not suffer from local minima, because the total tangent vector is the sum of unitary and Lindblad part. I.e. even if one of the constituents of the tangent vector vanishes, it only slows down the convergence of the evolution.

This approach has two main benefits: First of all, sampling the trajectories of successive tangent vectors (with intermediate projections to the variational manifold, of course) can be done in parallel. In contrast to other dissipative methods, the **Monte Carlo Time-Dependent Variational Principle (MCTDVP)** does not require longer computation times due to the fact that we can evaluate sampled evolution paths independently. The price we pay for this is quadratic expense in total computational cost due to the stochastic standard deviation scaling with $1/\sqrt{N}$. Computation power, if not needed as single-core application, has become increasingly cheap, however. In the following section we present a scheme to efficiently compute dissipative dynamics using a parallel and distributed computation approach in Python.

3. Algorithm and implementation

We proceed by sketching the algorithm and then take a detailed look at each step.

3.1. Preparations

Before giving the formulation of the iterative scheme that lets us evolve dissipative systems, we need to choose a suitable variational class. As we have seen, the choice of variational parameters need not be straightforward. While we can always decide on a bond dimension for a specific problem, this does not address computational considerations: While we can be sure that a bond-dimension of 16/24/32 and above will yield accurate results in most of the cases, values of even four or six may prove sufficient to capture the *relevant* dynamics. Obviously, the algorithm cannot make this choice for the operator. On the other hand, even for a well-educated physicist any decision must be based on experience and intuition rather than area laws alone. Finding the best tradeoff between computation time and accuracy is an art not to be underestimated and depends highly on the system itself, on its symmetries and interactions. The usual way of dealing with this challenge is to use both a very small system and hoping for limited finite-size effects as well as taking educated guesses about the entanglement behavior of the system. The aim is therefore to increase the number of parameters in a way that we can check the general behavior in small systems before starting the week-long calculations, that better be with the

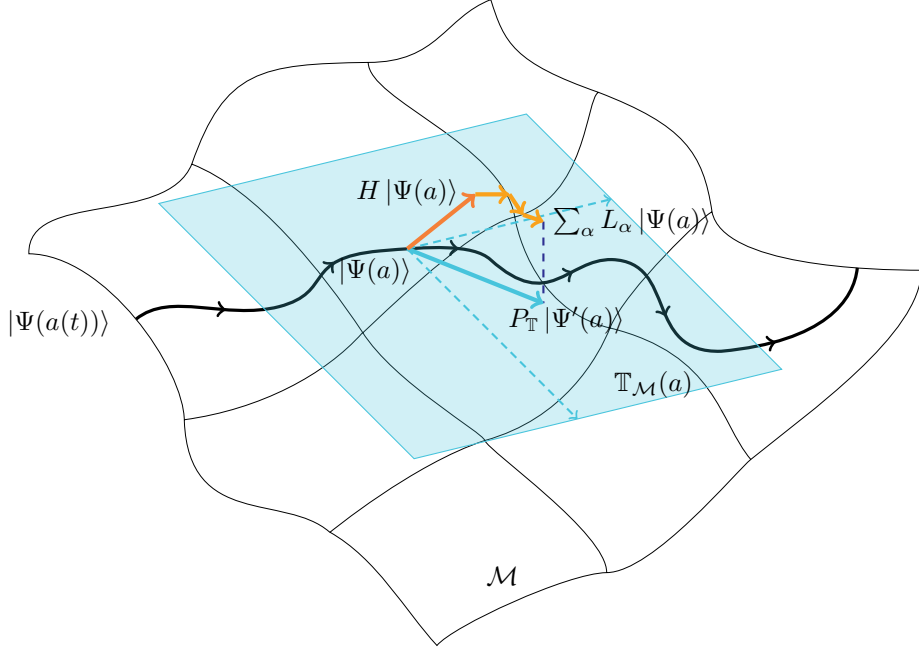


FIGURE 10. **Pictorial illustration of the variational manifold \mathcal{M} and its tangent plane \mathbb{T} under consideration of the Monte Carlo Time-Dependent Variational Principle.** Additional tangent vectors are calculated for the (randomly simulated) action of the dissipative Lindblad terms L_α on the state $|\Psi(a)\rangle$ and subsequently added to the Hamiltonian tangent vector $H|\Psi(a)\rangle$, resulting in a different position for the resulting approximation of the total time evolution $|\Psi'(a)\rangle$.

correct parameter choices. This includes the drudgery of checking all observables and basis choices.

3.2. Iteration step

After a suitable initial Matrix Product State has been constructed (or, as we will see, randomly sampled), we make sure the vector a^j of variational parameters has the canonical form, correct normalization etc. We then apply the following steps in order:

- (1) Evaluate Eq. (231) and set $a^j(t + dt) = a^j(t) + da^j(t)$.
- (2) Normalize $|\Psi(a)\rangle$ and restore the canonical form for a^j .
- (3) Calculate expectations of interest and go back to step 1.

Let us look at the steps in detail. First of all, we cannot compute $a^j(t + dt) = a^j(t) + da^j(t)$ directly, because it would be inefficient computationally, i.e. of order $\mathcal{O}(D^6)$. Instead, we need to calculate the two auxiliary quantities K and C , similarly to the way they are given in Eq. (153) and Eq. (155). However, since we are dealing with a Master equation, we have to adapt the instances of the TDVP where in coherent systems only the Hamiltonian factors in.

More concretely, this means that H is replaced by the expression Q : expression Q :

$$K' - \sum_{s=1}^d a^{s\dagger} K' a^s + \text{tr}[K' r] l = [(l|H_{aa}^{aa}) - hl], \quad (233)$$

$$\text{with } [(l|H_{aa}^{aa}) = \sum_{stuv} \langle st|h|uv \rangle (\bar{a}^s \bar{a}^t)^\dagger l(a^u a^v), \quad (234)$$

where K' is now defined as $(K'| = (l|Q_{aa}^{aa}(1 - E)^{-1}$.

Consequently, the auxiliary quantity C has also to be adapted:

$$C'^{st} = \sum_{uv} \langle st|q|uv \rangle a^u a^v, \quad (235)$$

where $h \rightarrow q$ substitutes the nearest-neighbor parts of the Hamiltonian with those from Q .

It should be noted that this simple substitution is only valid for nearest-neighbor interactions, and as such also the L_α s have to act on nearest neighbors only. This restriction can be lifted by applying Matrix Product Operators instead, but has the tradeoff of slightly higher complexity [185]. We considered changing the Gram matrices to accommodate for the more complicated impact of long-range-interacting Lindblad operators, but decided that the gain was not worth the effort because with MPOs one can study both long-range-interacting Hamiltonians and dissipations of Lindblad-type.

As a final modification, the tangent vectors b_α^j have to be multiplied by samples from a complex Wiener process dW_α . Since SciPy has built-in support for the normal distribution, all we need to do is make a call of the `random.normal()` subroutine and feed it with the correct mean $\mu = 0$ and variance $\sigma = \sqrt{dt}$.

Going forth, we see that the actual application of the TDVP does not change by adding dissipation. However, we did not yet discuss the fact that through adding the Monte Carlo part, the final result is much less accurate than for coherent real-time evolution in the TDVP, and we have to consider the variational parameters themselves as random variables. As such, the answer of the question we probe can only ever be the ensemble average of many instances of it.

There are two important points to clarify. First of all, we need to express what changes we make to the method in the Monte Carlo setting. While easy to state, the scope of the consequences is massive. We will have to evolve many sampling paths such that we can take the average, just like with every other Monte Carlo method. Luckily, we can perform all of these samples in parallel, given enough computational resources. It is worth noting though that compared to direct diagonalization the complexity is relatively tractable. Of course the tradeoff is skewed by the fact that we compare complexity of a deterministic process with a stochastic process. This means in particular that although the MCTDVP can provide accuracy at an acceptable level *on average*, there may be instances where this is not the case, but they are exponentially suppressed by the fact that for each time step we do not only sample one random number but rather a number of order of the bond dimension. Effectively this means that convergence of non-critical systems actually improves with more Lindblad operators due to the fact that more entanglement is produced which can act as accelerating the driving toward a steady state if one exists.

By the way, the last remark is not connected to criticality as it can be shown that solving critical systems itself is complicated for a multitude of theoretical reasons based on the spectral theorem – it is a simple observation that just like nature itself is not able to unravel critical systems, neither diagonalization nor the MCTDVP would do particularly well.

The question of the starting distribution, however, depends solely on the application at hand. If, like most of the times, we are looking for the steady state of a driven system, we expect that the initial configuration does not play a role with regards to the results, but it does influence the convergence time. Just like any other variational method, starting from a very entangled state far from equilibrium means that convergence will be slow. Still, even if convergence is slow, we can be certain to reach a global minimum. Thus, we can take the approach to just randomly generate states, if we don't have a precisely defined starting state, e.g. if we explicitly *want* to model dissipation from maximally mixed states.

As an aside mention, why do we evolve each *path* along the variational manifold **separately** instead of *taking averages after each step*? If we remember the ansatz for the mixed state distribution in Eq. (216), we can see that the underlying probability distribution is unknown. It is certainly true that an average of mixed states will with measure one be a mixed state again. Although the Time-Dependent Variational Principle is a scheme of evolving tangent vectors along the variational manifold, the average of tangent vectors need not necessarily be a tangent vector if the variational class does not span the full Hilbert space, i.e. the bond dimension is finite. If we are, on the other hand, to take the average of all projections of the tangent vectors, we find that the quantity

$$\bar{\rho}(t) = \frac{1}{M} \sum_{k=1}^M \rho_k(t) = \frac{1}{M} \sum_{k=1}^M |\Psi(a^k(t))\rangle \langle \Psi(\bar{a}^k(t))| \quad (236)$$

is well-defined. But taking averages after each time step means that we have to sample the Monte Carlo paths of the evolution not only in parallel, but synchronously. Instead we find that by the law of large numbers Eq. (194), the average of many trials will be close to the expectation value and we can conclude that

$$\langle \rho(t) \rangle = \lim_{k \rightarrow \infty} \bar{\rho}_k(t), \quad (237)$$

which allows us to compare expectations. This applies to all operators A measured by tracing over the state as $\text{tr}(\rho A)$, which allows us to apply measurements by measuring one sample and then averaging over all sample paths.

It is fortunate that all relevant results from this methods will always be averages of expectations, because it allows us to evolve sampling paths independently, as we see in the next section.

3.3. Distributed computation and sampling

By now we have explained in detail how one evolution, or *sampling path* can be obtained by splitting the master equation into drift part proportional to Q and a diffusion governed by $L_\alpha d\omega_\alpha$ and how the TDVP iteration step basically stays the same since we can come up with an adapted way of calculating the tangent vector to the variational manifold. However, this evolution is not very accurate from the perspective of a single sample path. Instead, we have to take the average over many instances due to the stochastic nature of the Wiener process: The sampled time evolutions will converge in mean-square only. While all of this process can be done sequentially by calculating one sampling path after the other, it is much more time efficient to evolve paths *in parallel*.

As mentioned in [16], the possibility, given enough computers, to evolve all sample paths at once, opens up to treat problems of this form in an “embarrassingly parallel” manner – basically, we can solve problems susceptible to this possibility much faster than sequential methods, if we can only control the computation time of the single instance. And indeed, this is the case: For dissipative dynamics as proposed, we can have calculation times of a single evolution path comparable to

coherent Hamiltonian real time evolutions up to a factor of the number of Lindblad operators, which will in general, i.e. for practical systems of interest, be of order $\mathcal{O}(10)$, if at all.

To exploit this feature of massive parallelizability we not only implemented the approach to simulate dissipative dynamics given in Section 3.2, but also used the Python programming language to build a framework allowing us to compute sample paths in a scalable manner.

Before giving the details, we take a look at the general framework:

- (1) Start the computation server and give a first number M of the sample paths to calculate.
- (2) Start the job queue subroutine and wait for computation clients to connect.
- (3) Once a client is connected, ask for the number of cores available at the machine and send an appropriate number of jobs.
- (4) Whenever a job is marked as finished, collect the results at the computation server and send out more jobs until M jobs have been started.
- (5) Wait for all jobs to terminate.
- (6) Wait for the operator to either start more jobs or execute the post-processing subroutine.

It is worth noting how this framework [121] gives maximal freedom to the operator, i.e. the physicist performing the simulation: At any stage of the process he has full access to the set of results, i.e. finished time evolutions and can decide to add more samples or export a result set to perform post-processing analyses, i.e. averaging and plotting of results. The only downside is that a time evolution, once finished, cannot easily be resumed.

The way the abstraction layer of the scheduler works is that of a standard “client-server” model: At the host computer we start the corresponding python program that will open a TCP/IP port at the network level and listen for connections. This is a fully transparent implementation using python’s multiprocessing package. The *evoMPS* dissipative multiprocessing extension includes the server executable as well as the corresponding client program.

Whenever we speak of “sufficient computational resources”, in the context of the *evoMPS* dissipation extension this means we need access to $\mathcal{O}(10)$ standard desktop computer systems with no special features apart from network access. For the purpose of this thesis the maximal arsenal of computers was about three older MacPro machines, two high-power computation servers with up-to-date (i.e. E5-2687W as of the year 2015) Intel Xeon processors and various notebook computers. One of the beauties of distributed, load-balanced computational grids is that there is no need for comparable hardware. Much like the distributed computation network BOINC (see [169]), any machine that can run Python with its SciPy and NumPy packages can contribute to the calculation of hundreds of sample paths of a single “experiment” – although of course faster hardware, as usual, is always better. (Note that even though the LAPACK [27] and openBLAS [26] libraries can substantially speed up the computations, they are not strictly necessary. Every line of code is written in such manner that the number-crunching back-end does not rely on optimizations available.)

In detail this means that the server has three kinds of queue modules running: First, the job queue where every sample path subroutine is stored along with the observables and the return format until a client connecting to the server picks some of them up. Second, the result queue, where clients can put the results of the sample path routines they ran. Third and finally, there is a meta queue that can be used to communicate with individual processes, e.g. for improving load balancing

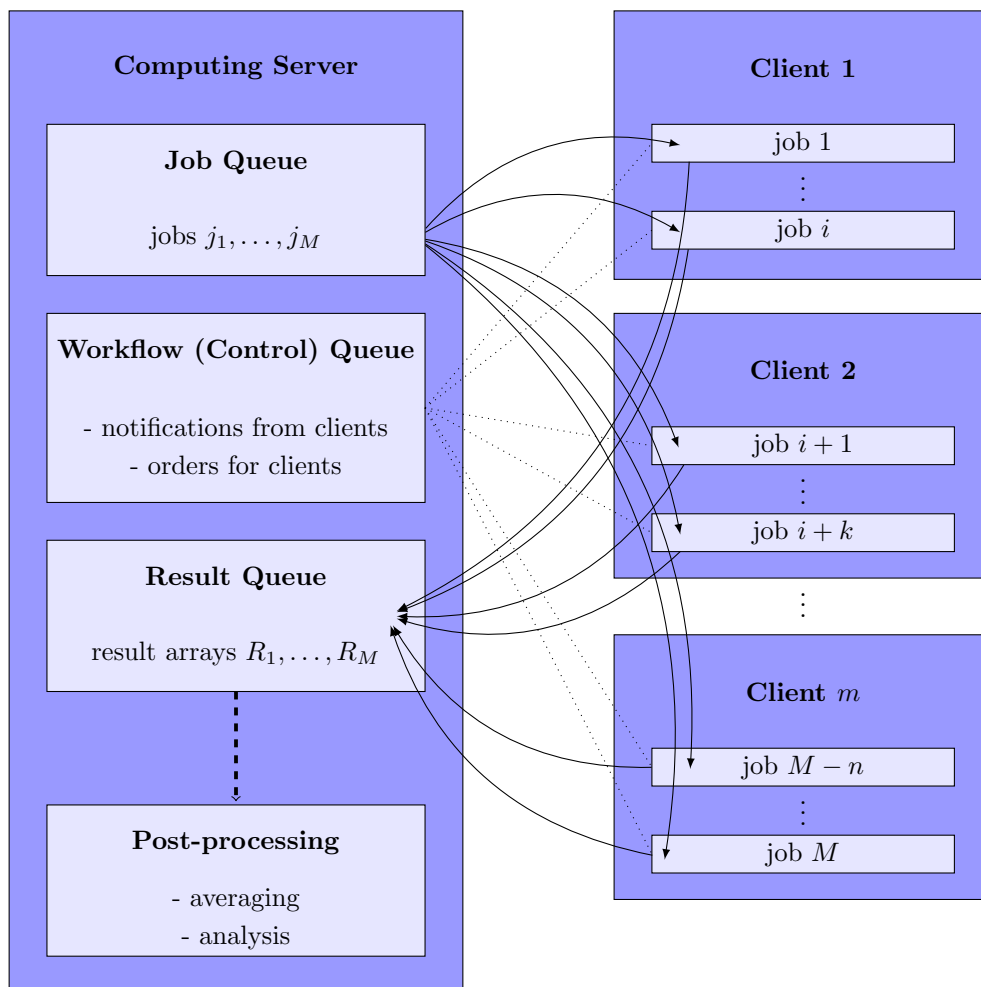


FIGURE 11. **Working of the distributed computing scheduling process.** The clients $\{1, 2, \dots, m\}$ obtain their jobs $\{1, \dots, i\}, \{i + 1, \dots, i + k\}, \dots, \{M - n, \dots, M\}$ from the specific queue, deposit the results in the result queue, while the logistics like load balancing are handled by the workflow queue. After enough results are calculated, post-processing is performed on the server.

or handling crashes. If there is a fixed number of samples we want to calculate, this should be done in the most efficient manner. That is, if the queue is empty, but we did not get enough results because there went something wrong with regards to network connectivity the operator should not need to manually add new jobs, but within these narrow bounds of scheduling the calculation server can handle some exceptions on its own.

3.4. Post-processing and analysis

After all results have been put into the results queue of the server, they can be processed and analyzed, i.e. in general we are going to calculate averages of measurements performed at certain time steps. If, for example, we are observing the convergence behavior of an Ising model, one way of doing this is to measure the system energy at every time step t_i of the evolution and store it in an array of memory positions, such that after the calculation is finished at N steps, we have

M vectors of tuples $(\{t_1, E_1\}, \{t_2, E_2\}, \dots, \{t_N, E_N\})$, one per sample path. From elementary statistics we know how we can calculate the average energy of all the samples: Remember that for a time evolution of $\rho(t)$, we have that

$$\dot{\rho}(t) = e^{t\mathcal{L}}\rho(0), \quad (238)$$

and thus any observable \hat{O} we might want to measure can be calculated as

$$\langle O(t) \rangle = \text{tr} [Oe^{t\mathcal{L}}\rho(0)], \quad (239)$$

such that the average expectation value over M samples simply resolves to

$$\langle \overline{O(t)} \rangle = \frac{1}{M} \sum_{l=1}^M \langle O(t) \rangle_l = \frac{1}{M} \sum_{l=1}^M \text{tr} [O\rho_l(t)] = \frac{1}{M} \sum_{l=1}^M \text{tr} [Oe^{t\mathcal{L}}\rho_l(0)], \quad (240)$$

where $\rho_l(t)$ denotes the state of the l -th sample path at time t . Note however, that we do not have access to the full density matrix at each step, but only the variational parameters a_i . Restoring the density matrix would require to unravel the whole chain of matrix product coefficients – an operation much less efficient than taking expectations as shown in Eq. (98). This should once more illustrate that the standard error of the mean \bar{X} of some random variable X becomes smaller, the more samples we can calculate – leading to the somewhat infamous statement

$$\text{SE}_{\bar{X}} = \frac{s_{\bar{X}}}{\sqrt{N}}. \quad (241)$$

The quantity $\text{SE}_{\bar{X}}$ can be easily misinterpreted as the *true* standard deviation of the sample mean – which itself is defined as $\text{SD}_{\bar{X}} = \frac{\sigma}{\sqrt{N}}$, where σ is the standard deviation of the distribution, not the standard error of the sample ensemble, which is defined as

$$s_{\bar{X}} = \sqrt{\frac{1}{M} \sum_{k=1}^M (X_k - \bar{X})^2}. \quad (242)$$

More concretely this means that we have to distinguish between the *expected values according to the distribution* we are sampling from (i.e. Wiener process based on the normal distribution) versus the *average values we get from actually sampling the ansatz*, that only approximate the “true” mean value.

To put the trade-off between sampling a quadratically growing number of samples and the exponentially growing complexity of direct diagonalization into perspective, we now proceed to present the systems that were actually solved with the method: Given a two-qubit system with $\mathcal{H} = \mathbb{C}^2 \otimes \mathbb{C}^2$, we define $H_{XZ} = \sum_{i=1}^{N-1} \sigma_i^x \sigma_{i+1}^x + \lambda \sigma_i^z \sigma_{i+1}^z$ together with dissipative dynamics of the form $L_\alpha = \sigma_\alpha^+ \forall \alpha$. Choosing a highly entangled MPS (within the constraints of the bond dimension), we can cross-check the simulation results with exact diagonalization. Indeed we find good agreement for sample number values beginning in $\mathcal{O}(100)$ and above. In Fig. 12, we show the expectation value of the average spin value in z -direction. Another instructive insight might be given by Fig. 13, where we illustrate how an average spin expectation actually looks like: We can see that although each individual sample is subject to random and (heuristically) misleading measurements, the average is much closer to the ensemble expectation and the behavior we *expect* from the experiment.

Usually we dedicate the computation server to fulfill the post-processing as well, because it is not as memory-consuming as the time evolution with high bond dimensions. Thus, it can very well be the case that post-processing a week worth of measurements takes no longer than 30 minutes.

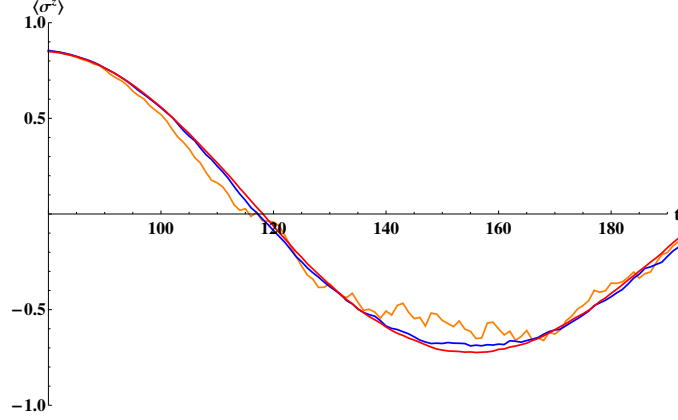


FIGURE 12. **Accuracy scaling of Monte Carlo simulation.** Expectation value of the spin value in a 2-qubit system with average taken over both sites and N samples, where $N \in \{480, 4800, 48000\}$ with yellow, blue and red color, respectively for a time evolution after 80 time steps of discretization size $dt = 0.001$. One clearly observes that the experiments with less samples show considerably more volatility.

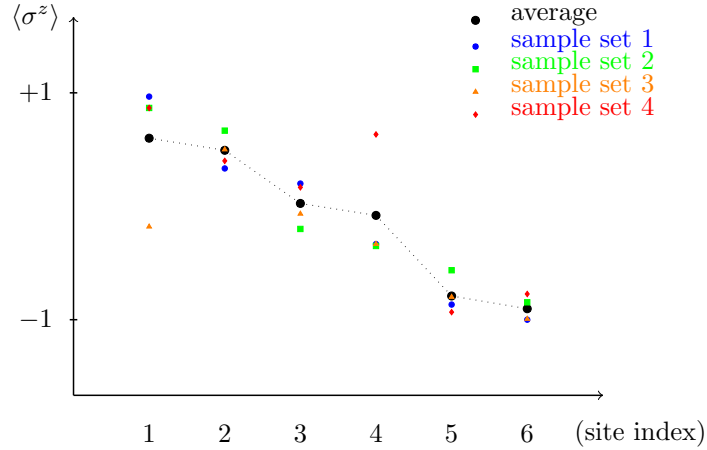


FIGURE 13. **Sample averaging.** Four sample configurations of σ^z -observables of a six-site lattice depicted together with its average value, taken from a system with $N = 6$, $H_{XZ} = \sum_{i=1}^5 \sigma_i^x \sigma_{i+1}^x + \lambda \sigma_i^z \sigma_{i+1}^z$, $\lambda = 1$ after 50 time steps of size $dt = 0.001$ with edge driving $L_1 = \sigma_1^+$, $L_2 = \sigma_6^-$. Although individual measurements may not even qualitatively give the correct behavior, the averages does.

4. Possible extensions

Apart from parametric changes and the aim to treat ever-increasing system size it seems worthwhile to take a different approach. We have shown how a complex problem like diagonalizing the generator of a Master Equation can be segmented into evolving stochastic processes. Still, 1-to-1-mapping of computational problems is a peculiar discipline. The question whether the method can be applied to

other problems than dissipative dynamics arises naturally. While the sampling of unknown probability distributions is undecidable, the idea of mapping the small problem to a larger one, like e.g. entanglement distillation, seems promising in the sense that for the larger problem there may be a different set of tools available.

One such direction could be the research of dynamics treated with Projected Entangled Pair States (PEPS). As an extension to Matrix Product States, PEPS systems aim to model higher-dimensional spin systems with large success [171]. However, much like the TDVP using MPS, also the PEPS formalism cannot defy complexity theory and has to cope with the fact that, as a rule of thumb, every dimension will square the calculation time. Nevertheless we can observe that in two dimensions of (unitary) time evolution one necessarily finds expressions like that of Eq. (221) where the tensor has to be contracted over two indices, leading to a double derivative. Although our approach does not straightaway solve that misery, it is a solid guesswork that sampling over the state distribution could help doing this precise operation more efficiently or at least make it parallelizable, which *in practice* means a speedup for a program that would be calculated sequentially, i.e. monolithic, otherwise.

One more perspective on using noise as a resource is to ask to what extent the presented method can be understood as a pseudo-diagonalization of the system's Lindblad generator. While this sentiment is certainly false for every single time step, this is not necessarily the case for averages of tangent vectors. Although such methods do exist [190, 36, 144], of course, we already know that the tangent projection of the TDVP is optimal. It could thus be worthwhile to investigate whether the existing methods can be improved by this knowledge.

This on the other hand opens up the possibility of turning away from time evolution dynamics toward the study of mixed states and the thermodynamic properties thereof, i.e. phase properties and ground states. By adding support for time-dependent Hamiltonians, the algorithm can already handle adiabatic ground state discrimination by changing the Wiener distribution to a less peaked representation. One would have to check whether the Fokker-Planck equation is a solution of the Master Equation in each individual instance, but that seems like an acceptable trade-off given the fact that the treatment of mixed states is implicit.

Another approach worth mentioning is the split-step integrator proposed in [71] that is based on the Dirac-Frenkel Time-Dependent Variational Principle, which was proposed for Matrix Product States in [73] and would allow for long-range interactions. A priori, there does not seem to be a general reason why this would not be possible with long-range Lindblad operators. Still, we have to keep in mind that in comparison to unitary dynamics a dissipative approach needs to account for the overlap of the jump operators. This could lead to non-optimal projection properties and thus unfavorable convergence behavior even for non-critical systems.

Applications to the Heisenberg model

The first system we investigate both acts as a benchmark and verification example: The spin-1/2 XXZ-Heisenberg model with edge driving has been solved analytically [143] by T. Prosen and is the perfect candidate to replicate and improve established results.

As already mentioned, Heisenberg chains are used to explore magnetic coupling behavior and phase transitions in quasi-local system where we have particles interacting with the next neighbor only.

Here, we explicitly restrict ourselves to cases with no external fields, because in dissipative settings it is often not so easy to distinguish between interactions that can be attributed to a heat bath and those that still change the energy of the system without physical energy transfer, i.e. if we turn off the magnetic field, the total energy of the system will be the same as it was before turning it on, but only if no dissipation irreversibly changed the energy.

Although the matter resorts in some way or the other to preference, adding external fields in this work will be treated by adding Lindblad operators of the respective form. Also, even if more complex systems can be investigated in the lab [128], the limits of homogenous models of Heisenberg or Hubbard form still leave much room for improvement, such that the thorough numerical treatment of systems with particles of mixed and varied characteristics is, unfortunately, still out of reach for extensive settings. For small number of particles, however, direct diagonalization is still the better approach.

1. Introduction

The Hamilton operator for this kind of system with N sites and closed boundary conditions can be given as

$$H = \sum_i^{N-1} \varepsilon [2\sigma_i^+ \sigma_{i+1}^- + 2\sigma_i^- \sigma_{i+1}^+ + \lambda \sigma_i^z \sigma_{i+1}^z], \quad (243)$$

where ε models the total interaction strength and λ models the specific exchange term in z-direction. Note that in general there can be a constant magnetic field of the form $h\sigma_i^z$ that acts locally, but for the matter of this investigation we set $h = 0$. Because all terms represent next-neighbor interaction, we only have $N - 1$ terms, i.e., the 2-local terms model the couplings between two sites of the form $\sum_i O_i \otimes O_{i+1}$, not the 1-local on-site dynamics, which can be included in the next-neighbor formulation as operators of the form $O_i \otimes \mathbb{1}_{i+1}$, like the Lindblad operators L_1 and L_2 that act on the outermost sites only:

$$L_1 = \sigma_i^+, \quad L_2 = \sigma_N^-. \quad (244)$$

Note that we omit all trivial tensor factors of the form $\bigotimes_{k=2}^{N-1} \mathbb{1}_k$ that are necessary to illustrate what the full form of the Lindblad operators on the full Hilbert space looks like.

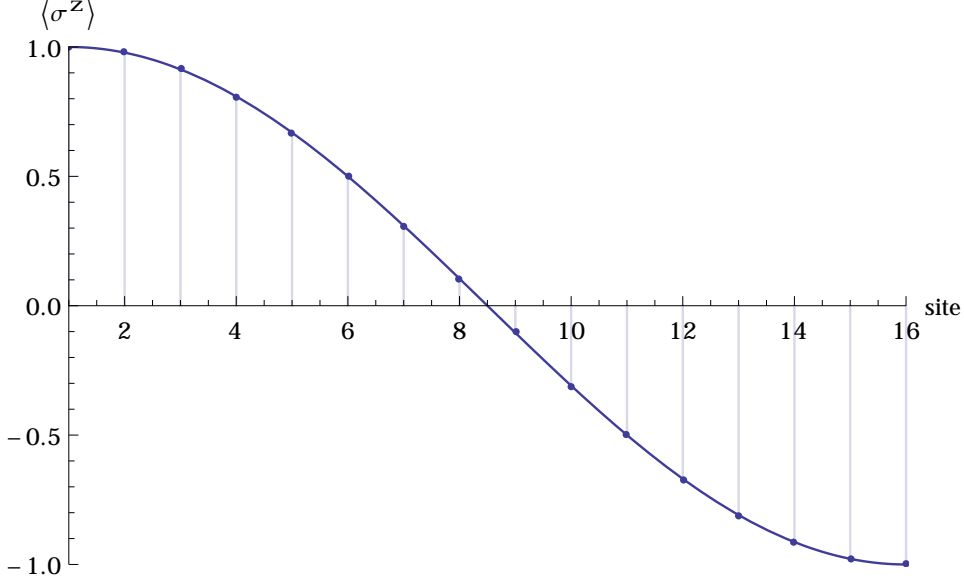


FIGURE 14. **Edge driven Heisenberg XXZ model.** Average magnetization in z -direction for a 16-site XXZ-Heisenberg model with edge driving $L_1 = \sigma^+$, $L_2 = \sigma^-$, interaction parameters $\varepsilon = 1$, $\lambda = 1$, $D = 24$ and 300 samples. The straight line is the analytic solution for the steady state from [143], while the dots are the simulation results.

2. Results for edge-driven models

As can be seen from Fig. 14, the numerical solution for a small number of sites matches the analytics from [143] so well that sampling error bars are below the optical resolution of the plot. In fact, the deviation from the analytic solution is below 10^{-3} at the center, being even more accurate at the edges due to the strong driving regime. Since there are analytics available, the statement that calculation of the results for 16 sites takes less than a day is of little noteworthiness. Still, the *evoMPS* implementation already outperforms exact diagonalization.

It should be noted though that this specific Hamiltonian is a prime example of a critical [173] spin system, i.e. the expected convergence to the steady state is very slow. Even though the TDVP is not stopped by local minima, we observe that the random noise from the Lindblad evolution somewhat amplifies the convergence behavior: While it is true that *on average* the TDVP tangent vectors will point toward an energetically correct direction, in the case of criticality some sample paths will converge very fast, while others will take longer than average. This is due to the fact that, although unlikely, but much like in Bernoulli statistics, there are instances of the time evolution where the White noise from the Wiener process will produce a few non-optimal tangent vectors in a row that can potentially throw back the convergence by many time steps. The observation of Bernoulli-like behavior is not limited to critical system of course, but very much overemphasized in this case. Although possible, the treatment of edge-driven XXZ-models for example is still a challenge: The information of the edges being driven has to be communicated to the bulk and in a critical system this is happening exponentially slow. That means that if we were to simulate a 100-site chain, we would not need an overly large bond dimension, but instead wait very long for its convergence: As mentioned earlier,

the monogamy of entanglement gives rise to an area law. Thus, moderate bond dimensions of 16 or more are sufficient to capture the behavior of those systems – at the expense of the speed the correlations travel at. However, even here we can find a good detail within. Since we are interested in a steady state, there is no need to be worried about loss of coherence due to long simulation time. The driving will take care of it eventually because when searching for a steady state, we can be sure that the equilibrium that eventually forms in the system under time evolution is actually accurate up to the computational precision, and can readily be checked, as we explain in the next section.

Still, critical systems are computationally hard to investigate anyways, that it seems worthwhile to stress that this is not a limitation of the presented method, but observable in any numerical treatment.

3. Probing the steady state

In numerical computations, it is often not easy to decide when a task has been accomplished. While the search for ground states often gives an upper bound on the ground state energy one can certify against, this is not so easy when probing for steady states of dissipative systems. While in general the steady state with regard to a system observable \hat{O} is defined by

$$\frac{\partial O}{\partial t} = 0, \quad (245)$$

this can be hard to verify because of the white noise that accompanies each individual time step, i.e. a steady state in Monte Carlo-TDVP time evolution will only ever fulfill

$$\frac{\partial O}{\partial t} \leq \sqrt{dt} \text{var}(O). \quad (246)$$

Under real conditions this means that we have to adopt a somewhat heuristic attitude: On the one hand we know that the presented method only allows us gain knowledge about ensemble averages in the mean, but on the other hand we would like to be able to stop computation of a sampling path when it is reasonably close to the steady state, which is an individual condition and thus in principle not accessible. Although computing resources are cheap, they are not free. That means that whenever we can stop a process and start another, one we save resources that will – with regards to constant number of operations (although parallel) – allow to improve the accuracy of the overall results.

This seems like a good rule-of-thumb, but fails miserably when dealing with critical systems, because the condition of Eq. (246) is fulfilled regularly, when the evolution temporarily sits in a local minimum. In this case all we can do is to look at many observables and verify that all of them are in a collective steady state – if we expect them to be, of course. However, if we think about prior examples of criticality, i.e. many configurations with comparable amounts of energy, it is clear that there is no way to probe them efficiently: The root cause of the criticality is also the reason for our inability to decide the steadiness of the state: a definite answer would require to explicitly calculate the energy variance of an exponentially growing number of configurations – and here lies the reason for our failure: In general, the variational class will not even allow for differentiation between those comparable configurations.

Summarized, what we can do in such cases is to evolve the system for a long time and many samples, obtain an ensemble average state and verify that it is suitably close to a true steady state by evolving this result for a comparably long time: if it stays within a noise threshold proportional to \sqrt{dt} , we can confidently assume it to be steady. This is of course interesting for cases where the numerical

simulation is the only reasonable prediction, i.e. a large number of sites, where we cannot compare the results to analytics or actual lab experiments.

4. Quasi-homogenous models

4.1. Introduction

Homogeneously driven dissipative spin models pose an interesting subset of dissipative Heisenberg chains. Although the prototype system that has the same local Lindblad operator acting on every site is prone to translation-invariant treatment, like mean field ansatzes, this class is in general non-integrable. Note the contrast of $L = \sum_{\alpha} L_{\alpha}$, where L_{α} is local, to a system with one large, highly nonlocal Lindblad operator \tilde{L} acting on all sites. Indeed, we find that the former has much more symmetry that is only revealed in the stochastic mean. We call the probed system with dissipation L *quasi-homogenous*, because in fact the stochastic nature of the Lindblad action means that the dissipation is essentially the same for all sites, but not steady with regard to single time steps.

The primary use of homogeneously driven Heisenberg models is to check for condensed matter systems that are, for any practical use, translation invariant. And indeed one finds that as long as translation invariance is not violated, there are very successful methods. However, physicists know that in real systems, finite size effects *do* play a role. As such, results from translation-invariant treatments can serve as a starting point for the thorough exploration of these effects, that can lead to much better understanding of, e.g. the behavior of a spin chain at its boundary. We use two different Hamiltonians in the following sections: First of all we will check an XZ-type with homogenous driving and then we will return to the already introduced XXZ-type with bihomogenous driving, i.e. to Lindblad operators driving one half of a chain respectively, simulating a system that is exposed to a steep magnetic field for example.

4.2. Homogenous dissipation

At the core of the class of homogeneously driven systems lies a very simple presumption: In a lab it is mildly difficult to catch, prepare and control single quantum particles. An easily implementable part of the experiments is thus, to enable low-end scalability by driving every particle in the exactly same way without the need to have multiple control mechanisms for individual particles. Granted, the amount of knowledge one can gain from directly, individually accessible quantum particles is much larger, but scalability is never as far advanced as the theoreticians would like [74].

The model we look at is this:

$$H_{KX} = \sum_{n=1}^{N-1} \sigma_n^x \sigma_{n+1}^x + \lambda \sigma_n^z \sigma_{n+1}^z, \quad L_n = \sigma_n^+, n \in \{1, \dots, N\}, \quad (247)$$

where compared to the XXZ-type from Eq. (243) we drop one $\sigma^y \sigma^y$ interaction. The main result is that we expect an anti-ferromagnetic order to form, but there is a caveat, as we will see.

4.2.1. *Results.* Plotting $\langle \overline{\sigma_i^z} \rangle$, we can check what form the magnetization of the steady state of the XZ-type Heisenberg chain takes (see Fig. 15). The structure of the Hamiltonian in Eq. (247) effectively forbids any negative z -alignment, but nevertheless has anti-ferromagnetic order, thus we observe that every even qubit's z -expectation is close to zero, while the Lindblads $L_i = \mu \sigma_i^+$ perform a driving that results in increase of magnetization. Unless noted otherwise, we set $\mu = 1$.

Another way to access the principal behavior of a spin system is to look at the correlation function of certain observables. For random variables X and Y with

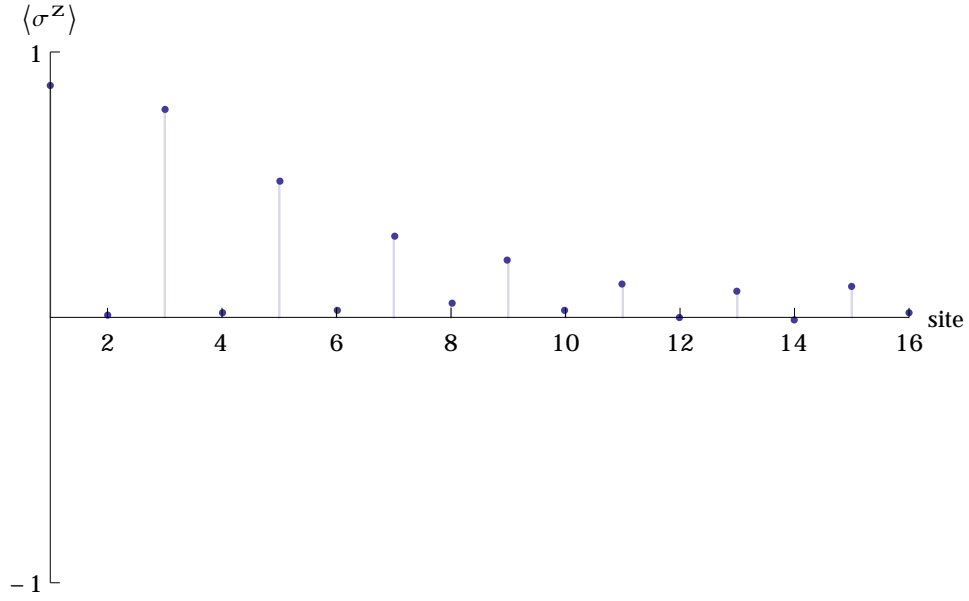


FIGURE 15. **Expectation value in z-direction for a KX type Heisenberg model.** Expectation value of the spin value in a 16-qubit system with average taken over 320 samples, $dt = 0.001$, $D = 16$.

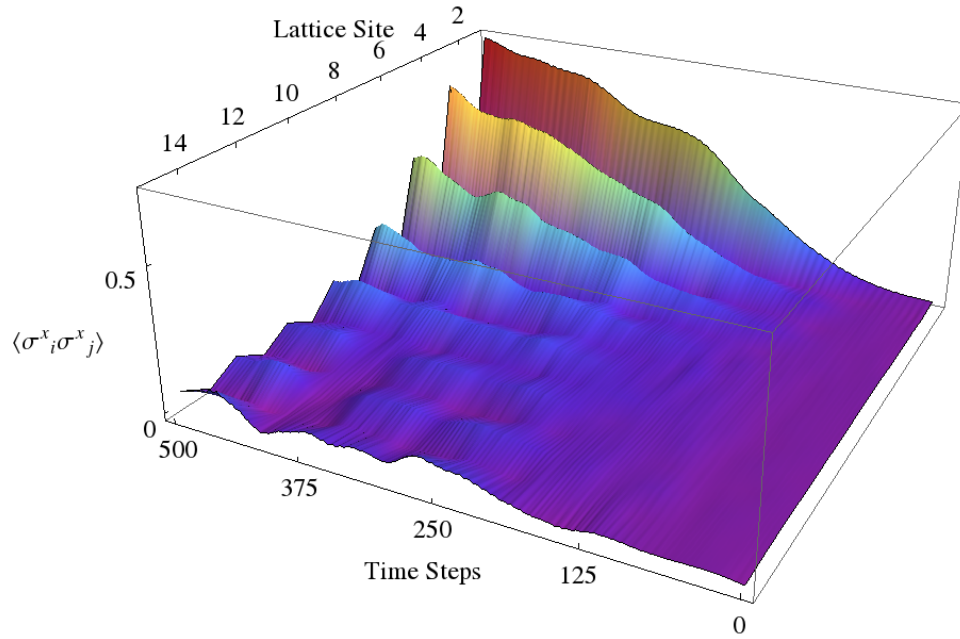


FIGURE 16. **Correlation behavior of the XZ Heisenberg model.** 2-point correlation function for the XZ Heisenberg model as given in Eq. (247).

standard error (s_X, s_Y) it is defined as

$$r_{XY} = \frac{\sum_{i=1}^N (X_i - \bar{X})(Y_i - \bar{Y})}{(N-1)s_X s_Y} = \frac{\sum_{i=1}^N (X_i - \bar{X})(Y_i - \bar{Y})}{\sqrt{\sum_{i=1}^N (X_i - \bar{X})^2 \sum_{i=1}^N (Y_i - \bar{Y})^2}}, \quad (248)$$

we can express correlations between different observables and check for their independence. In the present application, we calculate the correlation coefficients for different sites over the average of all sample paths, thus calculating a spatial correlation for fixed time:

$$r_{\sigma_i^z \sigma_j^z}(t) = \frac{\sum_{k=1}^N \left(\left[(\sigma_i^z(t))_k - \overline{\sigma_i^z(t)} \right] \left[(\sigma_j^z(t))_k - \overline{\sigma_j^z(t)} \right] \right)}{\sqrt{\sum_{k=1}^N \left[(\sigma_i^z(t))_k - \overline{\sigma_i^z(t)} \right]^2 \sum_{k=1}^N \left[(\sigma_j^z(t))_k - \overline{\sigma_j^z(t)} \right]^2}}, \quad (249)$$

where $r_{\sigma_i^z \sigma_j^z}(t)$ is to be read as the correlation coefficient of the observables σ^z at site i with σ^z at site j , all taken at time t . We consequently visualize the results of this calculation in Fig. 16. One can see that the z-component of the spin-1/2 particles are perfectly correlated: Even though we have the white noise from the Wiener-type driving, bearing infinite variance, the average correlation over all samples replicates the magnetization distribution depicted in Fig. 15. This is a clear indicator that the chosen bond dimension fully captures the system dynamics, because otherwise, while not necessarily qualitatively different, the quantitative correlation coefficients could not be close or equal to one.

4.3. Bihomogenous case

The research of domain and phase transitions is one of the most prominent in physics, because phase changes often drive the dynamics of systems with thermodynamic properties. It is thus only logical to probe systems with contradictory dissipation properties, like bihomogenous driving. Here, we use the same Hamiltonian as before, i.e., from Eq. (247), but chose different Lindblad operators

$$L_n = \mu \sigma_n^+, \text{ if } n \leq \frac{N}{2}, \quad L_n = \mu \sigma_n^- \text{ else,} \quad (250)$$

such that there are two magnetic domains: In the left half chain we predict positive sign for measurements of $\langle \sigma^z \rangle$, while the situation should reverse in the right half chain.

4.4. Results for bihomogenous case

Indeed, we find that for large interaction strength $\varepsilon = 1, \lambda = 1, \mu = 1$, and one subsequently obtains two clearly distinguished domains. (See Fig. 17.) If we, however, reduce the driving μ to values smaller than 0.75, we can observe that the next-neighbor interaction starts to mediate the magnetization alignment in a zone around the prior domain wall. (Compare Fig. 18).

This provides necessary insights to confidently study more dissipative systems with domain change without the need to model the whole state space. Since these calculations were carried out with bond dimensions $D \leq 32$, we are confident that the requirements of larger systems stay within reasonably achievable computational efforts for at least one additional order of magnitude in chain length. This is illustrated again by use of the 2-point correlation functions in Fig. 19. We start with completely random mixed states, such that all correlations are identical to zero throughout the lattice, but then are driven into the two corresponding domains,

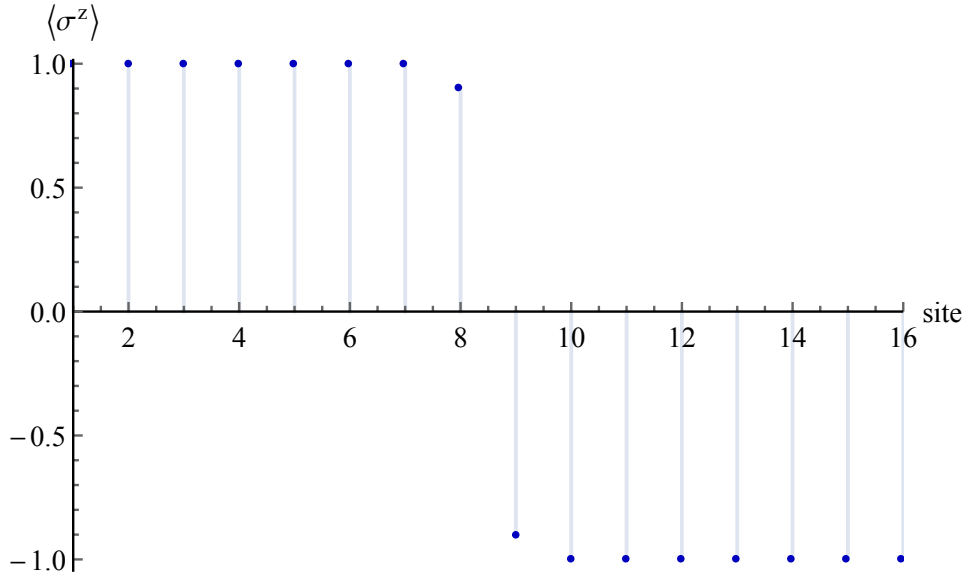


FIGURE 17. **Strong bihomogenous driving regime.** z -direction of average spin values per site for strong driving ($\mu = 1$) with bihomogenous Lindblads according to Eq. (250), 500 samples over 1000 time steps with discretization $dt = 0.001$ with bond dimension $D = 16$. The spins form two clearly distinguishable domains of opposite alignment with a minimal overlap zone in the center.

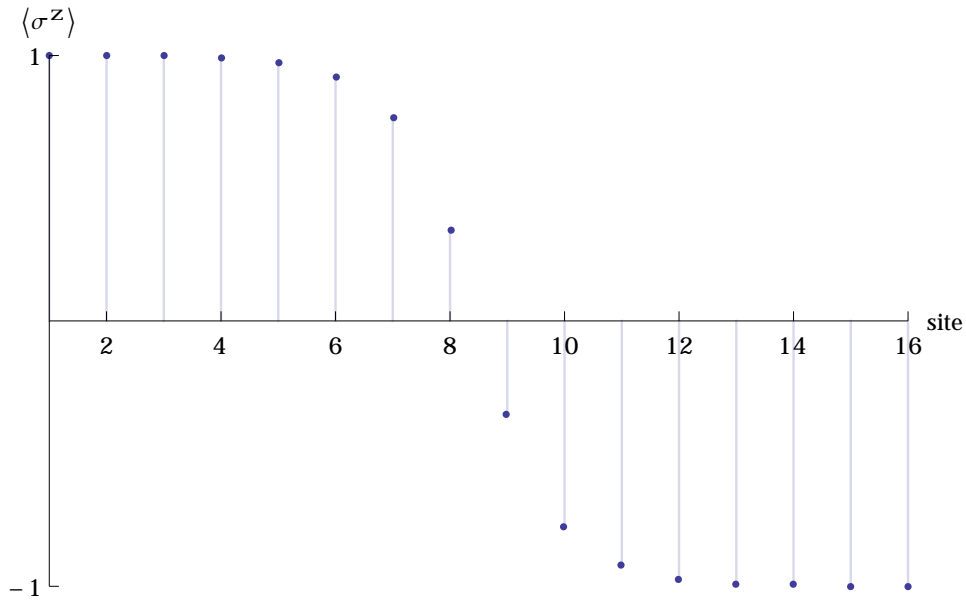


FIGURE 18. **Medium bihomogenous driving regime.** z -direction of average spin values per site for medium driving ($\mu = 0.75$) of bihomogenous Lindblads according to Eq. (250), 500 samples, 1000 time steps, $dt = 0.001$ with bond dimension $D = 16$. The domain interaction zone is considerably larger than in Fig. 17.

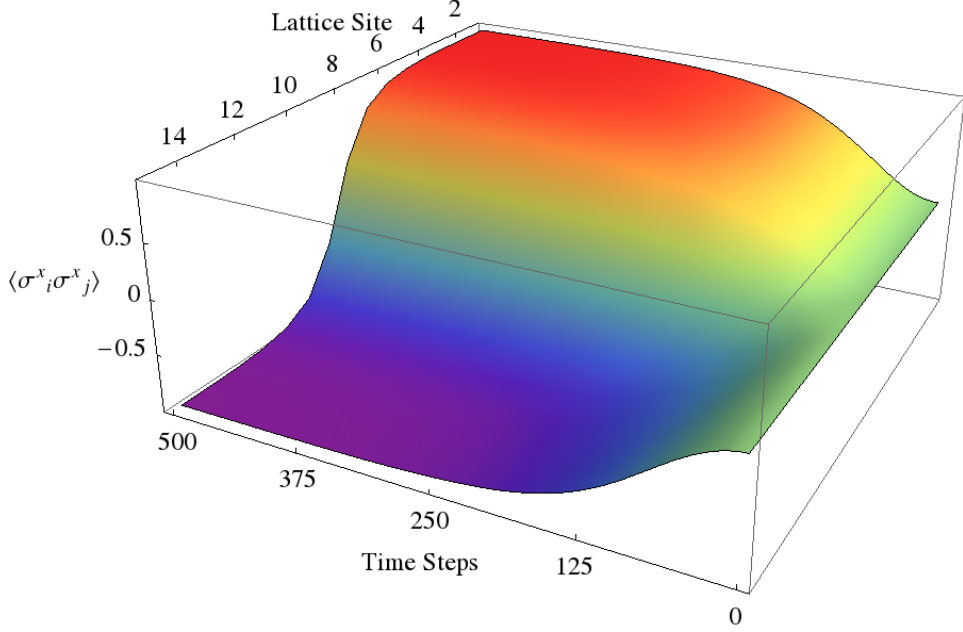


FIGURE 19. **Correlation function of strong bihomogenous driving regime.** 2-point correlation function for the bihomogeneous XZ-Heisenberg model given in Eq. (243) with the same parameters as in Fig. 18. We observe that the correlation corresponds 1-to-1 with the magnetization itself, which means that the chosen bond dimension suffices to capture the relevant dynamics.

which can effectively be seen after 100 time steps, after which the correlations increase in amplitude only, but do not change qualitatively.

5. Outlook

Although they have been widely studied for the last eighty years, models of Heisenberg type can still provide new insights into the inner working of extensive many-body systems, especially regarding the research of larger and larger systems – an endeavor that obviously cannot be solved by faster computers alone. Apart from further optimizing the implementation of the dissipative extension to the evoMPS framework, high-performance computing can potentially exploit the parallelizability of our approach to gain insights into system with particle numbers of order $\mathcal{O}(10^3)$ and above, most notable examples being molecule folding ansatzes of such a form. We will discuss other models after our treatment of the Fermi-Hubbard model in the next chapter, but it is already clear that, so long as the inner structure of an individual site does not exceed that of its couplings, the main caveat of the method, just like any numerical approximation, will always be the scaling behavior.

Applications to the Fermi-Hubbard model

1. Introduction

As a second application of the method, we investigate a particular example of a Fermi-Hubbard model. We insert a Hamiltonian of the form

$$H_{\text{FH}} = \sum_{i,j,\Delta}^{N-1} t_{ij} c_{i\Delta}^\dagger c_{j\Delta} + U \sum_i^N n_{i\uparrow} n_{i\downarrow} \quad (251)$$

into the Quantum master equation, where c^\dagger, c represent the creation and annihilation operators more comprehensively introduced in Eq. (256) ff. on page 95, using the number operators $n_{i\Delta} = c_{i\Delta}^\dagger c_{i\Delta}$, where i and j number the sites and Δ counts over the spin orientation $\{\uparrow / \downarrow\}$ and apply the Lindblad operators

$$j_{i,j,\Delta}^{(1)} = \sqrt{\gamma_1} c_{i,\bar{\Delta}}^\dagger c_{j,\Delta} P_{i,\Delta} P_{j,\Delta}, \quad (252)$$

$$j_{i,j,\Delta}^{(2)} = \left(j_{i,j,\Delta}^{(1)} \right)^\dagger, \quad (253)$$

$$j_{i,j}^{(3)} = \sqrt{\gamma_2} c_{i,\downarrow}^\dagger c_{j,\downarrow} n_{j,\uparrow}, \quad (254)$$

where $P_{i\sigma} = n_{i\sigma}(1 - n_{i\bar{\sigma}})$. Note that $\bar{\Delta}$ denotes a flip, such that $\bar{\uparrow} = \downarrow$ and vice versa. These propositions are not purely theoretical, but in fact represent part of the ^{40}K atomic level structure as depicted in Fig. 20.

It is possible to address and control a large number of ^{40}K atoms [149, 150] in optical cavities and experiment with them on a quantum level, where they show essential Fermi-statistical behavior. In detail[95], we refer to the levels $|\uparrow\rangle = |\frac{7}{2}; \frac{7}{2}\rangle$, $|\downarrow\rangle = |\frac{9}{2}; -\frac{7}{2}\rangle$, $|X\rangle = |\frac{9}{2}, \frac{9}{2}\rangle$.

In experimental realizations, the Lindblad operators $j^{(1)}$ and $j^{(2)}$ are implemented by Raman-assisted hopping [97], while sideband-cooling [123] is used to realize $j^{(3)}$. The aim of this section is to simulate the time evolution of the Master equation in order to find steady states of this particular setup, which can be used as starting configurations for experimental realizations of these Lindblad operators. Note that since this is a fermionic system, \uparrow / \downarrow denote the spin direction of an individual subsystem. That effectively means that instead of writing $|\frac{9}{2} \otimes \frac{7}{2}\rangle$ we can use $|\uparrow\downarrow\rangle$ instead and be sure that it really is the state $|11\rangle$ of a two-qubit system with *labeled* qubits, where we agree that the labels are (\uparrow) and (\downarrow). This may

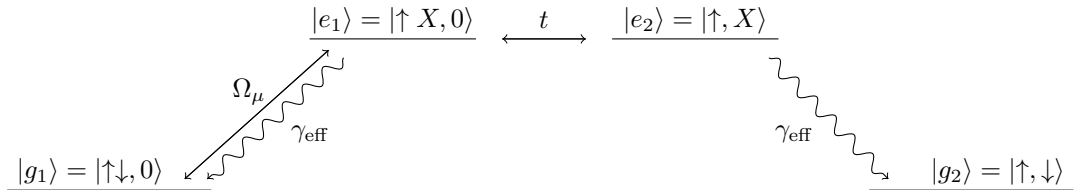


FIGURE 20. **Term scheme of ^{40}K .** Experimentally coupled $m = 7/2$, $m = 9/2$ and $m = 11/2$ electron levels in ^{40}K [95].

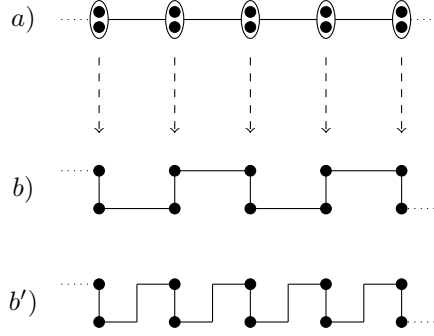


FIGURE 21. **One-dimensional Fermi Hubbard lattice.** a) Fermi-Hubbard model on a lattice. The Hilbert space is that of two coupled spins, their subspaces denoted (\uparrow) and (\downarrow) . This leads to $\mathcal{H}_{(\uparrow)+(\downarrow)} = \mathbb{C}^2 \otimes \mathbb{C}^2 = \mathbb{C}^4$. For computational convenience, this can be mapped to either b) A snake lattice with subspace order $\dots \uparrow\downarrow\uparrow\downarrow\uparrow\downarrow\uparrow \dots$ that is 2-site-translation invariant or b') a double snake lattice with 1-site-translation-invariance and configuration $\dots \uparrow\downarrow\uparrow\downarrow \dots$

seem overly complicated at first, but with the introduction of the Jordan-Wigner-transformed system it will become apparent why this distinction has to be made.

2. Model-specific adaptations to the Monte Carlo TDVP

One of the questions to this system is, what value the decay γ_{eff} frequency takes. We start by assuming that $t = U = \gamma_1 = \gamma_2 = 1$ and adapt the values both according to experimental results [149] and numerical findings [133]. Before, though, we have to derive the exact form of spin operators the current formulation is equivalent to, such that we are able to feed it into the evoMPS implementation of the Monte Carlo TDVP.

2.1. Jordan-Wigner transform

To be able to treat the system with the evoMPS implementation of the Monte Carlo Time-Dependent Variational Principle, we first need to transform the Fermionic Hubbard model into a spin chain. As mentioned before in Chapter 2, this can be achieved by applying a Jordan-Wigner transformation to the creation and annihilation operators c^\dagger and c . Instead of utilizing the standard form, it seems worthwhile to make use of an equivalent, but, in this case, more elegant formulation by M. Nielsen [126]. In place of the phase factor (see Eq. (126) for reference) at each site, we find that multiplication with Pauli z-matrices has the same effect:

$$c_j \equiv - \left(\bigotimes_{k=1}^{j-1} \sigma^z \right) \otimes \sigma_j. \quad (255)$$

We furthermore decide to use the ordering **b')** from Fig. 25, such that we obtain the following relations, which we show for the first two qubits of an open boundary chain and then prove that they are translation invariant. The subscripts (1) , resp. (2) hereby denote the lattice site while the individual index without parenthesis

represents the qubit position:

$$c_{(1),\uparrow} = \sigma^- \otimes \mathbb{1}_{\mathbb{C}^2}^{\otimes 2N-1}, \quad (256)$$

$$c_{(1),\uparrow}^\dagger = \sigma^+ \otimes \mathbb{1}_{\mathbb{C}^2}^{\otimes 2N-1}, \quad (257)$$

$$c_{(1),\downarrow} = \sigma^z \otimes \sigma^- \otimes \mathbb{1}_{\mathbb{C}^2}^{\otimes 2N-2}, \quad (258)$$

$$c_{(1),\downarrow}^\dagger = \sigma^z \otimes \sigma^+ \otimes \mathbb{1}_{\mathbb{C}^2}^{\otimes 2N-2}, \quad (259)$$

$$c_{(2),\uparrow} = \sigma^z \otimes \sigma^z \otimes \sigma^- \otimes \mathbb{1}_{\mathbb{C}^2}^{\otimes 2N-3}, \quad (260)$$

$$c_{(2),\uparrow}^\dagger = \sigma^z \otimes \sigma^z \otimes \sigma^+ \otimes \mathbb{1}_{\mathbb{C}^2}^{\otimes 2N-3}, \quad (261)$$

$$c_{(2),\downarrow} = \sigma^z \otimes \sigma^z \otimes \sigma^z \otimes \sigma^- \otimes \mathbb{1}_{\mathbb{C}^2}^{\otimes 2N-4}, \quad (262)$$

$$c_{(2),\downarrow}^\dagger = \sigma^z \otimes \sigma^z \otimes \sigma^z \otimes \sigma^+ \otimes \mathbb{1}_{\mathbb{C}^2}^{\otimes 2N-4}, \quad (263)$$

where we use the abbreviation $\mathbb{1}^{\otimes N} = \bigotimes_{i=1}^N \mathbb{1}$ to denote the identity on untouched subsystems. With this we can show that for the relation from Eq. (251) we get for $N = 2$

$$\begin{aligned} H_{\text{FH12}} &= t_{12}c_{1\uparrow}^\dagger c_{2\uparrow} + t_{12}c_{2\uparrow}^\dagger c_{1\uparrow} + t_{12}c_{1\downarrow}^\dagger c_{2\downarrow} + t_{12}c_{2\downarrow}^\dagger c_{1\downarrow} \\ &\quad + U \left(c_{1\uparrow}^\dagger c_{1\uparrow} c_{1\downarrow}^\dagger c_{1\downarrow} + c_{2\uparrow}^\dagger c_{2\uparrow} c_{2\downarrow}^\dagger c_{2\downarrow} \right) \\ &= t_{12}\hat{S}_{12,\uparrow} + t_{21}\hat{S}_{21,\uparrow} + t_{12}\hat{S}_{12,\downarrow} + t_{21}\hat{S}_{21,\downarrow} + U \left(\hat{U}_1 + \hat{U}_2 \right), \end{aligned} \quad (264)$$

where

$$\hat{S}_{12,\uparrow} = \sigma^+ \otimes \sigma^z \otimes \sigma^- \otimes \mathbb{1}, \quad (265)$$

$$\hat{S}_{21,\uparrow} = \sigma^- \otimes \sigma^z \otimes \sigma^+ \otimes \mathbb{1}, \quad (266)$$

$$\hat{S}_{12,\downarrow} = \mathbb{1} \otimes -\sigma^+ \otimes \sigma^z \otimes \sigma^-, \quad (267)$$

$$\hat{S}_{21,\downarrow} = \mathbb{1} \otimes \sigma^- \otimes \sigma^z \otimes \sigma^+, \quad (268)$$

$$\hat{U}_1 = \sigma^+ \sigma^- \otimes \sigma^+ \sigma^- \otimes \mathbb{1} \otimes \mathbb{1}, \quad (269)$$

$$\hat{U}_2 = \mathbb{1} \otimes \mathbb{1} \otimes \sigma^+ \sigma^- \otimes \sigma^+ \sigma^-, \quad (270)$$

for the Hamiltonian. We furthermore observe that

$$\sigma^+ = \begin{pmatrix} 0 & 1 \\ 0 & 0 \end{pmatrix}, \quad (271)$$

$$\sigma^- = \begin{pmatrix} 0 & 0 \\ 1 & 0 \end{pmatrix}, \quad (272)$$

$$\sigma^+ \sigma^- = \begin{pmatrix} 0 & 0 \\ 0 & 1 \end{pmatrix}, \quad (273)$$

$$\sigma^- \sigma^+ = \begin{pmatrix} 1 & 0 \\ 0 & 0 \end{pmatrix}, \quad (274)$$

and can subsequently reexpress the Lindblad operators as

$$j_{1,2,\uparrow}^{(1)} = \sqrt{\gamma_1} (\mathbb{1} \otimes \sigma^+ \sigma^z \otimes \sigma^- \otimes \mathbb{1}) P_{1\uparrow} P_{2\uparrow}, \quad (275)$$

$$j_{1,2,\downarrow}^{(1)} = \sqrt{\gamma_1} (\sigma^+ \otimes \sigma^z \otimes \sigma^z \otimes \sigma^-) P_{1\downarrow} P_{2\downarrow}, \quad (276)$$

$$j_{2,1,\uparrow}^{(1)} = \sqrt{\gamma_1} (\sigma^+ \otimes \sigma^z \otimes \sigma^z \otimes \sigma^-) P_{2\uparrow} P_{1\uparrow}, \quad (277)$$

$$j_{2,1,\downarrow}^{(1)} = \sqrt{\gamma_1} (\mathbb{1} \otimes \sigma^+ \sigma^z \otimes \sigma^- \otimes \mathbb{1}) P_{2\downarrow} P_{1\downarrow}, \quad (278)$$

$$j_{1,2}^{(3)} = \sqrt{\gamma_2} (\mathbb{1} \otimes \sigma^+ \sigma^z \otimes \sigma^z \sigma^+ \sigma^- \otimes \sigma^-), \quad (279)$$

$$j_{2,1}^{(3)} = \sqrt{\gamma_2} (\sigma^+ \sigma^- \otimes \sigma^z \sigma^- \otimes \sigma^z \otimes \sigma^+), \quad (280)$$

$$(281)$$

with

$$P_{i\Delta} = n_{i\Delta}(\mathbb{1} - n_{i\bar{\Delta}}) = c_{i\Delta}^\dagger c_{i\Delta} - c_{i\Delta}^\dagger c_{i\Delta} c_{i\Delta}^\dagger c_{i\bar{\Delta}}, \quad (282)$$

$$P_{1\uparrow} = [(\sigma^+ \sigma^- \otimes \mathbb{1} \otimes \mathbb{1} \otimes \mathbb{1}) - (\sigma^+ \sigma^- \otimes \sigma^+ \sigma^- \otimes \mathbb{1} \otimes \mathbb{1})], \quad (283)$$

$$P_{1\downarrow} = [(\mathbb{1} \otimes \sigma^+ \sigma^- \otimes \mathbb{1} \otimes \mathbb{1}) - (\sigma^+ \sigma^- \otimes \sigma^+ \sigma^- \otimes \mathbb{1} \otimes \mathbb{1})], \quad (284)$$

$$P_{2\uparrow} = [(\mathbb{1} \otimes \mathbb{1} \otimes \sigma^+ \sigma^- \otimes \mathbb{1}) - (\mathbb{1} \otimes \mathbb{1} \otimes \sigma^+ \sigma^- \otimes \sigma^+ \sigma^-)], \quad (285)$$

$$P_{2\downarrow} = [(\mathbb{1} \otimes \mathbb{1} \otimes \mathbb{1} \otimes \sigma^+ \sigma^-) - (\mathbb{1} \otimes \mathbb{1} \otimes \sigma^+ \sigma^- \otimes \sigma^+ \sigma^-)]. \quad (286)$$

With the relation $\sigma^z \cdot \sigma^z = \mathbb{1}$ we can then inductively show that for larger lattice sites we get back the canonical anti-commutation relations such that for site (3), we obtain the relations

$$c_{(3),\uparrow} = \sigma^{z\otimes 4} \otimes \sigma^- \otimes \mathbb{1}_{\mathbb{C}^2}^{\otimes 2N-5}, \quad (287)$$

$$c_{(3),\uparrow}^\dagger = \sigma^{z\otimes 4} \otimes \sigma^+ \otimes \mathbb{1}_{\mathbb{C}^2}^{\otimes 2N-5}, \quad (288)$$

$$c_{(3),\downarrow} = \sigma^{z\otimes 5} \otimes \sigma^- \otimes \mathbb{1}_{\mathbb{C}^2}^{\otimes 2N-6}, \quad (289)$$

$$c_{(3),\downarrow}^\dagger = \sigma^{z\otimes 5} \otimes \sigma^+ \otimes \mathbb{1}_{\mathbb{C}^2}^{\otimes 2N-6}. \quad (290)$$

Calculating the respective operators of the system, we see that indeed all actions on the first site's subspace are even products of σ^z and the identity operator: First we observe that the part of the Hamiltonian acting on sites 2 and 3, $H_{\text{FH}23}$ is composed of the following operators:

$$\hat{S}_{23,\uparrow} = \sigma^z \sigma^z \otimes \sigma^z \sigma^z \otimes \sigma^+ \otimes \sigma^z \otimes \sigma^- \otimes \mathbb{1}, \quad (291)$$

$$\hat{S}_{23,\downarrow} = \sigma^z \sigma^z \otimes \sigma^z \sigma^z \otimes \sigma^- \otimes \sigma^z \otimes \sigma^+ \otimes \mathbb{1}, \quad (292)$$

$$\hat{S}_{32,\downarrow} = \sigma^z \sigma^z \otimes \sigma^z \sigma^z \otimes \mathbb{1} \otimes -\sigma^+ \otimes \sigma^z \otimes \sigma^-, \quad (293)$$

$$\hat{S}_{32,\uparrow} = \sigma^z \sigma^z \otimes \sigma^z \sigma^z \otimes \mathbb{1} \otimes \sigma^- \otimes \sigma^z \otimes \sigma^+, \quad (294)$$

$$\hat{U}_2 = \sigma^z \sigma^z \otimes \sigma^z \sigma^z \otimes \sigma^+ \sigma^- \otimes \sigma^+ \sigma^- \otimes \mathbb{1} \otimes \mathbb{1}, \quad (295)$$

$$\hat{U}_3 = \sigma^z \sigma^z \otimes \sigma^z \sigma^z \otimes \mathbb{1} \otimes \mathbb{1} \otimes \sigma^+ \sigma^- \otimes \sigma^+ \sigma^-. \quad (296)$$

Note that these equations deviate in notation from Eq. (265) by including the two tensor factors of the first lattice site – given by $\sigma^z \sigma^z \otimes \sigma^z \sigma^z = \mathbb{1} \otimes \mathbb{1}$ to emphasize that all products of the form $c_{(2),\Delta} c_{(3),\Delta}$ are exactly the identity on non-relevant tensor factors – to highlight the fact that all interactions are local with respect to the interaction between lattice sites 2 and 3. By direct induction, this can be shown for any $N < \infty$ and open boundary conditions. In fact, for periodic boundary conditions it is true as well. The only caveat in this case is that the translation operators O_{N1} acting on sites N and 1 will add a phase proportional to σ^z for non-quadratic terms of the form $c_{N,\Delta}^\dagger c_{1,\Delta}$. With that in mind, locality only remains to be shown for the Lindblad operators. But since they are constructed from the same operators, plus the projections on the on-site subspaces $P_{j\Delta}$, we readily check

$$P_{i\uparrow} = \left[\left(\otimes^{(2N-2i)} \sigma^z \sigma^z \otimes \sigma^+ \sigma^- \otimes \mathbb{1} \otimes \mathbb{1} \otimes \mathbb{1} \otimes \dots \right) - \left(\otimes^{(2N-2i)} \sigma^z \sigma^z \otimes \sigma^+ \sigma^- \otimes \sigma^+ \sigma^- \otimes \mathbb{1} \otimes \mathbb{1} \otimes \dots \right) \right], \quad (297)$$

$$P_{i\downarrow} = \left[\left(\otimes^{(2N-2i)} \sigma^z \sigma^z \otimes \mathbb{1} \otimes \sigma^+ \sigma^- \otimes \mathbb{1} \otimes \mathbb{1} \otimes \dots \right) - \left(\otimes^{(2N-2i)} \sigma^z \sigma^z \otimes \sigma^+ \sigma^- \otimes \sigma^+ \sigma^- \otimes \mathbb{1} \otimes \mathbb{1} \otimes \dots \right) \right], \quad (298)$$

i.e. the projections cancel on non-relevant subspaces. However, we need to remember that the tensor product does not commute with the sums in the projectors, such

that we need to take the sum of the tensor products, which is, for large systems, marginally more complex.

Nevertheless this is a desirable result, because it means we can, within this set of interactions, deconstruct any N -site valence-bond lattice we might want to simulate into $2N$ spin-1/2 qubits of the presented form.

2.2. Algorithm

evoMPS can treat at most 3-site-interactions, but, in fact, the jump operators $j_{ji}^{(3)}$ are 4-local. Thus, we need to employ a trick to be able to simulate the dynamics: We realize that the deconstruction of the valence-bond picture was useful in undertaking the Jordan-Wigner transform, but now have to recombine the $(\uparrow), (\downarrow)$ subspaces into one tensor factor as input for the evoMPS algorithm. The resulting scheme is thus mapped to an N -site lattice again, with local dimension $(\mathbb{C}^2)^2 = \mathbb{C}^4$. This is an admissible tradeoff because we have at most 2-local interaction terms to treat.

In essence this means that with the preparations of the previous section we can apply the algorithm given in Chapter 5 right away, with the only change being the values of the jump operators and the Hamiltonian and the fact that there are more than one jump operator per site, but this poses, as already explained, no general problem.

Still, we need to briefly address the impact on computational complexity, given that we do have five jump operators per pair of interacting sites, $j_{\uparrow}^{(1)}, j_{\downarrow}^{(1)}, j_{\uparrow}^{(2)}, j_{\downarrow}^{(2)}$ and $j^{(3)}$. Unfortunately, it is necessary to recalculate the whole set of prerequisite matrices K and C given in Eqs. (153) and (155), respectively. That means that we have to account for an increase in computation time by a factor $\mathcal{O}(|\alpha|)$, $|\alpha|$ being the number of jump operators to be evaluated. Considering that increased accuracy calls for $\mathcal{O}(M^2)$ parallel samples, this seems like an acceptable tradeoff, because it has considerably more impact on the algorithm. That being said, we were comfortably able to perform investigations on a system of 8-10 sites, the results of which are presented in the next section.

2.3. Results for the one-dimensional case

The first step in any new model is to verify your results against an established results base. In cases where no analytic results are available, i.e. when numeric results are actually scientifically meaningful, the gold standard has always been to check against direct diagonalization with as large systems as possible, before increasing the lattice size of the approximate numeric method beyond the reach of the exact methods. An additional benefit of the MPS approach is that we can always run exact TDVP calculations as well – one calculates the maximal Schmidt rank of the interactions present and chooses the bond dimension accordingly. Obviously, this is limited to the same size as the diagonalization approach but provides a good benchmark nevertheless.

Thus, before explaining results of extensive lattice sizes, we give a direct comparison of diagonalization with an exact TDVP treatment of a 2-site system. Before, we highlight the stochastic nature of the observed process by plotting the sample path of a single time evolution instance in Fig. 22.

We can already see some very interesting observations about the behavior of the system: Starting from the pure state $|\uparrow, 0\rangle$, the total occupation number will stay close to one, i.e. per site there is at all times only about one particle, although up to two would be allowed. We will later see that this behavior can also be found in the larger system because it is the (energetically) preferred configuration of the interaction terms $c_i^\dagger c_j$ in the Hamiltonian. Though not the only useful measure of

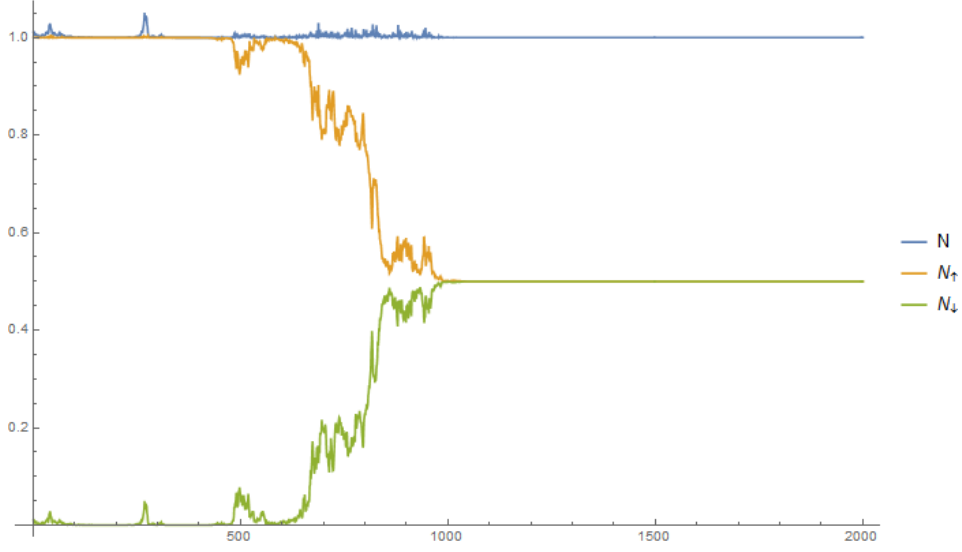


FIGURE 22. **Example of driven Fermi-Hubbard time evolution.** Occupation number for 2-site simulation (per site). 1 sample only. The system parameters are $t = 1$, $U = 100$, $\sqrt{\gamma_1} = 1$, $\sqrt{\gamma_2} = \sqrt{2}$, $D = 16$, $dt = 0.001$, $3 \cdot 10^4$ time steps.

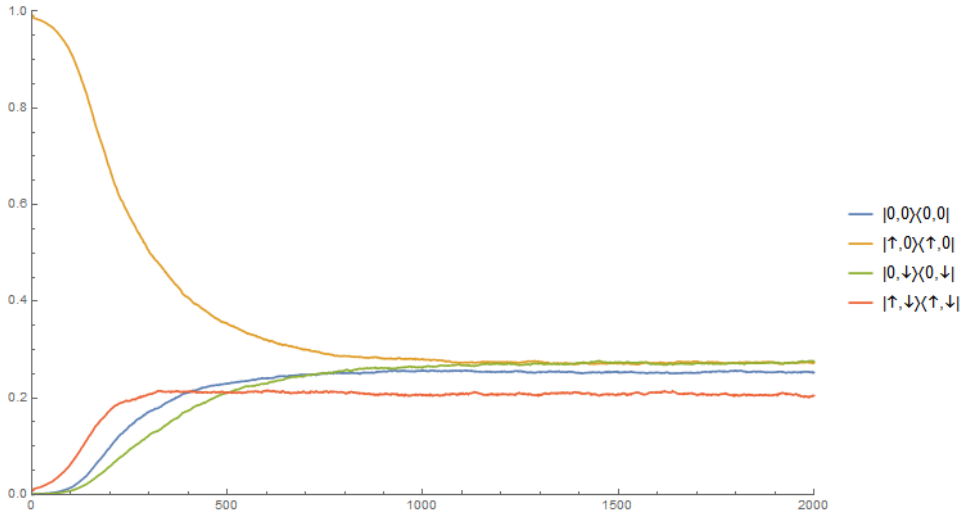


FIGURE 23. **Time evolution plot of diagonal elements.** Diagonal elements of the density matrix for lattice length 8. The system parameters are as in Fig. 22, but for 10^3 samples.

the Fermi-Hubbard dynamics, the occupation number often highlights the macroscopic behavior best insofar as the perspective of a magnet is concerned: We show that indeed the defined dissipation has a realization of anti-ferromagnetic alignment of spins as its steady state, and this can be deduced from occupation number and double occupation probability. In Fig. 27 we show the diagonal elements of the reduced one-site density matrix for a lattice of $N = 8$ sites, followed by the relevant system properties in Fig. 24.

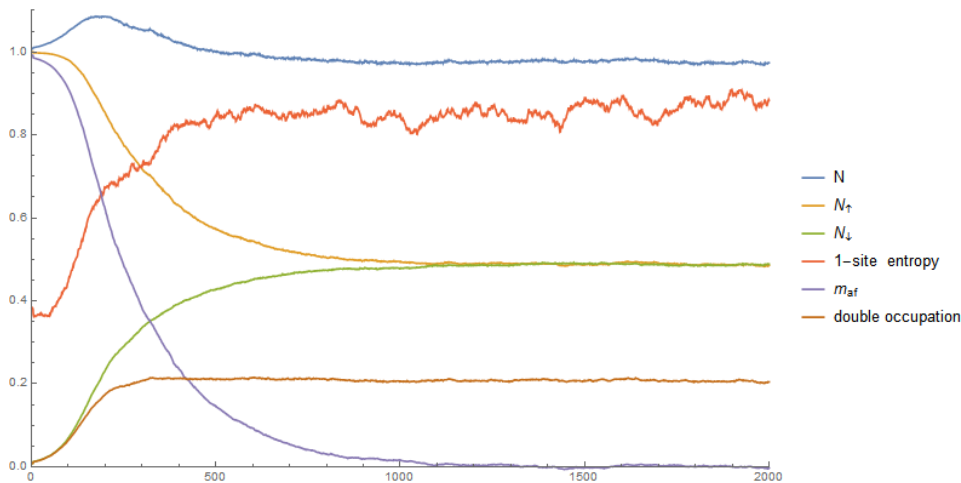


FIGURE 24. **Relevant observables of a lattice with 8 sites.**

Occupation number, both for total particle count N (per site) as well as the subsystems N_{\uparrow} and N_{\downarrow} . Furthermore the plot contains 1-site entropy, magnetization and double occupation probability. The system parameters are as in Fig. 22, but for 10^3 samples.

The starting configuration has been chosen as before, but composed through the lattice, i.e.

$$\bigotimes_{i=1}^N |\uparrow, 0\rangle. \quad (299)$$

As expected, the occupation numbers are qualitatively similar, although we have an increase of particle count *before* the magnetization evens out. We see that the steady state has an equal number of \uparrow - and \downarrow -components, which already points toward an anti-ferromagnetic alignment, but unlike the 2-site case, from these observables alone we could be missing the fact that there are configurations like $\uparrow\uparrow\downarrow\downarrow$ in between. To this end we calculate the reduced density matrix of all neighboring sites and measure the 2-site operator $\frac{1}{\sqrt{2}} (|\uparrow 0, 0 \downarrow\rangle \langle \uparrow 0, 0 \downarrow|) + \frac{1}{\sqrt{2}} (|0 \downarrow, \uparrow 0\rangle \langle 0 \downarrow, \uparrow 0|)$.

3. Treatment of higher spatial dimensions

Since the one-dimensional treatment of the given system has shown that there were some reserves on the computational side, it was a somewhat straightforward idea to see whether the scheme can be extended further. Using the same convolution trick we explained in Section 2.2 we now not only compose two qubits of one physical side together, but *all* sites of a horizontal slice through an extended square lattice. Although this is obviously expensive, it is still much less expensive than direct diagonalization. Considering 4 by 4 sites, i.e., $N = 16$, the full Hilbert space dimension would be $4^N \approx 4 \cdot 10^9$, a size for which direct diagonalization is only possible on a computation cluster. Given, we make use of a grid as well, but would not have to: A single consumer-range machine could solve the task within its memory capacity, although it would mean to calculate successive number of sample for a long time, given that the local dimension is $4^4 = 256$, so we actually have only four sites and can choose a suitable bond dimension. Thus, the magnitude of the computation utilizing evoMPS-MCTDVP is manageable.

| Supersite size | Memory requirement | Sparse memory requirement |
|----------------|--------------------|---------------------------|
| 2 | 1 MB | 77 KB |
| 3 | 256 MB | 3.2 MB |
| 4 | 64 GB | 1.5 GB |

TABLE 1. **Memory comparison for different lattice sizes.**

One can clearly see the exponential growth of the memory requirements for increasing lattice dimensions. In particular in comparison to the sparse memory allocation, the amount of “unnecessary” overhead, following from the fact that large parts of the respective matrices are filled with zeros, is striking.

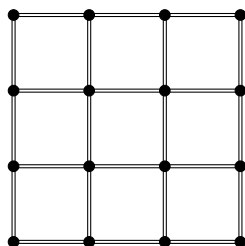


FIGURE 26. **Counting of graph bonds.** For the matter of bounding the maximal amount of memory the interaction operators will occupy we have to count every edge twice: The term H_{ji} is quantitatively different from H_{ij} and effectively doubles the amount of memory we need per edge. The same is, of course, true for the Lindblad operators j_1, \dots, j_3 .

We can see that for the internal dimension of $N_S = 4$, the memory required only for storing a single interaction matrix is so huge that only specialized machines can store them. However, for practical purposes we have more than one interaction term, such that for a system of 4×4 sites (given that the smaller spatial dimension always is turned into the supersite) we have $24 \times 2 \times 6 = 192$ interaction terms because we have to count each edge twice (since $H_{ij} \neq H_{ji}$) and multiply by the 6 different types of operators: The Hamiltonian part and the five Lindblad terms.

Luckily, the matrices we are talking about are generally sparse: To model a single interaction we generally find that no more than $\sqrt{\dim_{\text{Interaction}}(N_S)}$ elements of the matrix are non-zero, and they do not require the maximal 128 bit-accuracy of the NumPy package, but are integers, such that we could reduce the memory requirements immensely:

By using the sparse matrix implementation from the SciPy library `sp.sparse.coo_matrix`, we were able to reduce the memory needed by two orders of magnitude on average. This finding is illustrated in Fig. 27. However, it turns out that the data type we want to use is not fully implemented in Python 2.7.: Addition and multiplication, which was all we need for the preprocessing of the interaction operators, had to be implemented on our own. While this format *can* be converted to the usual `np.ndarray` format, there is no transparent overloading available without breaking compatibility with the evoMPS implementation: As a consequence, whenever an interaction matrix is needed for a calculation, the respective ndarray is initialized and the sparse matrix is converted such that the operation can be performed by the optimized evoMPS operation. After the calculation is complete,

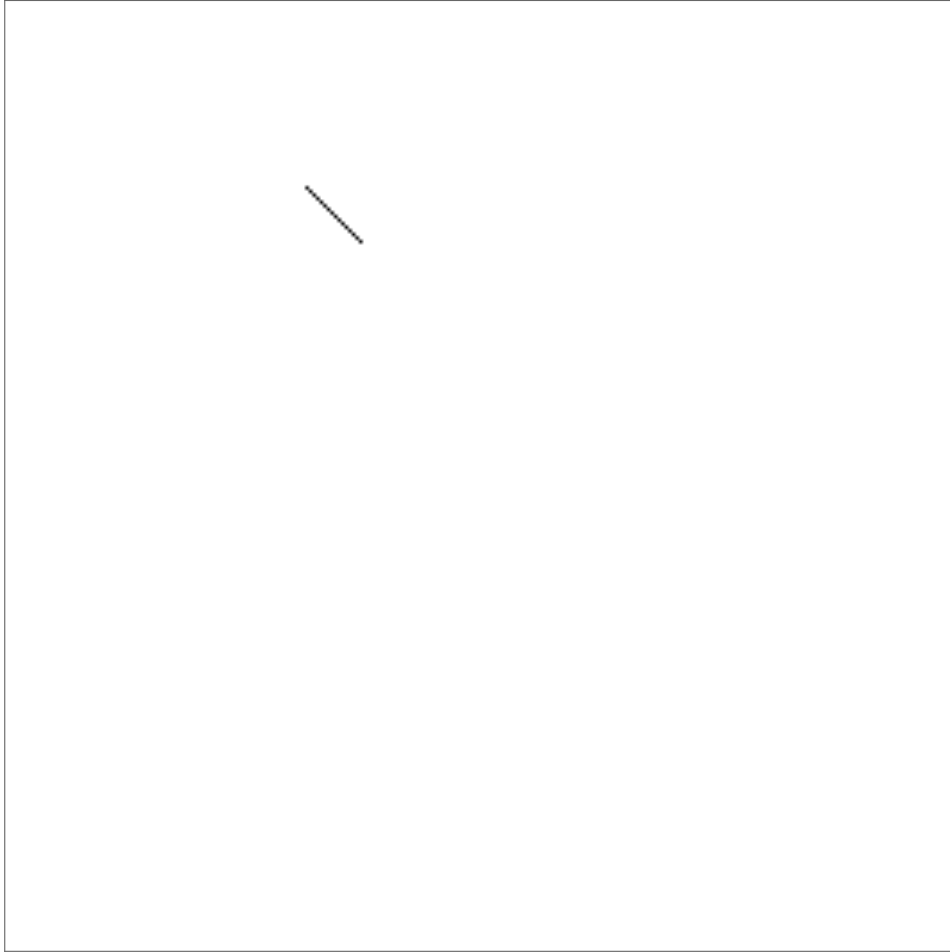


FIGURE 27. **Sparse array representation.** Pictorial representation of $j_{12}^{(3)}$ in a system with super site dimension 2. The matrix dimension of the operator is 256×256 , but there are 8 non-zero elements only (black dots), i.e. 97% of the allocated memory can be cut.

the memory has to be unallocated, because there can not be many instances of such big matrices within the RAM. While this tradeoff is worthwhile for large super sites, future implementations should circumvent this problem by implementing the TDVP in a way that fully supports sparse matrices as interaction terms.

The presented issue is the symptom of a much deeper lying systematic intricacy: In contrast to compiled languages like Fortran or C, Python is an interpreted language. This first and foremost means that heavy numeric calculations are slower if the code is not optimized. This is no problem since in general one can use the Python wrapper for the BLAS and LAPACK libraries. One of the characteristics of interpreted languages, however, is that the memory allocation is usually done in a way called *lazy evaluation*: Whenever an expression is assigned, only the part that is needed is evaluated. For a large matrix, it depends on the data type whether *at time of evaluation* the memory can actually be assigned, irrespective of the fact that it was declared before. On windows machines this leads to two problems: First of all, the maximal amount of memory that can be assigned is limited due to the

fact that Python's memory controller cannot be sure never to need more memory for operations that take place *before* the big chunk of assigned memory is accessed, which means that without very tricky memory allocation we can not certify that the big matrix of 65536×65536 entries (i.e. the size of the interaction matrix with supersite size of 4) can be allocated.

As an additional treat one has to keep track of the memory and explicitly delete even implicit allocations, because again the lazy evaluation means that the memory controller (in this instance referred to as *garbage collector*) does not delete unneeded memory just because the namespace ended. In a way, of course, this criticism is unfair, because in a compiled language one would also have to deal with memory management. In Python, however, it is worse because apart from explicitly deleting large matrices and hoping that the memory gets unallocated, there is not much one can do. In the end, we resorted to a rather lengthy probing game where every conceivable memory error that could come up while initializing a matrix was handled with the appropriate exception.

It seems opportune to ask whether further optimizations could lead to the treatment of even larger systems, and that is the case: In its present form, evoMPS stores the intermediate quantities K and C in array for performance reasons. However, they are of size $q_n \times q_n \times D \times D$, which is quite large for systems utilizing the super site formalism. Luckily, the TDVP can sweep through the lattice, such that every calculation of a tangent vector b only depends on the results for the preceding two sites. For large lattices, serializing these calculations and only allocating memory where necessary could save memory on the order of $(N - 2) \times D \times D$ at the expense of calculation and memory allocation time. However, for systems so large that this would make a difference, the sheer size of the interaction matrices will dominate all of these complexity considerations by far.

3.2. Results for the two-dimensional case

We apply the same observables to the system and shall compare the results to the one-dimensional case. It seems interesting to see whether the qualitative behavior changes, especially with regards to the expected anti-ferromagnetic ordering behavior. While there are methods based on superpositions of matrix product states [133] and of course based on projected entangles pair states (PEPS) [185, 34], this is to our knowledge the first proposition of a treatment of higher spatial dimensions with Matrix Product States alone.

First of all we notice that, although not surprising, the two-dimensional behavior of the Fermi-Hubbard system is similar. We expect to see mildly different steady states for the simple fact that in a 2-d lattice the entanglement structure has a different geometry, i.e. accounting for the fact that an individual site will have 3 or 4 bonds depending on whether they sit at the edge of the lattice or in the bulk. We proceed by giving the same measurements as in the one-dimensional case. For the diagonal elements of the reduced density matrix (see Fig. 28) we find good agreement with the one-dimensional case, but this is clear: Projecting the state to its single-site subspace must reveal its classical properties, which are, due to the same interactions, identical.

When we look at the more intricate observables of Fig. 29, however, we see that although the occupation numbers are comparable in the mean, we get a slightly different convergence behavior. There are two mechanism competing with each other: On the one hand, the system is two-dimensional, which means that with a higher density of bonds between sites we expect the dissipation to have even larger impact, but on the other hand the convergence is largely driven by the entanglement transport throughout the lattice, which is inhibited by frustrations stemming from the fact that there are so many bonds per site in the bulk.

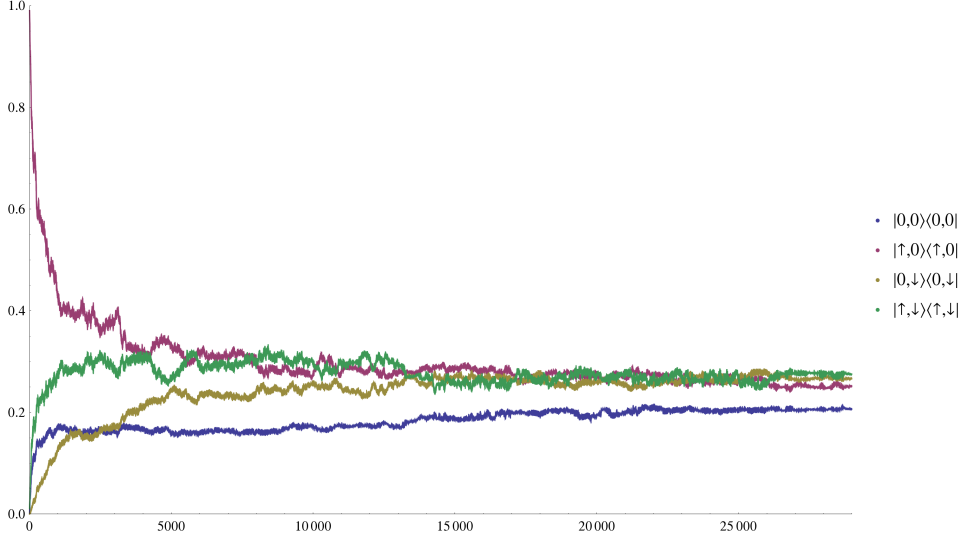


FIGURE 28. **Time evolution plot of diagonal elements.** Diagonal elements of the density matrix for a square lattice with 2×2 sites. The system parameters are $t = 1$, $U = 100$, $\sqrt{\gamma_1} = 1$, $\sqrt{\gamma_2} = \sqrt{2}$, $D = 16$, $dt = 0.001$, $3 \cdot 10^4$ time steps, 250 samples.

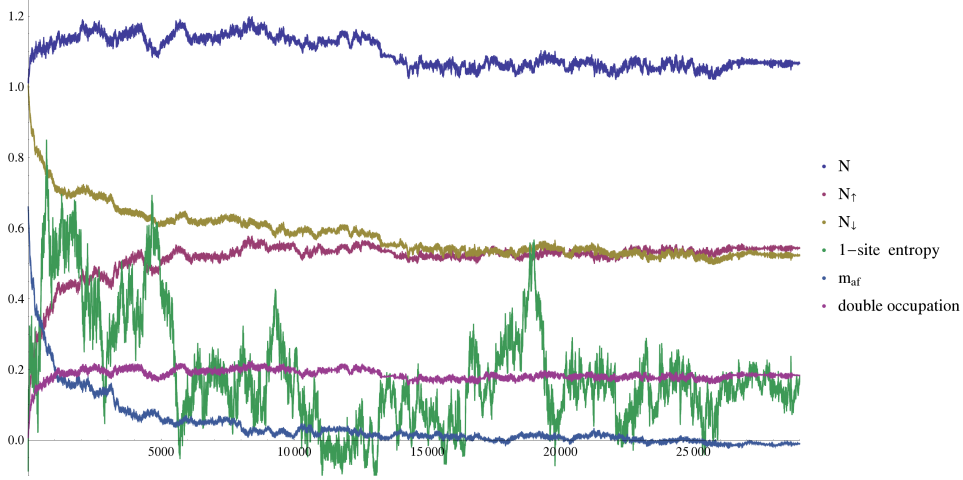


FIGURE 29. **Relevant observables of a 2×2 square lattice.** Occupation number, both for total particle count N (per site) as well as the subsystems N_\uparrow and N_\downarrow . Furthermore the plot contains 1-site entropy, magnetization and double occupation probability. The system parameters are as in Fig. 28.

Actually, this finding is expected to be an even larger problem in three dimensions: Limited by the monogamy of entanglement, sites with up to six bonds will either frustrate the lattice due to non-satisfiable conditions on the level of occupation or decohere into product states due to the fact that the amount of *entanglement per bond* is very low.

Even more interesting thus is the question how the double occupation probability behaves. Although the total number of occupations is moderated to be constant

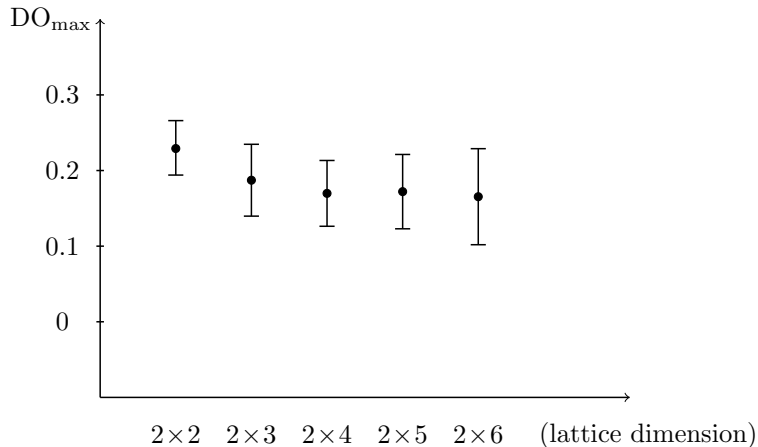


FIGURE 30. **Comparison of double occupations for varying spatial extension of a square lattice.** We compare the maximal value of the double occupation diagonal element $|\uparrow, \downarrow\rangle \langle \uparrow, \downarrow|$ for *one* increasing spatial dimension. The error becomes larger with higher number of sites because we chose to decrease the number of samples at the same time to accommodate for the increased runtime. The system parameters are as in Fig. 28 except for the sample number. Those are $2 \times 2 : 250$, $2 \times 3 : 200$, $2 \times 4 : 150$, $2 \times 5 : 100$, $2 \times 6 : 100$.

by magnetic part of the Hamiltonian, the dissipation drives it away from equilibrium and is counteracted by the correlation structure of the lattice. Indeed we find (see Fig. 30) that for increasing one spatial dimension, i.e. going from 2×2 to 2×4 , the maximal double occupation probability decreases as the lattice is less squared and behaves more like a double chain. Although we expect the double occupation to vanish in the steady state, the comparison of the equilibration behavior of the system for different sizes (e.g. 2×2 , 2×3 , 2×4) gives extended intuition into its correlation structure: It is a very uncommon event that at more than one site a particle is created from the driving. Since the situation where two particles $|\uparrow, \downarrow\rangle$ occupy the same site is energetically unfavorable, the lattice “absorbs” the particle into a superposition. This process faster in more extensive lattices due to its larger entanglement structure.

4. Outlook

There are two very interesting ideas to discuss in the Fermi-Hubbard setting. Apart from introducing other forms of dissipation, it now seems clear that in a one-dimensional chain we can use the snake-method to build super sites of two or possibly more logical sites to enable the evoMPS implementation to treat interactions more complex than next-neighbor or next-nearest-neighbor.

4.1. One-dimensional super sites

In fact, a simple estimation can be made to evaluate the maximal size of the super sites: Assuming consumer-level computation resources, we are limited by 16 GB of RAM, which in turn would be the maximal size a single interaction term could take up. Given that both the bond dimension be negligible (such that the total memory size of the MPS is very small compared to the interaction terms) and all operators build at runtime, such that only the MPS and the current interaction term need be present in the memory, we can estimate the maximal super site size minimizing

the expression

$$q_{n_{\max}} = \frac{C_{\text{mem}}}{256 * q_n^{2N}}, \quad q_{n_{\max}} > 1, \quad (301)$$

where C_{mem} is the amount of available memory. The number 256 comes from the fact that one generally would use 128-bit floats, which takes up 256 bits given that every degree of freedom is complex. For the aforementioned 16 GB and Fermi-Hubbard-type logical sites of dimension $q_n = 4$, we can see that this would be equal to

$$\frac{1}{137438953472} \cdot 16^N < 1 \quad (302)$$

$$\Leftrightarrow N < 9.25, \quad (303)$$

which gives an upper bound of super sites that can consist of 4 logical sites given the fact that the interaction operator will have squared super site dimension, thus facilitating a maximum of 7-next-nearest-neighbor actions to every site of the chain. This is obviously very similar to 'classical' DMRG approaches in the sense that there is a central super block that can be treated very accurately that is connected loosely to its edges. However, it has to be noted that there are conceptual differences. Using the MPS form of the total chain, the truncation error can also be estimated like a normal MPS and controlled via the value of the bond dimension between the super sites. Also, we still use the variational principle and not diagonalization, thus enabling us to sweep through the lattice, which, in theory, should keep the convergence on levels comparable to standard MPS approaches. Nevertheless, the full scope of this approach could not be examined in this dissertation and should be approached in future works, especially with regards to dissipative systems. While we have shown that local and next-neighbor Lindblad operators can be treated, using super sites to enable treatment of more complicated dissipation models seems absolutely worthwhile.

4.2. Nested MPS

Even more radical however is the following approach: Given the fact that we can decompose high-dimensional systems into super sites that contain the full Hilbert space of its constituents, it is only consequential to ask whether we can treat these super sites more efficiently to reduce its limiting impact on not only the memory usage but also computation time. The usual way would be to either resort to using next-neighbor Matrix Product Operators in order to incorporate the long-range interactions following the snake approach or straightaway decomposing the interaction into an MPO with true long-range interaction as has been done in, e.g. [140]. Recalling that we had to develop this data structure to be able to map terms of next-neighbor-interactions that would not be next-neighbor in higher dimensions, it would be too easy to simply conjecture that super sites can be formulated as Matrix Product States. However, this is what we do. And at least for the states on the lattice, it *is* obvious that this approach works: Considering the super sites as tensor products of single sites, we would get the standard MPS decomposition of the form

$$|\Psi_{\text{super}}\rangle = \sum_{i_1=0}^1 \sum_{i_2=0}^1 \cdots \sum_{i_n=0}^1 c_{i_1 \dots i_N} \bigotimes_{j=1}^N |i_j\rangle. \quad (304)$$

But this is just a product state with $D^2 \cdot d \cdot N$ parameters. As such, we can use its span, i.e. the variational class, as basis vectors for the high-level matrix product state. Using the super index β as a means of counting the elements $|i_j^N\rangle$, we can

write the nested MPS for M super sites using $|\beta\rangle \in \text{span}(|i_j^N\rangle)$

$$\begin{aligned}
 |\Psi_{\text{total}}\rangle &= \sum_{\beta_1=0}^1 \sum_{\beta_2=0}^2 \cdots \sum_{\beta_n=0}^M c_{\beta_1 \dots \beta_M} \bigotimes_{l=1}^M |\beta_l\rangle \quad (305) \\
 &= \sum_{\beta_1=0}^1 \sum_{\beta_2=0}^1 \cdots \sum_{\beta_n=0}^1 c_{\beta_1 \dots \beta_M} \bigotimes_{l=1}^M \left[\sum_{i_1=0}^1 \sum_{i_2=0}^1 \cdots \sum_{i_n=0}^1 c_{i_1 \dots i_N} \bigotimes_{j=1}^N |\beta_{i_j}^l\rangle \right]. \quad (306)
 \end{aligned}$$

Although this looks more like a tensor network, it still is a one-dimensional chain of length $M \cdot N$. While one can see that in this way of writing the state it is just a re-indexed MPS, there is no need to restrict to uniform basis states $|\beta_{i_k}\rangle = |\beta_{i_{k+1}}\rangle$. Precisely this property might be the benefit of a logically rearranging: We are able to couple clusters of matrix product states with local interactions and defer any long-range interactions to the outer matrix product. Although it does not solve the problem of long-range interactions straight away, one might be able to engineer outer variational classes to be tractable with the same methods as the inner variational classes, albeit different dynamics.

Whether operators can be mapped to obey the conditions from two (or more) nested MPS constructions is completely unclear at the moment, as is the question whether one can find suitable classes that are reasonably physical. Further research in this direction nevertheless seems worthwhile, because even if this worked only for next-neighbor interactions, it would potentially enable treatment of much larger systems.

Conclusion

Dissipative systems are hard to solve – and, unsurprisingly, this dissertation could not change that fact. However, we have shown that the treatment of problems that can be represented as spin chains with respective interactions, indeed has seen considerable advances.

The presented method of adding Monte Carlo-sampled dissipation to the well-established Time-Dependent Variational principle enables future research of systems previously regarded too complicated for treatment. It has to be noted that the Monte Carlo Time-Dependent Variational Principle is stochastic in nature, i.e. it can only give results about averages of observables – although this is not to be considered a general limitation since thermodynamic processes like dissipation hardly ever are exactly solvable.

We have furthermore shown that the computation scheme can be scaled (almost) arbitrarily, such that much larger quantum systems are within reach of high-performance applications because the MCTDVP trades complexity of the individual task in terms of memory and computation time with the number of samples to be calculated.

Summing up Chapters 6 and 7, we have seen how to study and examine Heisenberg and Fermi-Hubbard models – the two most common and theoretically rich examples of both well-established, yet not-fully-understood systems where the present approach can push the boundaries of the understanding of Condensed Matter Physics, Quantum Information and Thermodynamics into the previously unknown.

The problems encountered while applying the super site-snake algorithm to higher-dimensional Fermi-Hubbard models also marks the entry into uncharted territory as far as numeric libraries are concerned: Although there were neither secret nor overly complicated methods involved, the maturing from the pre-compiled packages at our disposal shows that some of the advances are truly unprecedented – although their use deserves further benchmarking in regards to both computational optimization as well as physical benefit.

We gave examples of both critical and well-converging models to see that the limitations of limited convergence in frustrated systems – still, the MCTDVP does here not perform worse than comparable methods. We then went on to propose setups in high-performance computing that could make previously unreachable amounts of particles treatable as well as pointed out that the specific way of unraveling the master equation we use could be suited to solving systems with higher spatial dimensions, because the stochastic nature of the MCTDVP mimics quasi-diagonalization of the semigroup generator, i.e. if the requirements of the PEPS configurations in question can be properly bounded, nested versions of our approach can be used to *simulate* solving the multi-dimensional PEPS evolution.

Complementing the comments from the previous chapters about extensions and applications of the Monte Carlo Time-Dependent Variational Principle, in Chapter 7 we gave a solid proposition of one straightforward extension that would allow for the treatment of more complicated systems, most notably two-dimensional

Hubbard models. It would certainly be interesting to see an implementation that is based on the current state-of-the-art, but could not be ventured within the scope of this dissertation. Nevertheless, the fact that the opportunities this work opens up regarding dissipative dynamics on Quantum spin chains are not exhaustively accounted for is actually a good thing from the scientific point of view: As dwarfs on the shoulders of other dwarfs on the shoulders of giants, it may not always be possible to know what to look for, but it is certainly good if we have better binoculars.

As such, it is the utmost hope of the author that the present dissertation can act as a refined tool for finding undiscovered physics – in other words, to continue the journey to where no dwarf – and no giant, for that matter – has gone before.

Appendix. List of tables

- 1 **Memory comparison for different lattice sizes.** One can clearly see the exponential growth of the memory requirements for increasing lattice dimensions. In particular in comparison to the sparse memory allocation, the amount of “unnecessary” overhead, following from the fact that large parts of the respective matrices are filled with zeros, is striking. 101

Appendix. List of figures

- 1 **The Bloch sphere.** The 2-dimensional state space of a qubit with basis states $|\uparrow\rangle = r$ and $|\downarrow\rangle = -r$ along the central axis. The convex hull is spanned by the polar decomposition (r, θ, ϕ) of the convex combinations $|\psi\rangle = \cos\left(\frac{\theta}{2}\right)|\downarrow\rangle + e^{i\phi}\sin\left(\frac{\theta}{2}\right)|\uparrow\rangle = \cos\left(\frac{\theta}{2}\right)|\downarrow\rangle + (\cos\phi + i\sin\phi)\sin\left(\frac{\theta}{2}\right)|\uparrow\rangle$. 16
- 2 **Conditional entropy.** Entropy overview for two non-separable random variables: The blue and green circles stand for the entropies $H(X)$ and $H(Y)$ respectively, while the parts without the intersection give the conditional entropies $H(X|Y)$ and $H(Y|X)$. The central, overlapping part is the mutual information $I(X, Y)$ and both sets together form the joint entropy $H(X, Y)$. 20
- 3 **Exemplary lattice configurations.** a) One-dimensional lattice with next-neighbor edges. b) (Two-dimensional) square lattice. c) Honeycomb lattice: vertices are connected in a hexagonal pattern. d) Irregular lattice: without translation invariance, this example is that of an arbitrary graph. 28
- 4 **Boundary of a sublattice.** ∂I is given by the blue nodes of the graph, because they share edges with nodes from *outside* the sublattice. a) One-dimensional lattice. b) Two-dimensional, non-regular example. Note that only one of the sites in the set I does not belong to its boundary, because of the geometry of the set. 30
- 5 **Valence bond theory.** One virtual lattice site consists of two atoms with one unpaired electron each. Either one of the two spins in such a bond then interacts with one of the spatial nearest neighbors, such that the resulting lattice has alternating pairs of spins connected physically and virtually. 32
- 6 **DMRG iteration scheme.** In the first step, the half-chain block [B] is diagonalized to find its approximate ground state. Afterward, a smaller block [a], comprised of one site (and possibly, but rarely more sites), is added at the center of the total chain. The superblock [B a] then is treated as the new block [B_{new}]. The dual [B'] is used to either model a heat bath coupling or for providing proper boundary conditions in case of finite length. 37
- 7 **Frustrated system.** Given a system of three mutually connected sites of qubit dimension representing spin orientation, it is easy to show how to geometrically frustrate that system. With the proposition that neighboring spins should, by action of the system Hamiltonian H , align anti-parallel, this can obviously not lead to a self-consistent ground state for the depicted graph. 42
- 8 **Pictorial illustration of the variational manifold \mathcal{M} and its tangent plane \mathbb{T} .** The path of the variational flow, represented by the Matrix Product State $|\Psi(a(t))\rangle$, on the variational manifold $\mathcal{M}(a)$, is

- shown together with its derivatives $\partial_i |\Psi(a)\rangle$ and $\partial_j |\Psi(a)\rangle$ with respect to variational parameters a_i, a_j at time t . The shaded area below depicts the tangent plane $\mathbb{T}_{\mathcal{M}}(a)$, to which the discretely with respect to time propagated state $H |\Psi(a)\rangle$ is projected, resulting in the expression $P_{\mathbb{T}} H |\Psi(a)\rangle$. 51
- 9 **Example of Brownian motion.** Simulated Markov process with drift coefficient $\mu = 0.5$, volatility $\sigma = 0.3$ and time discretization of 0.01 as given in Eq. (186). 61
- 10 **Pictorial illustration of the variational manifold \mathcal{M} and its tangent plane \mathbb{T} under consideration of the Monte Carlo Time-Dependent Variational Principle.** Additional tangent vectors are calculated for the (randomly simulated) action of the dissipative Lindblad terms L_α on the state $|\Psi(a)\rangle$ and subsequently added to the Hamiltonian tangent vector $H |\Psi(a)\rangle$, resulting in a different position for the resulting approximation of the total time evolution $|\Psi'(a)\rangle$. 77
- 11 **Working of the distributed computing scheduling process.** The clients $\{1, 2, \dots, m\}$ obtain their jobs $\{1, \dots, i\}, \{i+1, \dots, i+k\}, \dots, \{M-n, \dots, M\}$ from the specific queue, deposit the results in the result queue, while the logistics like load balancing are handled by the workflow queue. After enough results are calculated, post-processing is performed on the server. 81
- 12 **Accuracy scaling of Monte Carlo simulation.** Expectation value of the spin value in a 2-qubit system with average taken over both sites and N samples, where $N \in 480, 4800, 48000$ with yellow, blue and red color, respectively for a time evolution after 80 time steps of discretization size $dt = 0.001$. One clearly observes that the experiments with less samples show considerably more volatility. 83
- 13 **Sample averaging.** Four sample configurations of σ^z -observables of a six-site lattice depicted together with its average value, taken from a system with $N = 6$, $H_{XZ} = \sum_{i=1}^5 \sigma_i^x \sigma_{i+1}^x + \lambda \sigma_i^z \sigma_{i+1}^z$, $\lambda = 1$ after 50 time steps of size $dt = 0.001$ with edge driving $L_1 = \sigma_1^+$, $L_2 = \sigma_6^-$. Although individual measurements may not even qualitatively give the correct behavior, the averages does. 83
- 14 **Edge driven Heisenberg XXZ model.** Average magnetization in z -direction for a 16-site XXZ-Heisenberg model with edge driving $L_1 = \sigma^+$, $L_2 = \sigma^-$, interaction parameters $\varepsilon = 1, \lambda = 1, D = 24$ and 300 samples. The straight line is the analytic solution for the steady state from [143], while the dots are the simulation results. 86
- 15 **Expectation value in z -direction for a KX type Heisenberg model.** Expectation value of the spin value in a 16-qubit system with average taken over 320 samples, $dt = 0.001, D = 16$. 89
- 16 **Correlation behavior of the XZ Heisenberg model.** 2-point correlation function for the XZ Heisenberg model as given in Eq. (247). 89
- 17 **Strong bihomogenous driving regime.** z -direction of average spin values per site for strong driving ($\mu = 1$) with bihomogenous Lindblads according to Eq. (250), 500 samples over 1000 time steps with discretization $dt = 0.001$ with bond dimension $D = 16$. The spins form two clearly

- distinguishable domains of opposite alignment with a minimal overlap zone in the center. 91
- 18 **Medium bihomogenous driving regime.** z -direction of average spin values per site for medium driving ($\mu = 0.75$) of bihomogenous Lindblads according to Eq. (250), 500 samples, 1000 time steps, $dt = 0.001$ with bond dimension $D = 16$. The domain interaction zone is considerably larger than in Fig. 17. 91
- 19 **Correlation function of strong bihomogenous driving regime.** 2-point correlation function for the bihomogenous XZ-Heisenberg model given in Eq. (243) with the same parameters as in Fig. 18. We observe that the correlation corresponds 1-to-1 with the magnetization itself, which means that the chosen bond dimension suffices to capture the relevant dynamics. 92
- 20 **Term scheme of ^{40}K .** Experimentally coupled $m = 7/2$, $m = 9/2$ and $m = 11/2$ electron levels in ^{40}K [95]. 93
- 21 **One-dimensional Fermi Hubbard lattice.** Fermi-Hubbard model on a lattice. The Hilbert space is that of two coupled spins, their subspaces denoted (\uparrow) and (\downarrow). This leads to $\mathcal{H}_{(\uparrow)+(\downarrow)} = \mathbb{C}^2 \otimes \mathbb{C}^2 = \mathbb{C}^4$. For computational convenience, this can be mapped to either b) A snake lattice with subspace order $\dots \uparrow\downarrow\uparrow\downarrow\uparrow \dots$ that is 2-site-translation invariant or b') a double snake lattice with 1-site-translation-invariance and configuration $\dots \uparrow\downarrow\uparrow\downarrow \dots$ 94
- 22 **Example of driven Fermi-Hubbard time evolution.** Occupation number for 2-site simulation (per site). 1 sample only. The system parameters are $t = 1$, $U = 100$, $\sqrt{\gamma_1} = 1$, $\sqrt{\gamma_2} = \sqrt{2}$, $D = 16$, $dt = 0.001$, $3 \cdot 10^4$ time steps. 98
- 23 **Time evolution plot of diagonal elements.** Diagonal elements of the density matrix for lattice length 8. The system parameters are as in Fig. 22, but for 10^3 samples. 98
- 24 **Relevant observables of a lattice with 8 sites.** Occupation number, both for total particle count N (per site) as well as the subsystems N_\uparrow and N_\downarrow . Furthermore the plot contains 1-site entropy, magnetization and double occupation probability. The system parameters are as in Fig. 22, but for 10^3 samples. 99
- 25 **Two-dimensional Fermi Hubbard lattice.** evoMPS can only handle one-dimensional lattices in principle, we need to adapt the lattice representation in order to treat higher-dimensional systems: Note how we draw a snake through the lattice to map it to one-dimension (red arrows): First, we compose the two local subspaces like before (black ellipses) and then go all the way through one supersite (blue dashed area). We then move to the very top of the next supersite and repeat the pattern. 100
- 26 **Counting of graph bonds.** For the matter of bounding the maximal amount of memory the interaction operators will occupy we have to count every edge twice: The term H_{j_i} is quantitatively different from H_{i_j} and effectively doubles the amount of memory we need per edge. The same is, of course, true for the Lindblad operators j_1, \dots, j_3 . 101

- 27 **Sparse array representation.** Pictorial representation of $j_{12}^{(3)}$ in a system with super site dimension 2. The matrix dimension of the operator is 256×256 , but there are 8 non-zero elements only (black dots), i.e. 97% of the allocated memory can be cut. 102
- 28 **Time evolution plot of diagonal elements.** Diagonal elements of the density matrix for a square lattice with 2×2 sites. The system parameters are $t = 1$, $U = 100$, $\sqrt{\gamma_1} = 1$, $\sqrt{\gamma_2} = \sqrt{2}$, $D = 16$, $dt = 0.001$, $3 \cdot 10^4$ time steps, 250 samples. 104
- 29 **Relevant observables of a 2×2 square lattice.** Occupation number, both for total particle count N (per site) as well as the subsystems N_\uparrow and N_\downarrow . Furthermore the plot contains 1-site entropy, magnetization and double occupation probability. The system parameters are as in Fig. 28. 104
- 30 **Comparison of double occupations for varying spatial extension of a square lattice.** We compare the maximal value of the double occupation diagonal element $|\uparrow, \downarrow\rangle \langle \uparrow, \downarrow|$ for *one* increasing spatial dimension. The error becomes larger with higher number of sites because we chose to decrease the number of samples at the same time to accommodate for the increased runtime. The system parameters are as in Fig. 28 except for the sample number. Those are $2 \times 2 : 250$, $2 \times 3 : 200$, $2 \times 4 : 150$, $2 \times 5 : 100$, $2 \times 6 : 100$. 105

Resources / Hilfsmittel

The following materials were used in the making of this dissertation:

Die folgenden Hilfsmittel wurden für diese Dissertation verwendet:

- The MikTeX[28] typography and typesetting environment implementing the \LaTeX typesetting format.
- The TeXnicCenter[30] \LaTeX editor.
- The Wolfram Mathematica[147] computer algebra program, used for post processing and plotting simulation data.

No Bohmians were harmed during the writing of this dissertation. Probably.

Curriculum Vitae

Fabian W. G. Transchel

- Born in 1987
- 1993-1997:
Wilhelm-Stedler-Schule Barsinghausen
- 1997-1998:
Orientierungsstufe am Spalterhals, Barsinghausen
- 1998-2005:
Hannah-Arendt-Gymnasium Barsinghausen, Ganztagschule
- 2005-2010:
Studies in physics, Leibniz Universität Hannover, degree: Dipl.-Phys.
- 2011-2015:
Graduate assistant to Prof. R. F. Werner and Prof. T. J. Osborne

Bibliography

- [1] Ian Affleck et al. “Rigorous Results on Valence-Bond Ground States in Antiferromagnets”. English. In: *Condensed Matter Physics and Exactly Soluble Models*. Ed. by Bruno Nachtergaele, JanPhilip Solovej, and Jakob Yngvason. Springer Berlin Heidelberg, 2004, pp. 249–252. ISBN: 978-3-642-06093-9. DOI: 10.1007/978-3-662-06390-3_18. URL: http://dx.doi.org/10.1007/978-3-662-06390-3_18.
- [2] Ian Affleck et al. “Valence bond ground states in isotropic quantum antiferromagnets”. In: *Comm. Math. Phys.* 115.3 (1988), pp. 477–528. URL: <http://projecteuclid.org/euclid.cmp/1104161001>.
- [3] M. Aizenman et al. “Matrix regularizing effects of Gaussian perturbations”. In: *ArXiv e-prints* (Sept. 2015). arXiv: 1509.01799 [math.PR].
- [4] C. Alexandre Brasil, F. Fernandes Fanchini, and R. d. J. Napolitano. “A simple derivation of the Lindblad equation”. In: *ArXiv e-prints* (Oct. 2011). arXiv: 1110.2122 [quant-ph].
- [5] Rnyi Alfrd. “On measures of information and entropy”. In: *Proceedings of the fourth Berkeley Symposium on Mathematics, Statistics and Probability*. 1961, pp. 547–561.
- [6] Huzihiro Araki and ElliottH. Lieb. “Entropy inequalities”. English. In: *Communications in Mathematical Physics* 18.2 (1970), pp. 160–170. ISSN: 0010-3616. DOI: 10.1007/BF01646092. URL: <http://dx.doi.org/10.1007/BF01646092>.
- [7] A. Aspect et al. “Laser Cooling below the One-Photon Recoil Energy by Velocity-Selective Coherent Population Trapping”. In: *Phys. Rev. Lett.* 61 (7 Aug. 1988), pp. 826–829. DOI: 10.1103/PhysRevLett.61.826. URL: <http://link.aps.org/doi/10.1103/PhysRevLett.61.826>.
- [8] M. Bal et al. “Matrix product state renormalization”. In: *ArXiv e-prints* (Sept. 2015). arXiv: 1509.01522 [quant-ph].
- [9] Howard Barnum et al. “Noncommuting Mixed States Cannot Be Broadcast”. In: *Phys. Rev. Lett.* 76 (15 Apr. 1996), pp. 2818–2821. DOI: 10.1103/PhysRevLett.76.2818. URL: <http://link.aps.org/doi/10.1103/PhysRevLett.76.2818>.
- [10] D. Benoit. “Matrix Product States approach to non-Markovian processes”. In: *ArXiv e-prints* (Oct. 2014). arXiv: 1410.0877 [quant-ph].
- [11] H. Bethe. “Zur Theorie der Metalle”. German. In: *Zeitschrift für Physik* 71.3-4 (1931), pp. 205–226. ISSN: 0044-3328. DOI: 10.1007/BF01341708. URL: <http://dx.doi.org/10.1007/BF01341708>.
- [12] S. M. Bhattacharjee and A. Khare. “Fifty Years of the Exact Solution of the Two-Dimensional Ising Model by Onsager”. In: *eprint arXiv:cond-mat/9511003* (Nov. 1995). eprint: cond-mat/9511003.
- [13] Enrico Bibbona, Gianna Panfilò, and Patrizia Tavella. “The Ornstein-Uhlenbeck process as a model of a low pass filtered white noise”. In: *Metrologia* 45.6 (2008), S117. URL: <http://stacks.iop.org/0026-1394/45/i=6/a=S17>.

- [14] Rainer Blatt and David Wineland. “Entangled states of trapped atomic ions”. In: *Nature* 453.7198 (June 2008), pp. 1008–1015. ISSN: 0028-0836. URL: <http://dx.doi.org/10.1038/nature07125>.
- [15] O. Bratteli and D. W. Robinson. *Operator Algebras and Quantum Statistical Mechanics*. Vol. 1. 2. Springer, Berlin, 1997, p. 587.
- [16] Barbara J. Breen et al. “Invitation to embarrassingly parallel computing”. In: *American Journal of Physics* 76.4 (2008), pp. 347–352. DOI: <http://dx.doi.org/10.1119/1.2834738>. URL: <http://scitation.aip.org/content/aapt/journal/ajp/76/4/10.1119/1.2834738>.
- [17] Lowell S. Brown and Gerald Gabrielse. “Geonium theory: Physics of a single electron or ion in a Penning trap”. In: *Rev. Mod. Phys.* 58 (1 Jan. 1986), pp. 233–311. DOI: 10.1103/RevModPhys.58.233. URL: <http://link.aps.org/doi/10.1103/RevModPhys.58.233>.
- [18] Ralf Bulla, Theo A. Costi, and Thomas Pruschke. “Numerical renormalization group method for quantum impurity systems”. In: *Rev. Mod. Phys.* 80 (2 Apr. 2008), pp. 395–450. DOI: 10.1103/RevModPhys.80.395. URL: <http://link.aps.org/doi/10.1103/RevModPhys.80.395>.
- [19] John C Butcher. “The Numerical Analysis of Ordinary Differential Equations. Runge-Kutta and General Linear methods”. In: Wiley, 1987.
- [20] Giuseppe Carleo. *Spectral And Dynamical Properties Of Strongly Correlated Systems*. PhD thesis, 2011.
- [21] Giuseppe Carleo et al. “Light-cone effect and supersonic correlations in one- and two-dimensional bosonic superfluids”. In: *Phys. Rev. A* 89 (3 Mar. 2014), p. 031602. DOI: 10.1103/PhysRevA.89.031602. URL: <http://link.aps.org/doi/10.1103/PhysRevA.89.031602>.
- [22] Giuseppe Carleo et al. “Localization and Glassy Dynamics Of Many-Body Quantum Systems”. In: *Sci. Rep.* 2 (Feb. 2012), pp. –. URL: <http://dx.doi.org/10.1038/srep00243>.
- [23] D. Ceperley, G. V. Chester, and M. H. Kalos. “Monte Carlo simulation of a many-fermion study”. In: *Phys. Rev. B* 16 (7 Oct. 1977), pp. 3081–3099. DOI: 10.1103/PhysRevB.16.3081. URL: <http://link.aps.org/doi/10.1103/PhysRevB.16.3081>.
- [24] John F. Clauser et al. “Proposed Experiment to Test Local Hidden-Variable Theories”. In: *Phys. Rev. Lett.* 23 (15 Oct. 1969), pp. 880–884. DOI: 10.1103/PhysRevLett.23.880. URL: <http://link.aps.org/doi/10.1103/PhysRevLett.23.880>.
- [25] Valerie Coffman, Joydip Kundu, and William K. Wootters. “Distributed entanglement”. In: *Phys. Rev. A* 61 (5 Apr. 2000), p. 052306. DOI: 10.1103/PhysRevA.61.052306. URL: <http://link.aps.org/doi/10.1103/PhysRevA.61.052306>.
- [26] The BLAS community. “openBLAS source code: Basic Linear Algebra Subprograms”. In: (2012). URL: <http://www.netlib.org/blas/>.
- [27] The LAPACK community. “Linear Algebra PACKage”. In: (2013). URL: <http://www.netlib.org/lapack/>.
- [28] The MikTeX community. “MikTeX - a L^AT_EX typesetting engine”. In: (2015). URL: <http://miktex.org/>.
- [29] The SciPy community. “SciPy – A Python-based ecosystem of open-source software for mathematics, science, and engineering”. In: (2015). URL: <https://www.scipy.org/>.
- [30] The TeXnicCenter community. “TeXnicCenter - a L^AT_EX editor”. In: (2015). URL: <http://www.texniccenter.org/>.

- [31] David L. Copper, Joseph Gerratt, and Mario Raimondi. “The electronic structure of the benzene molecule”. In: *Nature* 323.6090 (Oct. 1986), pp. 699–701. URL: <http://dx.doi.org/10.1038/323699a0>.
- [32] T. Cubitt, D. Perez-Garcia, and M. M. Wolf. “Undecidability of the Spectral Gap (full version)”. In: *ArXiv e-prints* (Feb. 2015). arXiv: 1502.04573 [quant-ph].
- [33] J. Cui, J. I. Cirac, and M. C. Bañuls. “Variational Matrix Product Operators for the Steady State of Dissipative Quantum Systems”. In: *Physical Review Letters* 114.22, 220601 (June 2015), p. 220601. DOI: 10.1103/PhysRevLett.114.220601. arXiv: 1501.06786 [quant-ph].
- [34] P. Czarnik and J. Dziarmaga. “Variational approach to projected entangled pair states at finite temperature”. In: *Phys. Rev. B* 92.3, 035152 (July 2015), p. 035152. DOI: 10.1103/PhysRevB.92.035152. arXiv: 1503.01077 [cond-mat.str-el].
- [35] E. R. Davidson. “The iterative calculation of a few of the lowest eigenvalues and corresponding eigenvectors of large real symmetric matrices”. In: *J. Comp. Phys* 17 (1975), pp. 87–94.
- [36] H. De Raedt and W. von der Linden. “Monte Carlo diagonalization of many-body problems: Application to fermion systems”. In: *Phys. Rev. B* 45 (15 Apr. 1992), pp. 8787–8790. DOI: 10.1103/PhysRevB.45.8787. URL: <http://link.aps.org/doi/10.1103/PhysRevB.45.8787>.
- [37] E.W. Dijkstra. “A note on two problems in connexion with graphs”. English. In: *Numerische Mathematik* 1.1 (1959), pp. 269–271. ISSN: 0029-599X. DOI: 10.1007/BF01386390. URL: <http://dx.doi.org/10.1007/BF01386390>.
- [38] P. A. M. Dirac. “On the Annihilation of Electrons and Protons”. In: *Mathematical Proceedings of the Cambridge Philosophical Society* 26 (03 July 1930), pp. 361–375. ISSN: 1469-8064. DOI: 10.1017/S0305004100016091. URL: http://journals.cambridge.org/article_S0305004100016091.
- [39] P. A. M. Dirac. “On the Theory of Quantum Mechanics”. In: *Proceedings of the Royal Society of London A: Mathematical, Physical and Engineering Sciences* 112.762 (1926), pp. 661–677. ISSN: 0950-1207. DOI: 10.1098/rspa.1926.0133.
- [40] D. P. Divincenzo. “The Physical Implementation of Quantum Computation”. In: *Fortschritte der Physik* 48 (2000), pp. 771–783. DOI: 10.1002/1521-3978(200009)48:9/11<771::AID-PROP771>3.0.CO;2-E. eprint: quant-ph/0002077.
- [41] W. Dür, G. Vidal, and J. I. Cirac. “Three qubits can be entangled in two inequivalent ways”. In: *Phys. Rev. A* 62.6, 062314 (Dec. 2000), p. 062314. DOI: 10.1103/PhysRevA.62.062314. eprint: quant-ph/0005115.
- [42] A. Einstein. “Über die von der molekularkinetischen Theorie der Wärme geforderte Bewegung von in ruhenden Flüssigkeiten suspendierten Teilchen.” In: 1905, pp. 549–560.
- [43] A. Einstein, B. Podolsky, and N. Rosen. “Can Quantum-Mechanical Description of Physical Reality Be Considered Complete?” In: *Phys. Rev.* 47 (10 May 1935), pp. 777–780. DOI: 10.1103/PhysRev.47.777. URL: <http://link.aps.org/doi/10.1103/PhysRev.47.777>.
- [44] J. Eisert, M. Cramer, and M. B. Plenio. “Colloquium : Area laws for the entanglement entropy”. In: *Rev. Mod. Phys.* 82 (1 Feb. 2010), pp. 277–306. DOI: 10.1103/RevModPhys.82.277. URL: <http://link.aps.org/doi/10.1103/RevModPhys.82.277>.
- [45] Ivar Ekeland. “On the variational principle”. In: *Journal of Mathematical Analysis and Applications* 47.2 (1974), pp. 324–353.

- [46] Sheer El-Showk et al. “Solving the 3d Ising Model with the Conformal Bootstrap II. c-Minimization and Precise Critical Exponents”. English. In: *Journal of Statistical Physics* 157.4-5 (2014), pp. 869–914. ISSN: 0022-4715. DOI: 10.1007/s10955-014-1042-7. URL: <http://dx.doi.org/10.1007/s10955-014-1042-7>.
- [47] M. Fannes, B. Nachtergaele, and R. F. Werner. “Exact Antiferromagnetic Ground States of Quantum Spin Chains”. In: *EPL (Europhysics Letters)* 10.7 (1989), p. 633. URL: <http://stacks.iop.org/0295-5075/10/i=7/a=005>.
- [48] M. Fannes, B. Nachtergaele, and R. F. Werner. “Finitely correlated states on quantum spin chains”. In: *Comm. Math. Phys.* 144.3 (1992), pp. 443–490. URL: <http://projecteuclid.org/euclid.cmp/1104249404>.
- [49] M. Fannes, B. Nachtergaele, and R.F. Werner. “Finitely Correlated Pure States”. In: *Journal of Functional Analysis* 120.2 (1994), pp. 511–534. DOI: <http://dx.doi.org/10.1006/jfan.1994.1041>.
- [50] E. Fermi. “On the Quantization of the Monoatomic Ideal Gas”. In: *eprint arXiv:cond-mat/9912229* (Dec. 1999). Ed. by A. Zannoni. eprint: [cond-mat/9912229](http://arxiv.org/abs/cond-mat/9912229).
- [51] C. Fernández-González et al. “Frustration Free Gapless Hamiltonians for Matrix Product States”. In: *Communications in Mathematical Physics* 333.1 (2015), pp. 299–333. ISSN: 1432-0916. DOI: 10.1007/s00220-014-2173-z. URL: <http://dx.doi.org/10.1007/s00220-014-2173-z>.
- [52] P. E. Finch et al. “Quantum phases of a chain of strongly interacting anyons”. In: *Phys. Rev. B* 90.8, 081111 (Aug. 2014), p. 081111. DOI: 10.1103/PhysRevB.90.081111. arXiv: 1404.2439 [[cond-mat.str-el](http://arxiv.org/abs/cond-mat.str-el)].
- [53] V. Fock. “Konfigurationsraum und zweite Quantelung”. German. In: *Zeitschrift für Physik* 75.9-10 (1932), pp. 622–647. ISSN: 0044-3328. DOI: 10.1007/BF01344458. URL: <http://dx.doi.org/10.1007/BF01344458>.
- [54] V. Fock. “Näherungsmethode zur Lösung des quantenmechanischen Mehrkörperproblems”. In: *Zeitschrift für Physik* 61.1-2 (1930), pp. 126–148. ISSN: 0044-3328. DOI: 10.1007/BF01340294. URL: <http://dx.doi.org/10.1007/BF01340294>.
- [55] G B Folland. “Fourier Analysis and its Applications”. In: Belmont, CA, USA, 1992.
- [56] J. Frenkel. *Wave Mechanics, Advanced General Theory*. Oxford, 1934.
- [57] J. J. Garcia-Ripoll. “Time evolution of Matrix Product States”. In: *eprint arXiv:cond-mat/0602305* (Feb. 2006). eprint: [cond-mat/0602305](http://arxiv.org/abs/cond-mat/0602305).
- [58] C. W. Gardiner. *Handbook of Stochastic Methods for Physics, Chemistry and the Natural Sciences*. Ed. by H. Haken. 2nd. Springer, 1985.
- [59] C W Gardiner and P Zoller. “Quantum Noise”. In: Springer Series in Synergetics, 3rd ed. Berlin Heidelberg: Springer-Verlag, 2010.
- [60] *Geometry of the Time-Dependent Variational Principle in Quantum Mechanics*. Vol. 140. Lecture Notes in Physics, Berlin Springer Verlag. 1981. DOI: 10.1007/3-540-10579-4.
- [61] Walther Gerlach and Otto Stern. “Das magnetische Moment des Silberatoms”. German. In: *Zeitschrift für Physik* 9.1 (1922), pp. 353–355. ISSN: 0044-3328. DOI: 10.1007/BF01326984. URL: <http://dx.doi.org/10.1007/BF01326984>.
- [62] Walther Gerlach and Otto Stern. “Der experimentelle Nachweis der Richtungsquantelung im Magnetfeld”. German. In: *Zeitschrift für Physik* 9.1 (1922), pp. 349–352. ISSN: 0044-3328. DOI: 10.1007/BF01326983. URL: <http://dx.doi.org/10.1007/BF01326983>.

- [63] Neil A. Gershenfeld and Isaac L. Chuang. “Bulk Spin-Resonance Quantum Computation”. In: *Science* 275.5298 (1997), pp. 350–356. DOI: 10.1126/science.275.5298.350. eprint: <http://www.sciencemag.org/content/275/5298/350.full.pdf>.
- [64] Daniel T. Gillespie. “Exact numerical simulation of the Ornstein-Uhlenbeck process and its integral”. In: *Phys. Rev. E* 54 (2 Aug. 1996), pp. 2084–2091. DOI: 10.1103/PhysRevE.54.2084. URL: <http://link.aps.org/doi/10.1103/PhysRevE.54.2084>.
- [65] N Gisin and I C Percival. “The quantum-state diffusion model applied to open systems”. In: *Journal of Physics A: Mathematical and General* 25.21 (1992), p. 5677. URL: <http://stacks.iop.org/0305-4470/25/i=21/a=023>.
- [66] D. Gosset and Y. Huang. “Correlation length versus gap in frustration-free systems”. In: *ArXiv e-prints* (Sept. 2015). arXiv: 1509.06360 [quant-ph].
- [67] D. M. Greenberger, M. A. Horne, and A. Zeilinger. “Going Beyond Bell’s Theorem”. In: *ArXiv e-prints* (Dec. 2007). arXiv: 0712.0921 [quant-ph].
- [68] John Gribbin. “In Search of Schrödinger’s Cat”. In: *Transworld Publishers, Ltd* (1984).
- [69] Bennett Charles H et al. “Concentrating Partial Entanglement by Local Operations”. In: *Phys. Rev. A* 53 (1996), pp. 2046–2052.
- [70] Bennett Charles H et al. “Mixed State Entanglement and Quantum Error Correction”. In: *Phys. Rev. A* 54 (1996), pp. 3824–3851.
- [71] J. Haegeman et al. “Unifying time evolution and optimization with matrix product states”. In: *ArXiv e-prints* (Aug. 2014). arXiv: 1408.5056 [quant-ph].
- [72] Jutho Haegeman. *Variational Renormalization Group Methods for Extended Quantum Systems*. Ed. by PhD thesis. 2011.
- [73] Jutho Haegeman et al. “Time-Dependent Variational Principle for Quantum Lattices”. In: *Phys. Rev. Lett.* 107 (7 Aug. 2011), p. 070601. DOI: 10.1103/PhysRevLett.107.070601. URL: <http://link.aps.org/doi/10.1103/PhysRevLett.107.070601>.
- [74] G. Hager and G. Wellein. *Introduction to High Performance Computing for Scientists and Engineers*. Chapman & Hall/CRC Computational Science. CRC Press, 2010. ISBN: 9781439811931. URL: <https://books.google.de/books?id=rkWPojgfeM8C>.
- [75] E Hairer and G Wanner. “Solving Ordinary Differential Equations. Band 2: Stiff and differential-algebraic problems. 2. revised edition. Corrected 2. print”. In: Springer, 2002.
- [76] Ernst Hairer, Christian Lubich, and Gerhard Wanner. *Geometric Numerical Integration*. Vol. 31. Springer Series in Computational Mathematics. Springer, 2006. DOI: 10.1007/3-540-30666-8.
- [77] D. R. Hartree. “The Wave Mechanics of an Atom with a Non-Coulomb Central Field. Part I. Theory and Methods”. In: *Mathematical Proceedings of the Cambridge Philosophical Society* 24 (01 Jan. 1928), pp. 89–110. ISSN: 1469-8064. DOI: 10.1017/S0305004100011919. URL: http://journals.cambridge.org/article_S0305004100011919.
- [78] D. R. Hartree. “The Wave Mechanics of an Atom with a Non-Coulomb Central Field. Part II. Some Results and Discussion”. In: *Mathematical Proceedings of the Cambridge Philosophical Society* 24 (01 Jan. 1928), pp. 111–132. ISSN: 1469-8064. DOI: 10.1017/S0305004100011920. URL: http://journals.cambridge.org/article_S0305004100011920.

- [79] M B Hastings. “An area law for one-dimensional quantum systems”. In: *Journal of Statistical Mechanics: Theory and Experiment* 2007.08 (2007), P08024. URL: <http://stacks.iop.org/1742-5468/2007/i=08/a=P08024>.
- [80] W. K. HASTINGS. “Monte Carlo sampling methods using Markov chains and their applications”. In: *Biometrika* 57.1 (1970), pp. 97–109. DOI: 10.1093/biomet/57.1.97. eprint: <http://biomet.oxfordjournals.org/content/57/1/97.full.pdf+html>. URL: <http://biomet.oxfordjournals.org/content/57/1/97.abstract>.
- [81] P. Hohenberg and W. Kohn. “Inhomogeneous Electron Gas”. In: *Phys. Rev.* 136 (3B Nov. 1964), B864–B871. DOI: 10.1103/PhysRev.136.B864. URL: <http://link.aps.org/doi/10.1103/PhysRev.136.B864>.
- [82] A. Honecker and S. Wessel. “Magneto-caloric effect in quantum spin-s chains”. In: *ArXiv e-prints* (July 2009). arXiv: 0907.3736 [cond-mat.str-el].
- [83] J. Hubbard. “Electron Correlations in Narrow Energy Bands”. In: *Proceedings of the Royal Society of London A: Mathematical, Physical and Engineering Sciences* 276.1365 (1963), pp. 238–257. ISSN: 0080-4630. DOI: 10.1098/rspa.1963.0204.
- [84] R.L. Hudson and K.R. Parthasarathy. “Quantum Ito’s formula and stochastic evolutions”. English. In: *Communications in Mathematical Physics* 93.3 (1984), pp. 301–323. ISSN: 0010-3616. DOI: 10.1007/BF01258530. URL: <http://dx.doi.org/10.1007/BF01258530>.
- [85] David A. Huse and Eric D. Siggia. “The density distribution of a weakly interacting bose gas in an external potential”. English. In: *Journal of Low Temperature Physics* 46.1-2 (1982), pp. 137–149. ISSN: 0022-2291. DOI: 10.1007/BF00655448. URL: <http://dx.doi.org/10.1007/BF00655448>.
- [86] Ernst Ising. “Beitrag zur Theorie des Ferromagnetismus”. In: *Zeitschrift für Physik* 31.1 (1925), pp. 253–258. ISSN: 0044-3328. DOI: 10.1007/BF02980577. URL: <http://dx.doi.org/10.1007/BF02980577>.
- [87] Kiyosi Itô. *Diffusion Processes*. Wiley Online Library, 1974.
- [88] A.R. Its and V.E. Korepin. “Generalized entropy of the Heisenberg spin chain”. English. In: *Theoretical and Mathematical Physics* 164.3 (2010), pp. 1136–1139. ISSN: 0040-5779. DOI: 10.1007/s11232-010-0091-6. URL: <http://dx.doi.org/10.1007/s11232-010-0091-6>.
- [89] R Jackiw and A Kerman. “Time-dependent variational principle and the effective action”. In: *Physics Letters A* 71.2 (1979), pp. 158–162.
- [90] H. Jia, C. Moore, and B. Selman. “From spin glasses to hard satisfiable formulas”. In: *eprint arXiv:cond-mat/0408190* (Aug. 2004). eprint: cond-mat/0408190.
- [91] Bell John. “On the Einstein Podolsky Rosen Paradox”. In: *Physics* 1.3 (1964).
- [92] P. Jordan and E. Wigner. “Über das Paulische Äquivalenzverbot”. In: *Zeitschrift für Physik* 47.9-10 (1928), pp. 631–651. DOI: 10.1007/bf01331938. URL: <http://dx.doi.org/10.1007/bf01331938>.
- [93] B.D. Josephson. “Possible new effects in superconductive tunnelling”. In: *Physics Letters* 1.7 (1962), pp. 251–253. ISSN: 0031-9163. DOI: [http://dx.doi.org/10.1016/0031-9163\(62\)91369-0](http://dx.doi.org/10.1016/0031-9163(62)91369-0). URL: <http://www.sciencedirect.com/science/article/pii/0031916362913690>.
- [94] Richard Jozsa and Benjamin Schumacher. “A new proof of the quantum noiseless coding theorem”. In: *Journal of Modern Optics* 41.12 (1994).
- [95] J. Kaczmarczyk, H. Weimer, and M. Lemeshko. “Dissipative Preparation of Antiferromagnetic Order in the Fermi-Hubbard Model”. In: *ArXiv e-prints* (Jan. 2016). arXiv: 1601.00646 [cond-mat.quant-gas].

- [96] Christian Karlewski and Michael Marthaler. “Time-local master equation connecting the Born and Markov approximations”. In: *Phys. Rev. B* 90 (10 Sept. 2014), p. 104302. DOI: 10.1103/PhysRevB.90.104302. URL: <http://link.aps.org/doi/10.1103/PhysRevB.90.104302>.
- [97] Mark Kasevich and Steven Chu. “Laser cooling below a photon recoil with three-level atoms”. In: *Phys. Rev. Lett.* 69 (12 Sept. 1992), pp. 1741–1744. DOI: 10.1103/PhysRevLett.69.1741. URL: <http://link.aps.org/doi/10.1103/PhysRevLett.69.1741>.
- [98] E.H. Kennard. “Zur Quantenmechanik einfacher Bewegungstypen”. German. In: *Zeitschrift für Physik* 44.4-5 (1927), pp. 326–352. ISSN: 0044-3328. DOI: 10.1007/BF01391200. URL: <http://dx.doi.org/10.1007/BF01391200>.
- [99] P. R. C. Kent, R. J. Needs, and G. Rajagopal. “Monte Carlo energy and variance-minimization techniques for optimizing many-body wave functions”. In: *Physical Review B* 59.19 (May 1999), pp. 344–351.
- [100] T. D. Kieu and C. J. Griffin. “Monte Carlo simulations with indefinite and complex-valued measures”. In: *Phys. Rev. E* 49 (5 May 1994), pp. 3855–3859. DOI: 10.1103/PhysRevE.49.3855. URL: <http://link.aps.org/doi/10.1103/PhysRevE.49.3855>.
- [101] Achim Klenke. “Wahrscheinlichkeitstheorie”. In: Springer.
- [102] M. Kliesch, D. Gross, and J. Eisert. “Matrix-Product Operators and States: NP-Hardness and Undecidability”. In: *Phys. Rev. Lett.* 113 (16 Oct. 2014), p. 160503. DOI: 10.1103/PhysRevLett.113.160503. URL: <http://link.aps.org/doi/10.1103/PhysRevLett.113.160503>.
- [103] R. Koenig, R. Renner, and C. Schaffner. “The operational meaning of min- and max-entropy”. In: *ArXiv e-prints* (July 2008). arXiv: 0807.1338 [quant-ph].
- [104] W. Kohn and L. J. Sham. “Self-Consistent Equations Including Exchange and Correlation Effects”. In: *Phys. Rev.* 140 (4A Nov. 1965), A1133–A1138. DOI: 10.1103/PhysRev.140.A1133. URL: <http://link.aps.org/doi/10.1103/PhysRev.140.A1133>.
- [105] A. Kossakowski. “On quantum statistical mechanics of non-Hamiltonian systems”. In: *Reports on Mathematical Physics* 3.4 (1972), pp. 247–274. ISSN: 0034-4877. DOI: [http://dx.doi.org/10.1016/0034-4877\(72\)90010-9](http://dx.doi.org/10.1016/0034-4877(72)90010-9). URL: <http://www.sciencedirect.com/science/article/pii/0034487772900109>.
- [106] M. Kotzian et al. “Channel Blockade in a Two-Path Triple-Quantum-Dot System”. In: *ArXiv e-prints* (July 2015). arXiv: 1507.03595 [cond-mat.mes-hall].
- [107] C. V. Kraus and T. J. Osborne. “Time-dependent variational principle for dissipative dynamics”. In: *Physical Review A: Atomic, Molecular, and Optical Physics* 86.6, 062115 (Dec. 2012), p. 062115. DOI: 10.1103/PhysRevA.86.062115. arXiv: 1206.3102 [quant-ph].
- [108] H. R. Krishna-Murthy, J. W. Wilkins, and K. G. Wilson. “Renormalization-group approach to the Anderson model of dilute magnetic alloys. I. Static properties for the symmetric case”. In: *Phys. Rev. B* 21 (3 Feb. 1980), pp. 1003–1043. DOI: 10.1103/PhysRevB.21.1003. URL: <http://link.aps.org/doi/10.1103/PhysRevB.21.1003>.
- [109] W. Kutta. “Beitrag zur näherungsweise Integration totaler Differentialgleichungen”. In: vol. 46. 1901, pp. 435–453.
- [110] C. Lanczos. “An iteration method for the solution of the eigenvalue problem of linear differential and integral operators”. In: *J. Res. Natl Bur. Std.* 45 (1950), pp. 225–282.

- [111] L. D. Landau and E. M. Lifschitz. “Lehrbuch der theoretischen Physik V. Statistische Physik”. In: Berlin: Akademie Verlag, 1970.
- [112] P. W. LANGHOFF, S. T. EPSTEIN, and M. KARPLUS. “Aspects of Time-Dependent Perturbation Theory”. In: *Rev. Mod. Phys.* 44 (3 July 1972), pp. 602–644. DOI: 10.1103/RevModPhys.44.602. URL: <http://link.aps.org/doi/10.1103/RevModPhys.44.602>.
- [113] D. Leibfried et al. “Creation of a six-atom Schrödinger cat state”. In: *Nature* 438.7068 (Dec. 2005), pp. 639–642. ISSN: 0028-0836. URL: <http://dx.doi.org/10.1038/nature04251>.
- [114] G. Lindblad. “On the generators of quantum dynamical semigroups”. English. In: *Communications in Mathematical Physics* 48.2 (1976), pp. 119–130. ISSN: 0010-3616. DOI: 10.1007/BF01608499. URL: <http://dx.doi.org/10.1007/BF01608499>.
- [115] F. Livet. “The Cluster Updating Monte Carlo Algorithm Applied to the 3d Ising Problem”. In: *Europhysics Letters* 16.2 (1991), p. 139. URL: <http://stacks.iop.org/0295-5075/16/i=2/a=003>.
- [116] E. Y. Loh et al. “Sign problem in the numerical simulation of many-electron systems”. In: *Phys. Rev. B* 41 (13 May 1990), pp. 9301–9307. DOI: 10.1103/PhysRevB.41.9301. URL: <http://link.aps.org/doi/10.1103/PhysRevB.41.9301>.
- [117] Daniel Loss and David P. DiVincenzo. “Quantum computation with quantum dots”. In: *Phys. Rev. A* 57 (1 Jan. 1998), pp. 120–126. DOI: 10.1103/PhysRevA.57.120. URL: <http://link.aps.org/doi/10.1103/PhysRevA.57.120>.
- [118] JC Luke. “A variational principle for a fluid with a free surface”. In: *Journal of Fluid Mechanics* 27.02 (1967), pp. 395–397.
- [119] Nicholas Metropolis et al. “Equation of State Calculations by Fast Computing Machines”. In: *The Journal of Chemical Physics* 21.6 (1953), pp. 1087–1092. DOI: <http://dx.doi.org/10.1063/1.1699114>. URL: <http://scitation.aip.org/content/aip/journal/jcp/21/6/10.1063/1.1699114>.
- [120] A. Milsted, M. Lewerenz, and F. W. G. Transchel. “evoMPS source code”. In: <https://github.com/amilsted/evoMPS> (2012). URL: <https://github.com/amilsted/evoMPS>.
- [121] A. Milsted and F. W. G. Transchel. “evoMPS dissipation multiprocessing extension”. In: (2014). URL: <https://github.com/ftranschel/evoMPS>.
- [122] A. Milsted et al. “Variational matrix product ansatz for nonuniform dynamics in the thermodynamic limit”. In: *Phys. Rev. B* 88.15, 155116 (Oct. 2013), p. 155116. DOI: 10.1103/PhysRevB.88.155116. arXiv: 1207.0691 [cond-mat.str-el].
- [123] C. Monroe et al. “Resolved-Sideband Raman Cooling of a Bound Atom to the 3D Zero-Point Energy”. In: *Phys. Rev. Lett.* 75 (22 Nov. 1995), pp. 4011–4014. DOI: 10.1103/PhysRevLett.75.4011. URL: <http://link.aps.org/doi/10.1103/PhysRevLett.75.4011>.
- [124] R. J. Needs et al. “TOPICAL REVIEW: Continuum variational and diffusion quantum Monte Carlo calculations”. In: *Journal of Physics Condensed Matter* 22.2, 023201 (Jan. 2010), p. 023201. DOI: 10.1088/0953-8984/22/2/023201. arXiv: 1002.2127 [cond-mat.mtrl-sci].
- [125] N. Nemec. “Diffusion Monte Carlo: Exponential scaling of computational cost for large systems”. In: *Physical Review B* 81.3, 035119 (Jan. 2010), p. 035119. DOI: 10.1103/PhysRevB.81.035119. arXiv: 0906.0501 [physics.comp-ph].

- [126] M. Nielsen. “Complete note on fermions and the Jordan-Wigner transform”. In: (2005). URL: <http://michaelnielsen.org/blog/complete-notes-on-fermions-and-the-jordan-wigner-transform/>.
- [127] M. A. Nielsen and I. L. Chuang. *Quantum Computation and Quantum Information*. 10th Anniversary Edition. Cambridge University Press, 2000.
- [128] S. Nimmrichter et al. “Master equation for the motion of a polarizable particle in a multimode cavity”. In: *New Journal of Physics* 12.8, 083003 (Aug. 2010), p. 083003. DOI: 10.1088/1367-2630/12/8/083003. arXiv: 1004.0807 [quant-ph].
- [129] Lars Onsager. “Crystal Statistics. I. A Two-Dimensional Model with an Order-Disorder Transition”. In: *Phys. Rev.* 65 (3-4 Feb. 1944), pp. 117–149. DOI: 10.1103/PhysRev.65.117. URL: <http://link.aps.org/doi/10.1103/PhysRev.65.117>.
- [130] T J Osborne and M A Nielsen. In: *Phys. Rev. A* 66 (2002), p. 032110.
- [131] Tobias J. Osborne. “Efficient Approximation of the Dynamics of One-Dimensional Quantum Spin Systems”. In: *Phys. Rev. Lett.* 97 (15 Oct. 2006), p. 157202. DOI: 10.1103/PhysRevLett.97.157202. URL: <http://link.aps.org/doi/10.1103/PhysRevLett.97.157202>.
- [132] Tobias J. Osborne and Frank Verstraete. “General Monogamy Inequality for Bipartite Qubit Entanglement”. In: *Phys. Rev. Lett.* 96 (22 June 2006), p. 220503. DOI: 10.1103/PhysRevLett.96.220503. URL: <http://link.aps.org/doi/10.1103/PhysRevLett.96.220503>.
- [133] V. R. Overbeck and H. Weimer. “Time evolution of open quantum many-body systems”. In: *ArXiv e-prints* (Oct. 2015). arXiv: 1510.01339 [quant-ph].
- [134] Wolfgang Paul. “Electromagnetic traps for charged and neutral particles”. In: *Rev. Mod. Phys.* 62 (3 July 1990), pp. 531–540. DOI: 10.1103/RevModPhys.62.531. URL: <http://link.aps.org/doi/10.1103/RevModPhys.62.531>.
- [135] Wolfgang Pauli. “Remarks on the History of the Exclusion Principle”. In: *Science* 103.2669 (1946), pp. 213–215. DOI: 10.1126/science.103.2669.213. eprint: <http://www.sciencemag.org/content/103/2669/213.full.pdf>. URL: <http://www.sciencemag.org/content/103/2669/213.short>.
- [136] P. Pearle. “Simple derivation of the Lindblad equation”. In: *European Journal of Physics* 33 (July 2012), pp. 805–822. DOI: 10.1088/0143-0807/33/4/805. arXiv: 1204.2016 [math-ph].
- [137] D. Perez-Garcia et al. “Matrix Product State Representations”. In: *Quantum Info. Comput.* 7.5 (July 2007), pp. 401–430. ISSN: 1533-7146. URL: <http://dl.acm.org/citation.cfm?id=2011832.2011833>.
- [138] “Density-Matrix Renormalization”. In: *A New Numerical Method in Physics Lectures of a Seminar and Workshop Held at the Max-Planck-Institut für Physik komplexer Systeme Dresden, Germany, August 24th to September 18th*. Ed. by I. Peschel et al. Vol. 528. Lecture Notes in Physics. Springer, Aug. 1998, pp. 0075–8450.
- [139] William D. Phillips. “Nobel Lecture: Laser cooling and trapping of neutral atoms”. In: *Rev. Mod. Phys.* 70 (3 July 1998), pp. 721–741. DOI: 10.1103/RevModPhys.70.721. URL: <http://link.aps.org/doi/10.1103/RevModPhys.70.721>.
- [140] B. Pirvu et al. “Matrix product operator representations”. In: *New Journal of Physics* 12.2 (2010), p. 025012. URL: <http://stacks.iop.org/1367-2630/12/i=2/a=025012>.

- [141] M. B. Plenio and S. Virmani. “An introduction to entanglement measures”. In: *eprint arXiv:quant-ph/0504163* (Apr. 2005). eprint: [quant-ph/0504163](http://arxiv.org/abs/quant-ph/0504163).
- [142] Tobias Preis et al. “GPU accelerated Monte Carlo simulation of the 2D and 3D Ising model”. In: *Journal of Computational Physics* 228.12 (2009), pp. 4468–4477. ISSN: 0021-9991. DOI: <http://dx.doi.org/10.1016/j.jcp.2009.03.018>. URL: <http://www.sciencedirect.com/science/article/pii/S0021999109001387>.
- [143] Tomaz Prosen. “Exact Nonequilibrium Steady State of a Strongly Driven Open XXZ Chain”. In: *Phys. Rev. Lett.* 107 (13 Sept. 2011), p. 137201. DOI: [10.1103/PhysRevLett.107.137201](https://doi.org/10.1103/PhysRevLett.107.137201). URL: <http://link.aps.org/doi/10.1103/PhysRevLett.107.137201>.
- [144] H. de Raedt and W. von der Linden. “Monte Carlo Diagonalization of very large matrices: application to fermion systems”. In: *International Journal of Modern Physics C* 03.01 (1992), pp. 97–104. DOI: [10.1142/S0129183192000087](https://doi.org/10.1142/S0129183192000087). URL: <http://www.worldscientific.com/doi/abs/10.1142/S0129183192000087>.
- [145] J W Rayleigh. “In Finding the Correction for the Open End of an Organ-Pipe”. In: *Philosophical Transactions* 161.1870 (), p. 77.
- [146] P. Reinhardt et al. “Quantum Monte Carlo facing the Hartree-Fock symmetry dilemma: The case of hydrogen rings”. In: *ArXiv e-prints* (July 2011). arXiv: 1107.3537 [physics.chem-ph].
- [147] Wolfram Research. “Mathematica 10”. In: (2015). URL: <http://www.wolfram.com/mathematica/>.
- [148] Giacomo Della Riccia and Norbert Wiener. “Wave Mechanics in Classical Phase Space, Brownian Motion, and Quantum Theory”. In: *Journal of Mathematical Physics* 7.8 (1966), pp. 1372–1383. DOI: <http://dx.doi.org/10.1063/1.1705047>. URL: <http://scitation.aip.org/content/aip/journal/jmp/7/8/10.1063/1.1705047>.
- [149] A. Ridinger et al. “Large atom number dual-species magneto-optical trap for fermionic ${}^6\text{Li}$ and ${}^{40}\text{K}$ atoms”. In: *European Physical Journal D* 65 (Nov. 2011), pp. 223–242. DOI: [10.1140/epjd/e2011-20069-4](https://doi.org/10.1140/epjd/e2011-20069-4). arXiv: 1103.0637 [cond-mat.quant-gas].
- [150] D. Rio Fernandes et al. “Sub-Doppler laser cooling of fermionic ${}^{40}\text{K}$ atoms in three-dimensional gray optical molasses”. In: *EPL (Europhysics Letters)* 100 (Dec. 2012), p. 63001. DOI: [10.1209/0295-5075/100/63001](https://doi.org/10.1209/0295-5075/100/63001). arXiv: 1210.1310 [cond-mat.quant-gas].
- [151] W. Ritz. “Über eine neue Methode zur Lösung gewisser Variationsprobleme der mathematischen Physik”. In: *Journal für die reine und angewandte Mathematik* 135.1 (1908).
- [152] C Runge. “Über die numerische Auflösung von Differentialgleichungen”. In: *Math. Annalen* 46 (1895), pp. 167–178.
- [153] A. Ruschhaupt and R. F. Werner. “Quantum mechanics of time”. In: *The message of quantum science – attempts towards a synthesis*. Ed. by P. Blanchard and J. Fröhlich. Springer, 2015.
- [154] E. K. H. Salje. “Phase Transitions in Ferroelastic and Co-elastic Crystals”. In: Cambridge University Press, 1993.
- [155] A. W. Sandvik. “Computational Studies of Quantum Spin Systems”. In: *American Institute of Physics Conference Series*. Ed. by A. Avella and F. Mancini. Vol. 1297. American Institute of Physics Conference Series. Nov. 2010, pp. 135–338. DOI: [10.1063/1.3518900](https://doi.org/10.1063/1.3518900). arXiv: 1101.3281 [cond-mat.str-el].

- [156] U. Schollwöck. “The density-matrix renormalization group in the age of matrix product states”. In: *Annals of Physics* 326 (Jan. 2011), pp. 96–192. DOI: 10.1016/j.aop.2010.09.012. arXiv: 1008.3477 [cond-mat.str-el].
- [157] C. E. Shannon and W. Weaver. *The Mathematical Theory of Information*. Urbana, Illinois: University of Illinois Press, 1949.
- [158] J. C. Slater. “Note on Hartree’s Method”. In: *Phys. Rev.* 35 (2 Jan. 1930), pp. 210–211. DOI: 10.1103/PhysRev.35.210.2. URL: <http://link.aps.org/doi/10.1103/PhysRev.35.210.2>.
- [159] E M Stoudenmire and Steven R White. “Minimally entangled typical thermal state algorithms”. In: *Journal of New Physics* 12.055026 (2010).
- [160] T. Tao. “Sunset and inverse sunset theorems for Shannon entropy”. In: *ArXiv e-prints* (June 2009). arXiv: 0906.4387 [math.CO].
- [161] Gérard Toulouse. “Theory of the frustration effect in spin glasses: I”. In: *Commun. Phys* 2.4 (1977), pp. 115–119.
- [162] J. Toulouse and C. J. Umrigar. “Optimization of quantum Monte Carlo wave functions by energy minimization”. In: *Journal of Chemical Physics* 126.8 (Feb. 2007), p. 084102. DOI: 10.1063/1.2437215. eprint: physics/0701039.
- [163] F. W. G. Transchel, A. Milsted, and T. J. Osborne. “A Monte Carlo Time-Dependent Variational Principle”. In: *ArXiv e-prints* (Nov. 2014). arXiv: 1411.5546 [quant-ph].
- [164] Christian Trippe et al. “Exact calculation of the magnetocaloric effect in the spin- $\frac{1}{2}$ XXZ chain”. In: *Phys. Rev. B* 81 (5 Feb. 2010), p. 054402. DOI: 10.1103/PhysRevB.81.054402. URL: <http://link.aps.org/doi/10.1103/PhysRevB.81.054402>.
- [165] H F Trotter. “On the product of semi-groups of operators”. In: 1959, pp. 545–551.
- [166] Matthias Troyer and Uwe-Jens Wiese. “Computational Complexity and Fundamental Limitations to Fermionic Quantum Monte Carlo Simulations”. In: *Phys. Rev. Lett.* 94 (17 May 2005), p. 170201. DOI: 10.1103/PhysRevLett.94.170201. URL: <http://link.aps.org/doi/10.1103/PhysRevLett.94.170201>.
- [167] K. Ueda et al. “Least Action Principle for the Real-Time Density Matrix Renormalization Group”. In: *eprint arXiv:cond-mat/0612480* (Dec. 2006). eprint: cond-mat/0612480.
- [168] G. E. Uhlenbeck and L. S. Ornstein. “On the Theory of the Brownian Motion”. In: *Phys. Rev.* 36 (5 Sept. 1930), pp. 823–841. DOI: 10.1103/PhysRev.36.823. URL: <http://link.aps.org/doi/10.1103/PhysRev.36.823>.
- [169] Berkeley University. “Berkeley Open Infrastructure for Network Computing”. In: (2003). URL: <https://boinc.berkeley.edu/>.
- [170] F. Verstraete, J. J. García-Ripoll, and J. I. Cirac. “Matrix Product Density Operators: Simulation of Finite-Temperature and Dissipative Systems”. In: *Phys. Rev. Lett.* 93 (20 Nov. 2004), p. 207204. DOI: 10.1103/PhysRevLett.93.207204. URL: <http://link.aps.org/doi/10.1103/PhysRevLett.93.207204>.
- [171] F. Verstraete, V. Murg, and J. I. Cirac. “Matrix product states, projected entangled pair states, and variational renormalization group methods for quantum spin systems”. In: *Advances in Physics* 57 (Mar. 2008), pp. 143–224. DOI: 10.1080/14789940801912366. arXiv: 0907.2796 [quant-ph].
- [172] F. Verstraete, D. Porras, and J. I. Cirac. “Density Matrix Renormalization Group and Periodic Boundary Conditions: A Quantum Information Perspective”. In: *Phys. Rev. Lett.* 93 (22 Nov. 2004), p. 227205. DOI: 10.1103/

- PhysRevLett.93.227205. URL: <http://link.aps.org/doi/10.1103/PhysRevLett.93.227205>.
- [173] F. Verstraete et al. “Criticality, the Area Law, and the Computational Power of Projected Entangled Pair States”. In: *Physical Review Letters* 96.22, 220601 (June 2006), p. 220601. DOI: 10.1103/PhysRevLett.96.220601. eprint: [quant-ph/0601075](http://arxiv.org/abs/quant-ph/0601075).
- [174] G. Vidal and R. F. Werner. “Computable measure of entanglement”. In: *Phys. Rev. A* 65 (3 Feb. 2002), p. 032314. DOI: 10.1103/PhysRevA.65.032314. URL: <http://link.aps.org/doi/10.1103/PhysRevA.65.032314>.
- [175] G. Vidal et al. “Entanglement in Quantum Critical Phenomena”. In: *Phys. Rev. Lett.* 90 (22 June 2003), p. 227902. DOI: 10.1103/PhysRevLett.90.227902. URL: <http://link.aps.org/doi/10.1103/PhysRevLett.90.227902>.
- [176] Guifré Vidal. “Efficient Classical Simulation of Slightly Entangled Quantum Computations”. In: *Phys. Rev. Lett.* 91 (14 Oct. 2003), p. 147902. DOI: 10.1103/PhysRevLett.91.147902. URL: <http://link.aps.org/doi/10.1103/PhysRevLett.91.147902>.
- [177] John Von Neumann. *Mathematische Grundlagen der Quantenmechanik*. Berlin: Springer, 1932.
- [178] A. Weichselbaum et al. “Variational matrix-product-state approach to quantum impurity models”. In: *Phys. Rev. B* 80 (16 Oct. 2009), p. 165117. DOI: 10.1103/PhysRevB.80.165117. URL: <http://link.aps.org/doi/10.1103/PhysRevB.80.165117>.
- [179] A. H. Werner et al. “A positive tensor network approach for simulating open quantum many-body systems”. In: *ArXiv e-prints* (Dec. 2014). arXiv: 1412.5746 [quant-ph].
- [180] R. F. Werner. “Arrival time observables in quantum mechanics”. In: *Ann. Inst. H. Poincaré Phys. Théor.* 47 (1987), pp. 429–449.
- [181] H Weyl. “Gruppentheorie und Quantenmechanik”. In: Leipzig: Hirzel, 1928.
- [182] Steven R. White. “Density-matrix algorithms for quantum renormalization groups”. In: *Phys. Rev. B* 48 (14 1993), pp. 10345–10356. DOI: 10.1103/PhysRevB.48.10345. URL: <http://link.aps.org/doi/10.1103/PhysRevB.48.10345>.
- [183] Steven R. White. “Density matrix formulation for quantum renormalization groups”. In: *Phys. Rev. Lett.* 69 (19 1992), pp. 2863–2866. DOI: 10.1103/PhysRevLett.69.2863. URL: <http://link.aps.org/doi/10.1103/PhysRevLett.69.2863>.
- [184] G. C. Wick. “Properties of Bethe-Salpeter Wave Functions”. In: *Physical Review* 96 (Nov. 1954), pp. 1124–1134. DOI: 10.1103/PhysRev.96.1124.
- [185] D. J. Williamson et al. “Matrix product operators for symmetry-protected topological phases”. In: *ArXiv e-prints* (Dec. 2014). arXiv: 1412.5604 [quant-ph].
- [186] Kenneth G. Wilson. “The renormalization group: Critical phenomena and the Kondo problem”. In: *Rev. Mod. Phys.* 47 (4 Oct. 1975), pp. 773–840. DOI: 10.1103/RevModPhys.47.773. URL: <http://link.aps.org/doi/10.1103/RevModPhys.47.773>.
- [187] W. K. Wootters and W. H. Zurek. “A single quantum cannot be cloned”. In: *Nature* 299.5886 (Oct. 1982), pp. 802–803. URL: <http://dx.doi.org/10.1038/299802a0>.
- [188] Sebastian Wouters et al. “Thouless theorem for matrix product states and subsequent post density matrix renormalization group methods”. In: *Phys.*

- Rev. B* 88 (7 Aug. 2013), p. 075122. DOI: 10.1103/PhysRevB.88.075122. URL: <http://link.aps.org/doi/10.1103/PhysRevB.88.075122>.
- [189] Jianling Xu et al. “Monte Carlo simulation of liquid-crystal alignment and chiral symmetry-breaking”. In: *The Journal of Chemical Physics* 115.9 (2001). URL: <http://scitation.aip.org/content/aip/journal/jcp/115/9/10.1063/1.1389857>.
- [190] T. Yanagisawa. “Quantum Monte Carlo diagonalization for many-fermion systems”. In: *Phys. Rev. B* 75.22, 224503 (June 2007), p. 224503. DOI: 10.1103/PhysRevB.75.224503. arXiv: 0707.1929 [cond-mat.str-el].
- [191] Michael Zwolak and Guifré Vidal. “Mixed-State Dynamics in One-Dimensional Quantum Lattice Systems: A Time-Dependent Superoperator Renormalization Algorithm”. In: *Phys. Rev. Lett.* 93 (20 Nov. 2004), p. 207205. DOI: 10.1103/PhysRevLett.93.207205. URL: <http://link.aps.org/doi/10.1103/PhysRevLett.93.207205>.